

Forecasting special events in cosmic history

Christophe Pichon

IAP / KIAS

C. Cadiou, S. Codis, C. Gay D. Pogosyan, C. Laigle, T.Sousbie, M. Musso

A 15-year long project initiated by S. Colombi



Statistics of Merging Peaks of Random Gaussian Fluctuations: Skeleton Tree Formalism

Hitoshi HANAMI

Physics Section, Faculty of Humanities and Social Sciences, Iwate University, Morioka 020 JAPAN

horizon-AGN

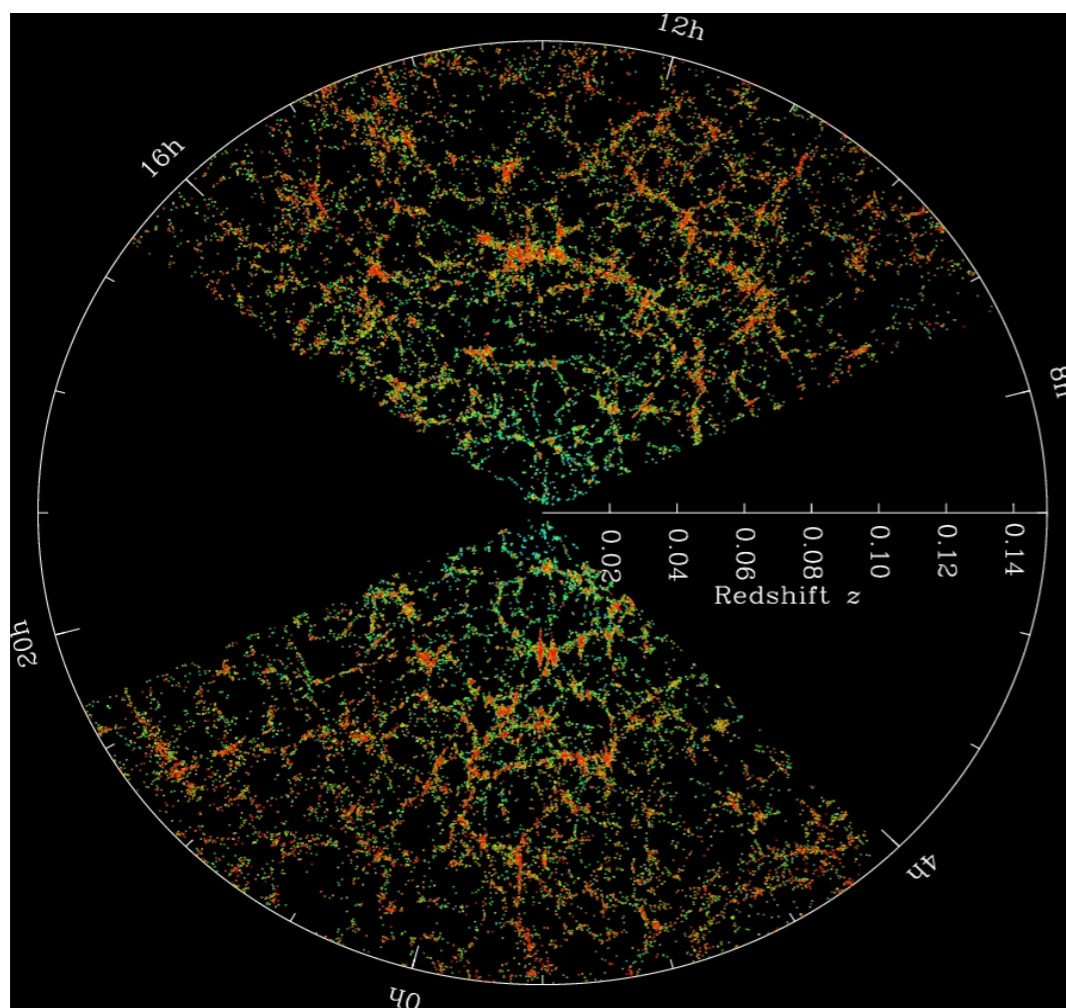
12/04/2019

Kyoto

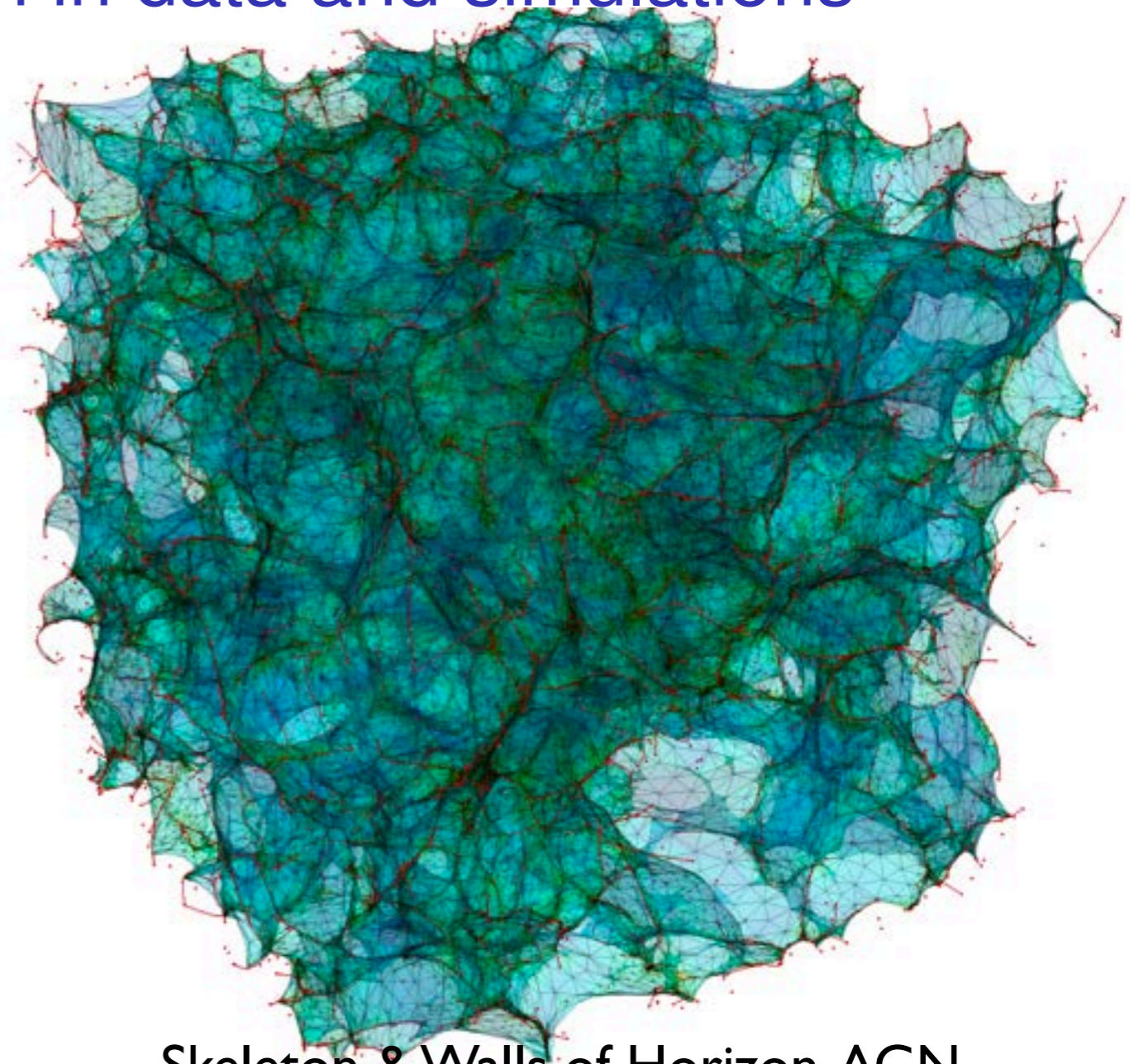
Thursday, 11 April, 19

Context: geometry & Topology

Large scale filamentary structure connecting clusters of galaxies is evident both in data and simulations



Sloan DS Survey

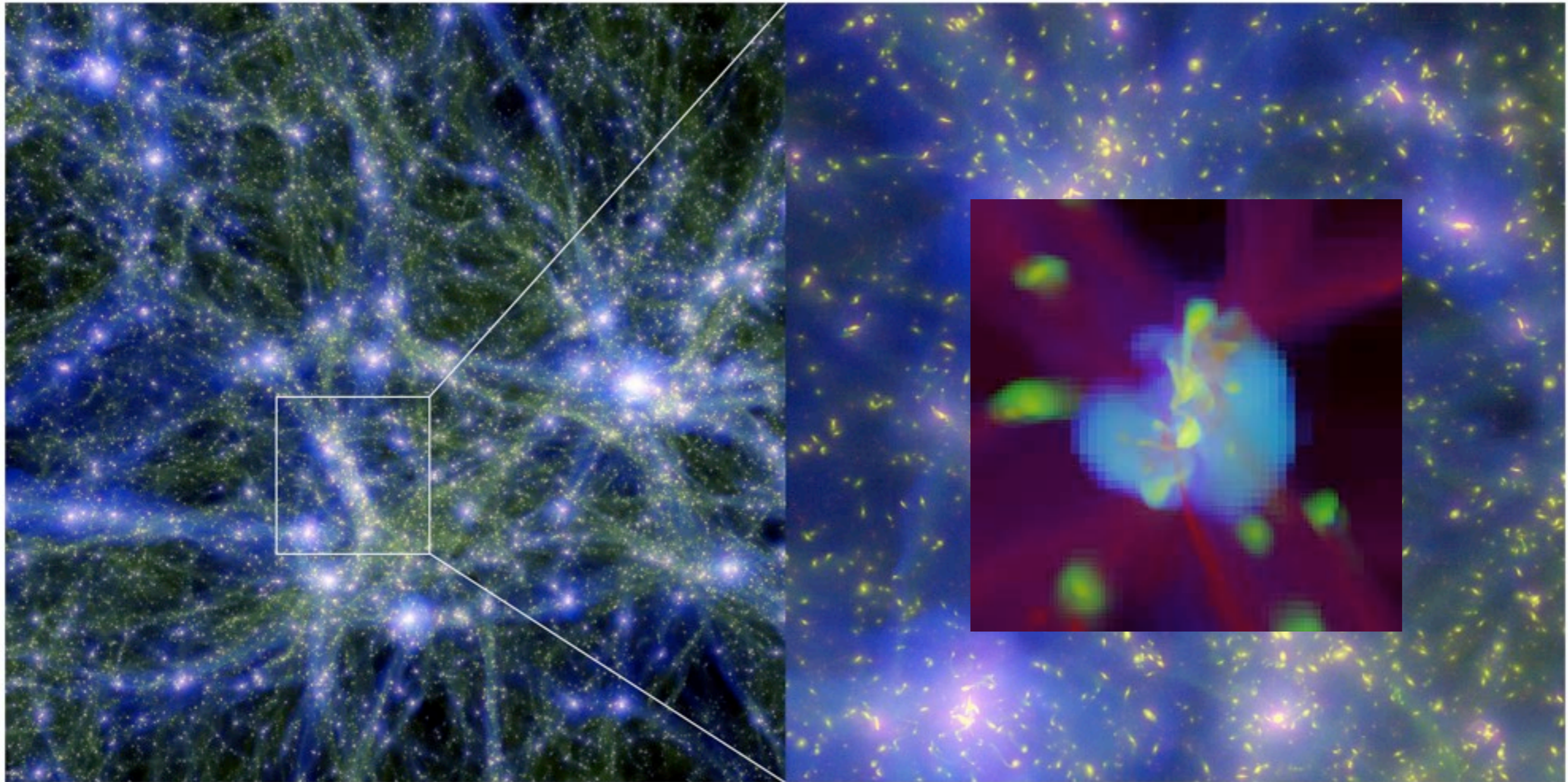


Skeleton & Walls of Horizon-AGN

Geometry of LSS as a probe of cosmology

Context: feeding galaxies via cold flows?

Large scale filamentary structure connecting clusters of galaxies is evident both in data and simulations



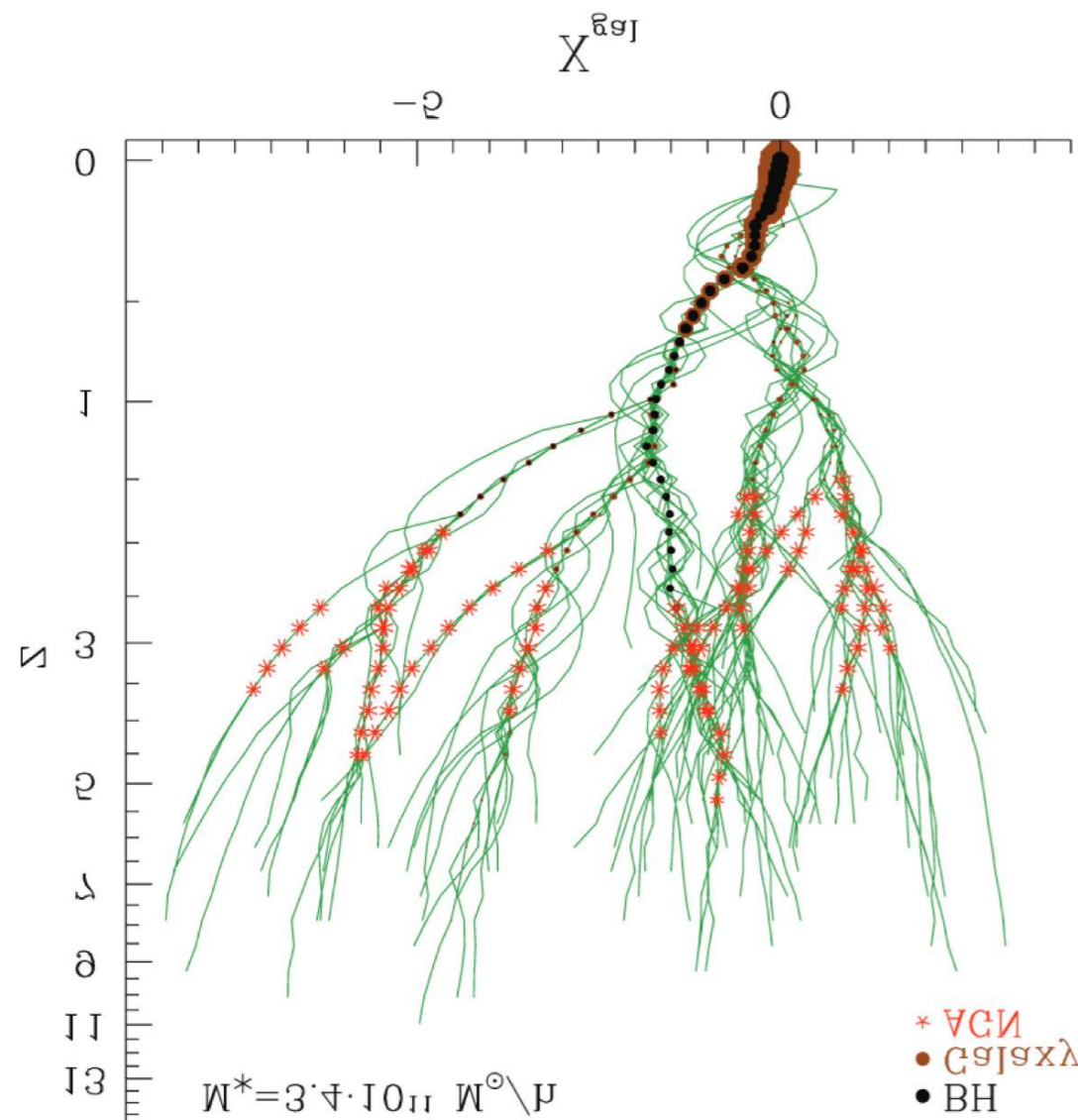
Filamentary accretion regulating stellar formation / AGN feedback/AM acquisition

Context: skeleton tree

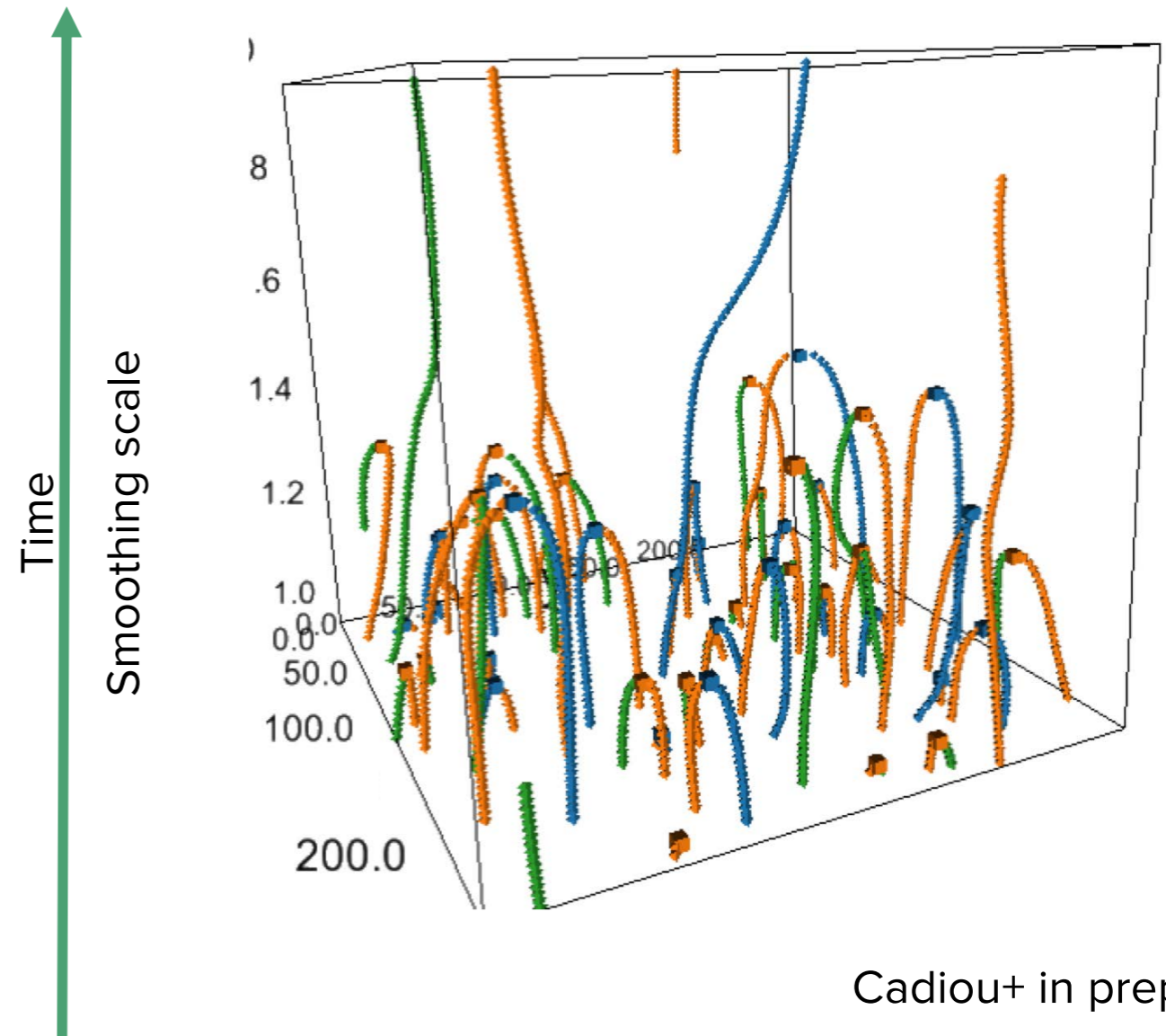
The skeleton tree formalism

Can we build a merger-tree like structure from the initial conditions?

⇒ Yes! Study the topological structure of the ICs at different scales (Hanami 2001)



Marulli+2009



Cadiou+ in prep

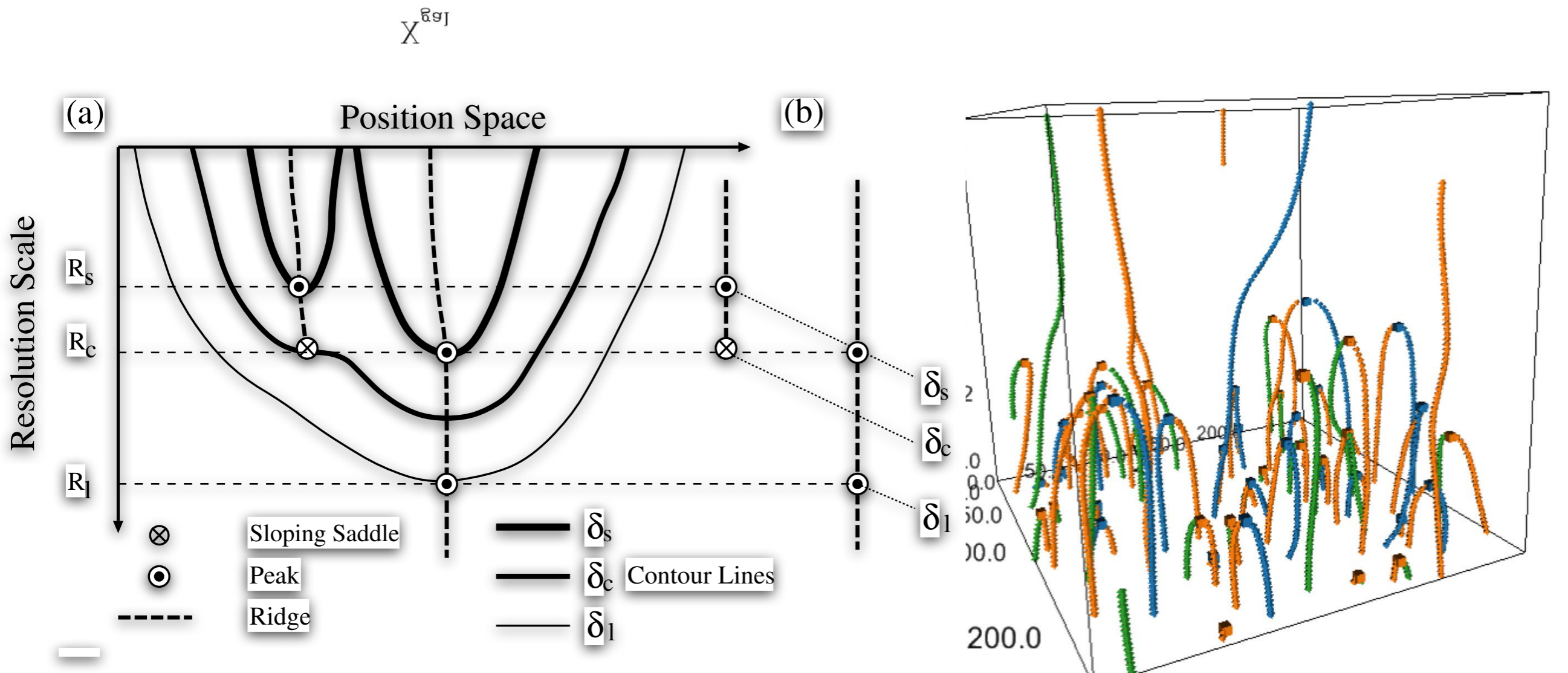
Extend Hanami '01 to *other* critical events

Context: skeleton tree

The skeleton tree formalism

Can we build a merger-tree like structure from the initial conditions?

⇒ Yes! Study the topological structure of the ICs at different scales (Hanami 2001)



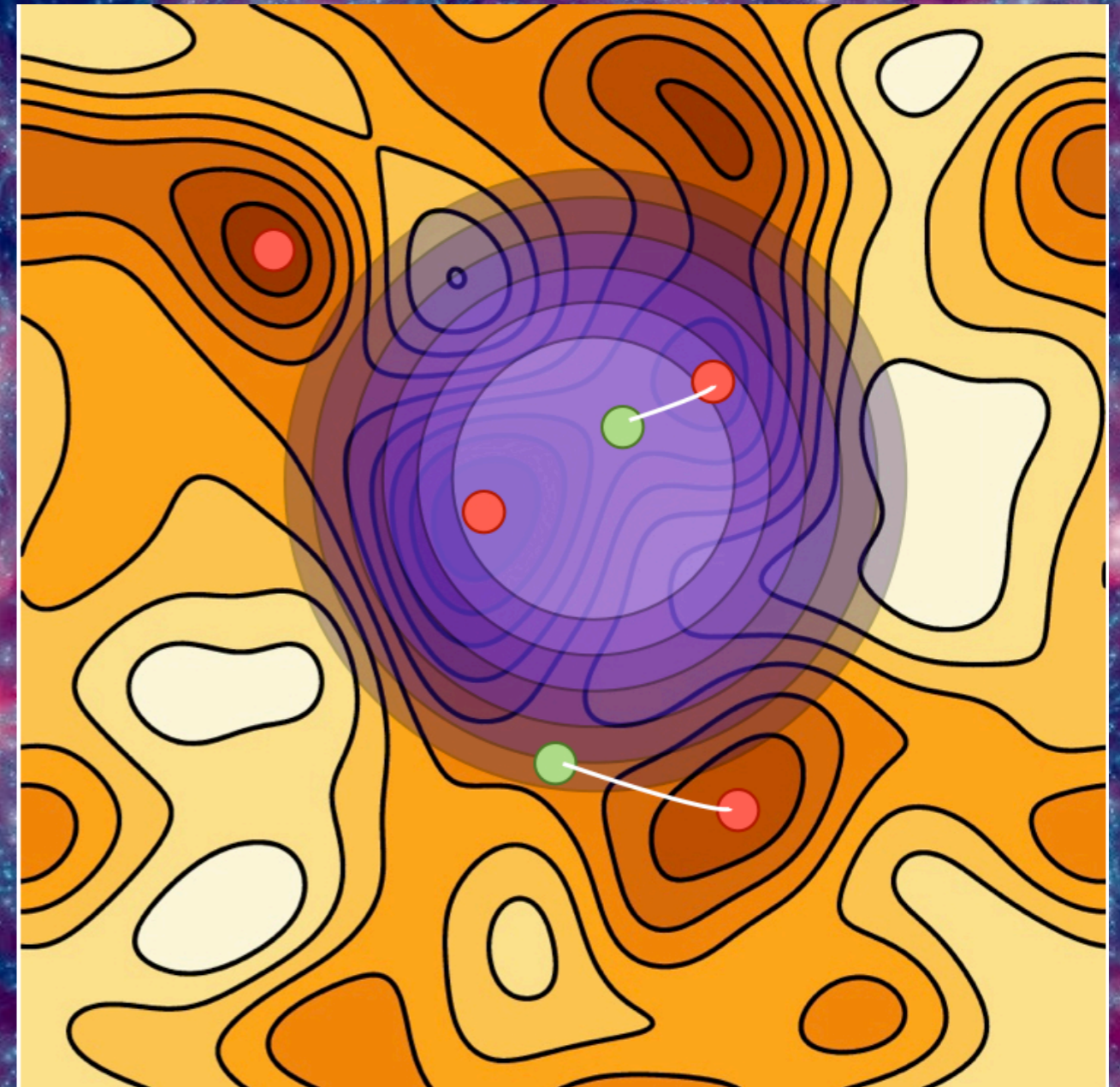
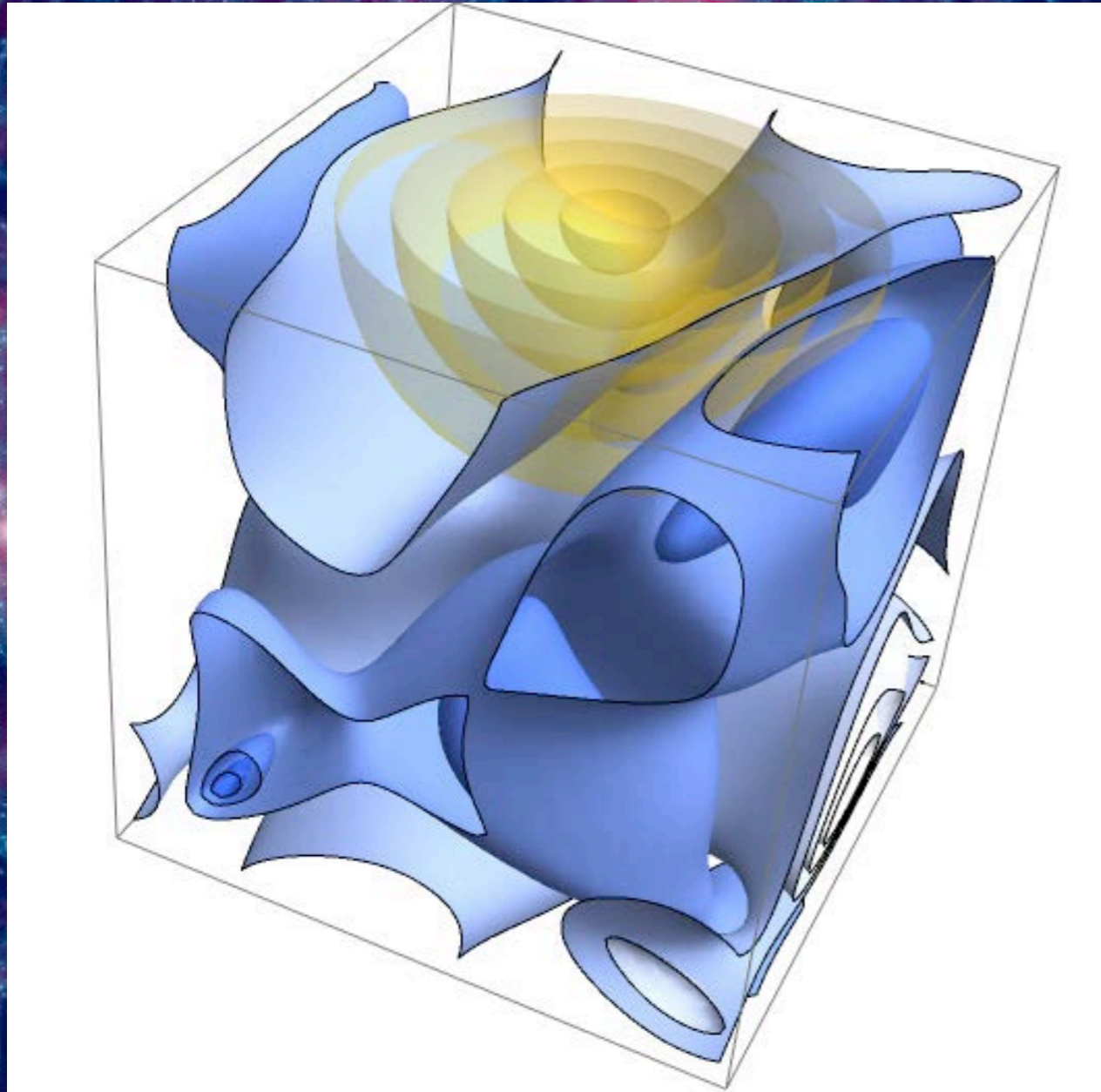
Marulli+2009

Cadiou+ in prep

Extend Hanami '01 to *other* critical events

Context

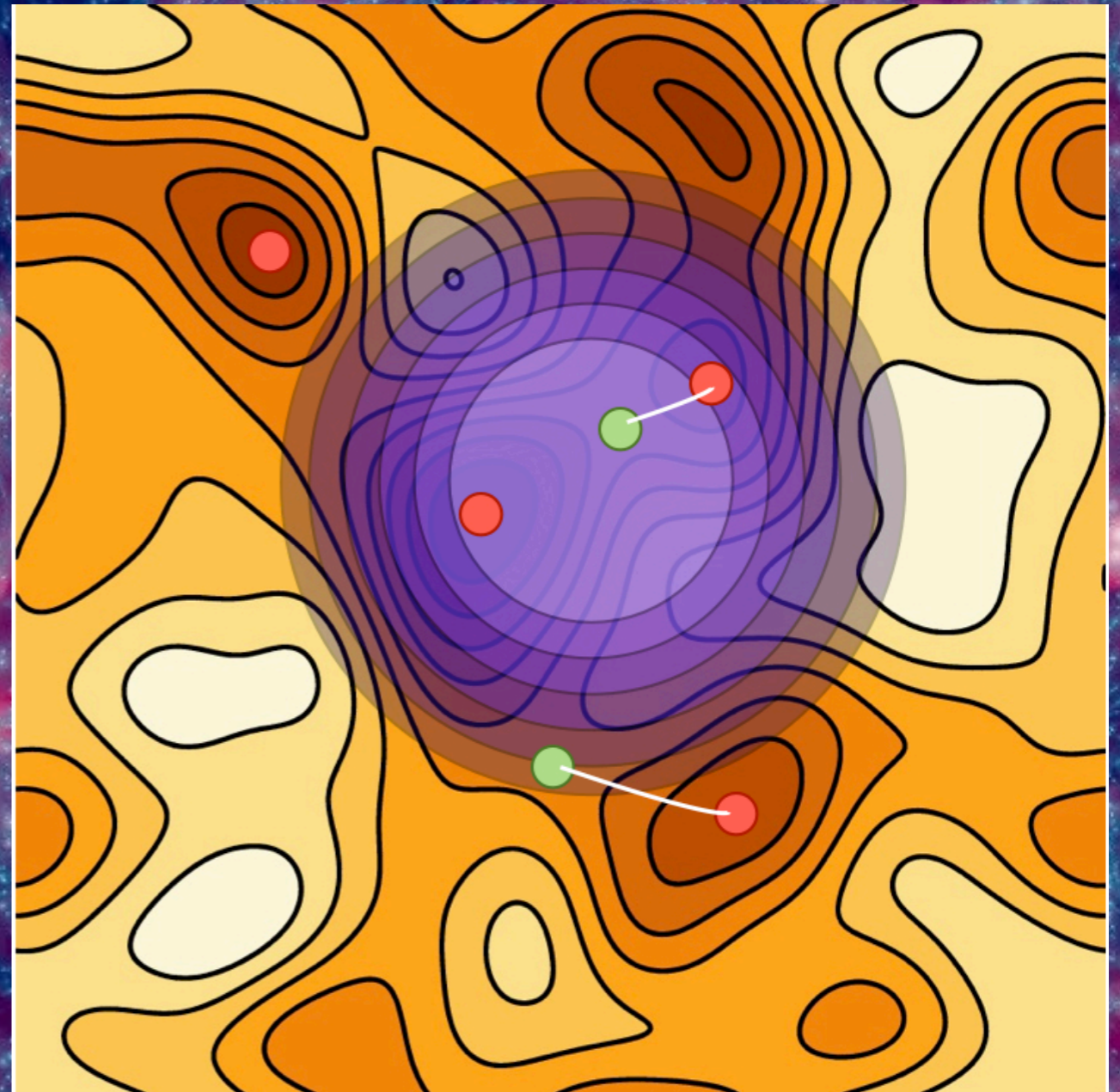
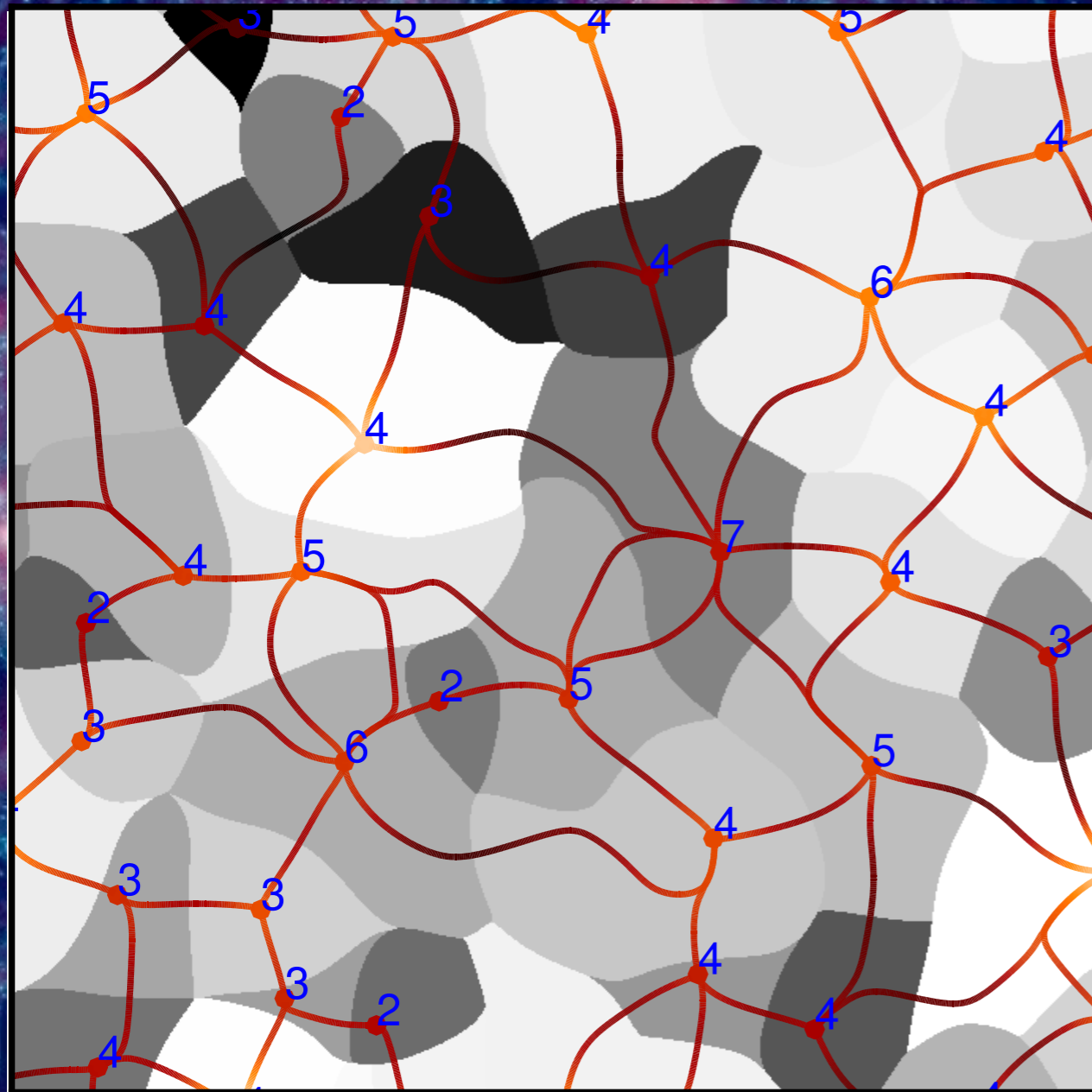
Spherical collapse: time-smoothing duality



Understand special events in evolution of cosmic web

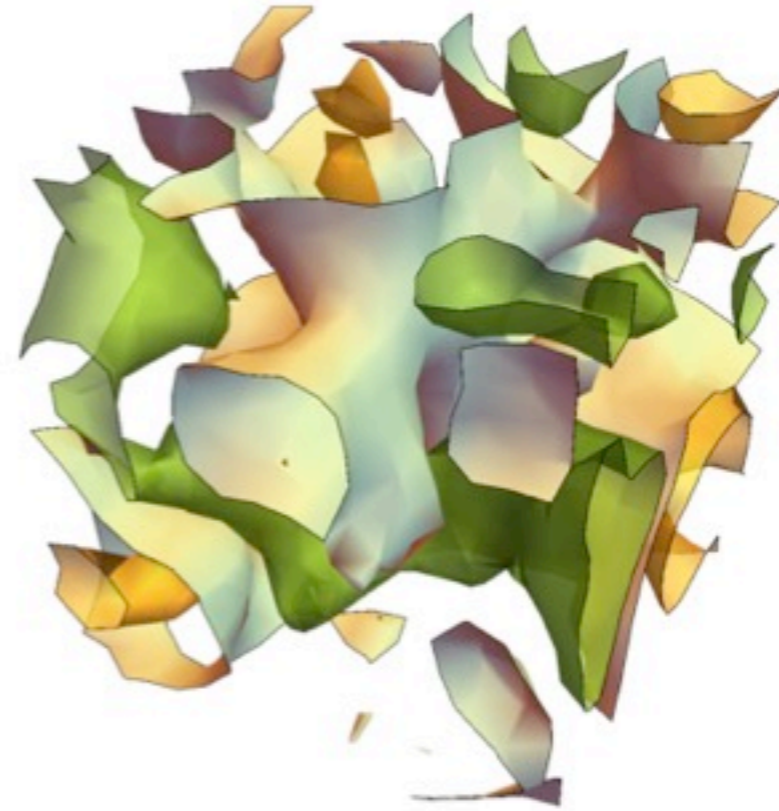
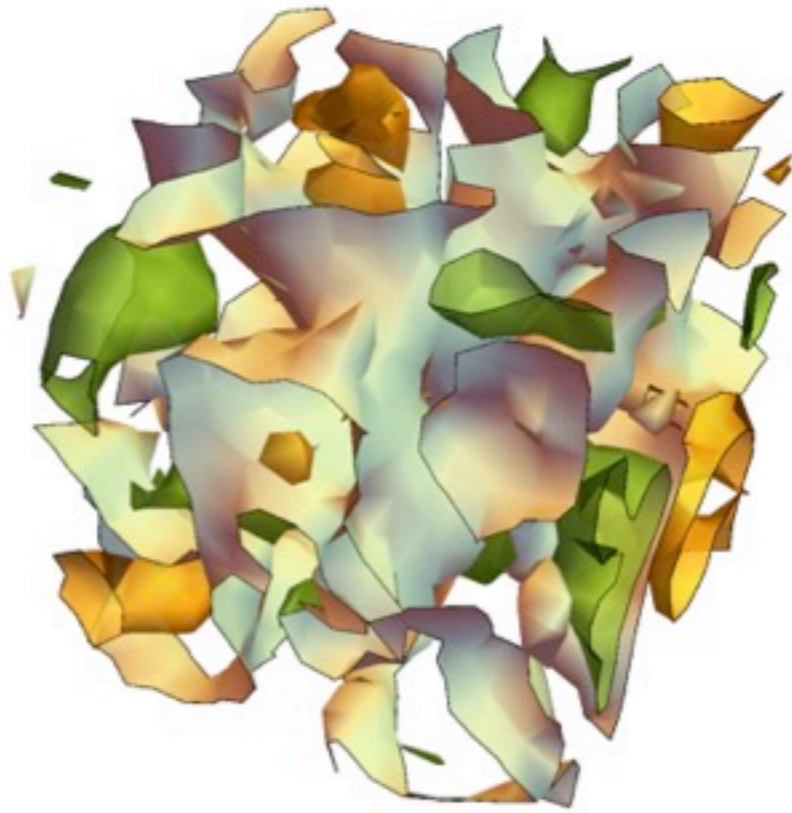
Context

Spherical collapse: time-smoothing duality

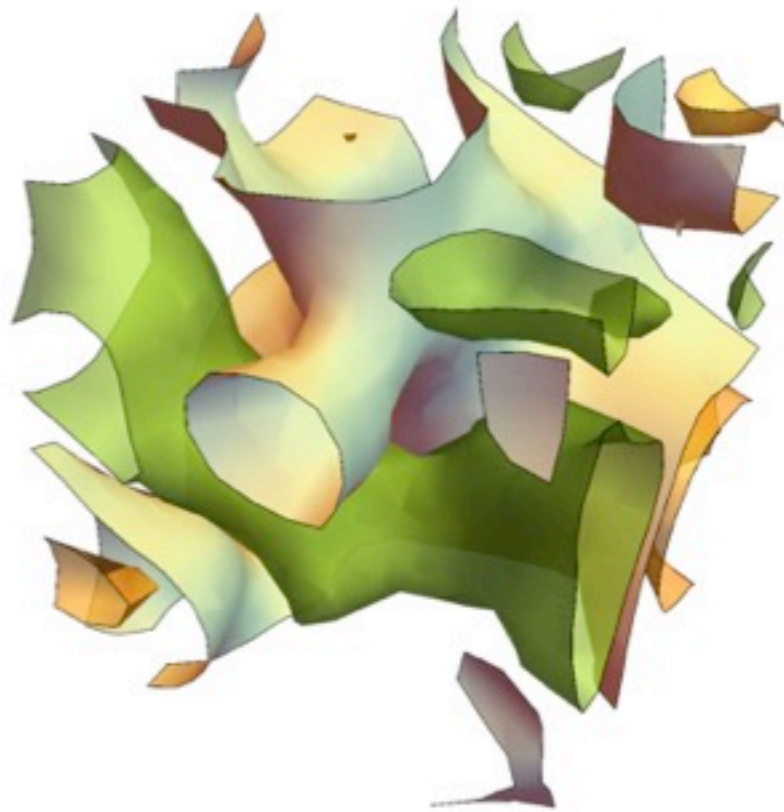


Understand special events in evolution of cosmic web

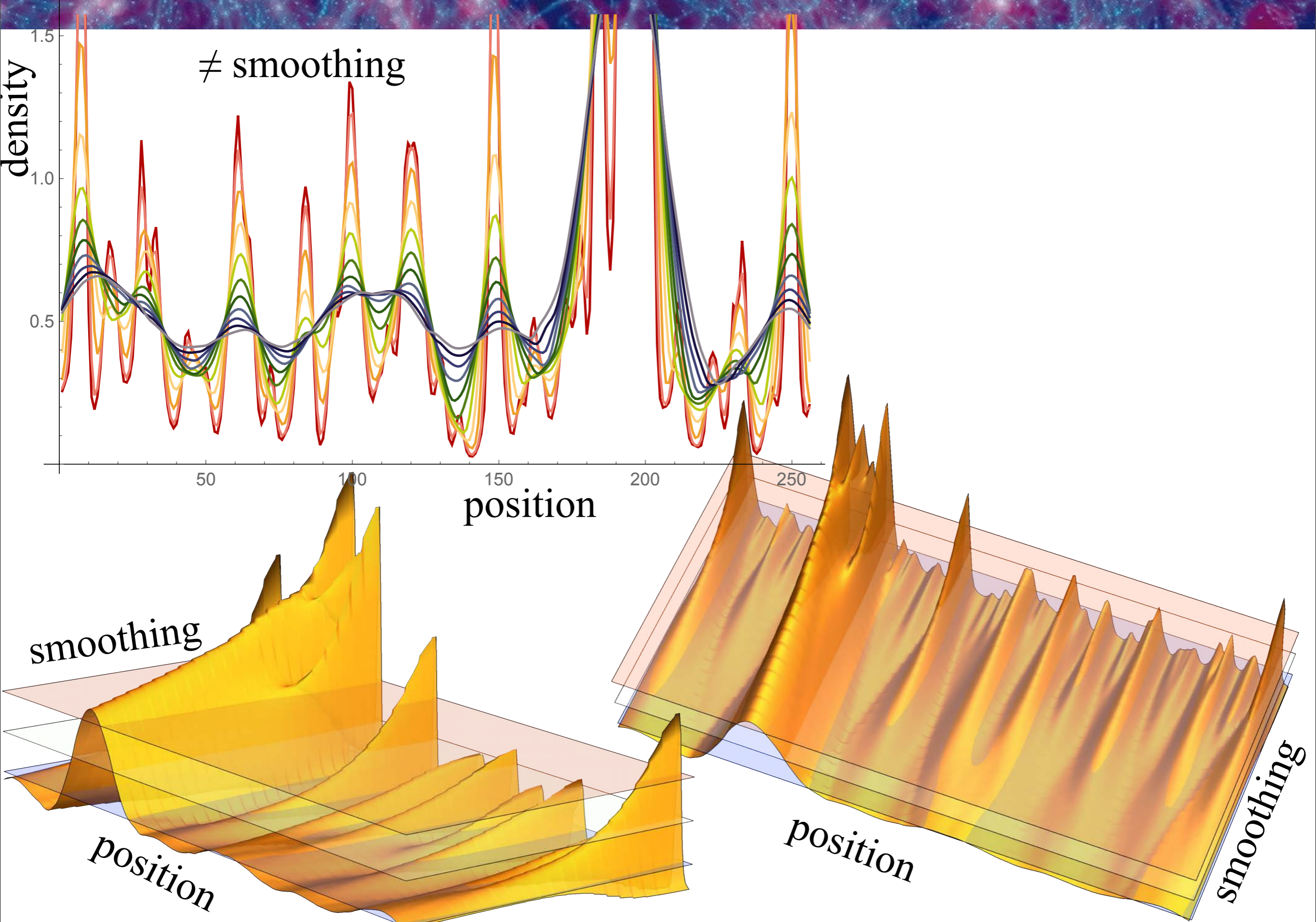
Context



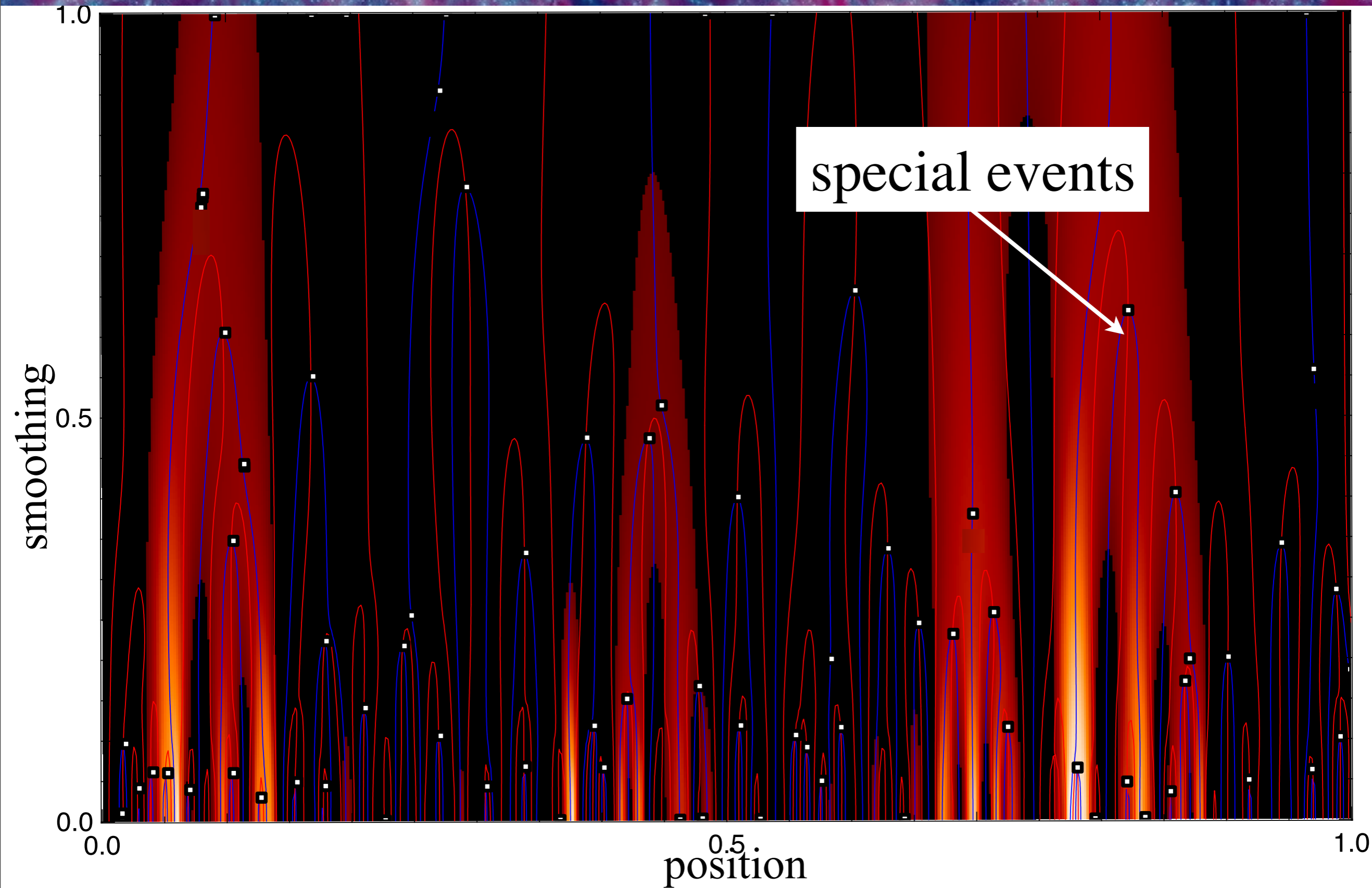
Change in excursion's topology impacts galaxy formation



1D outlook: ridges in position-smoothing landscape

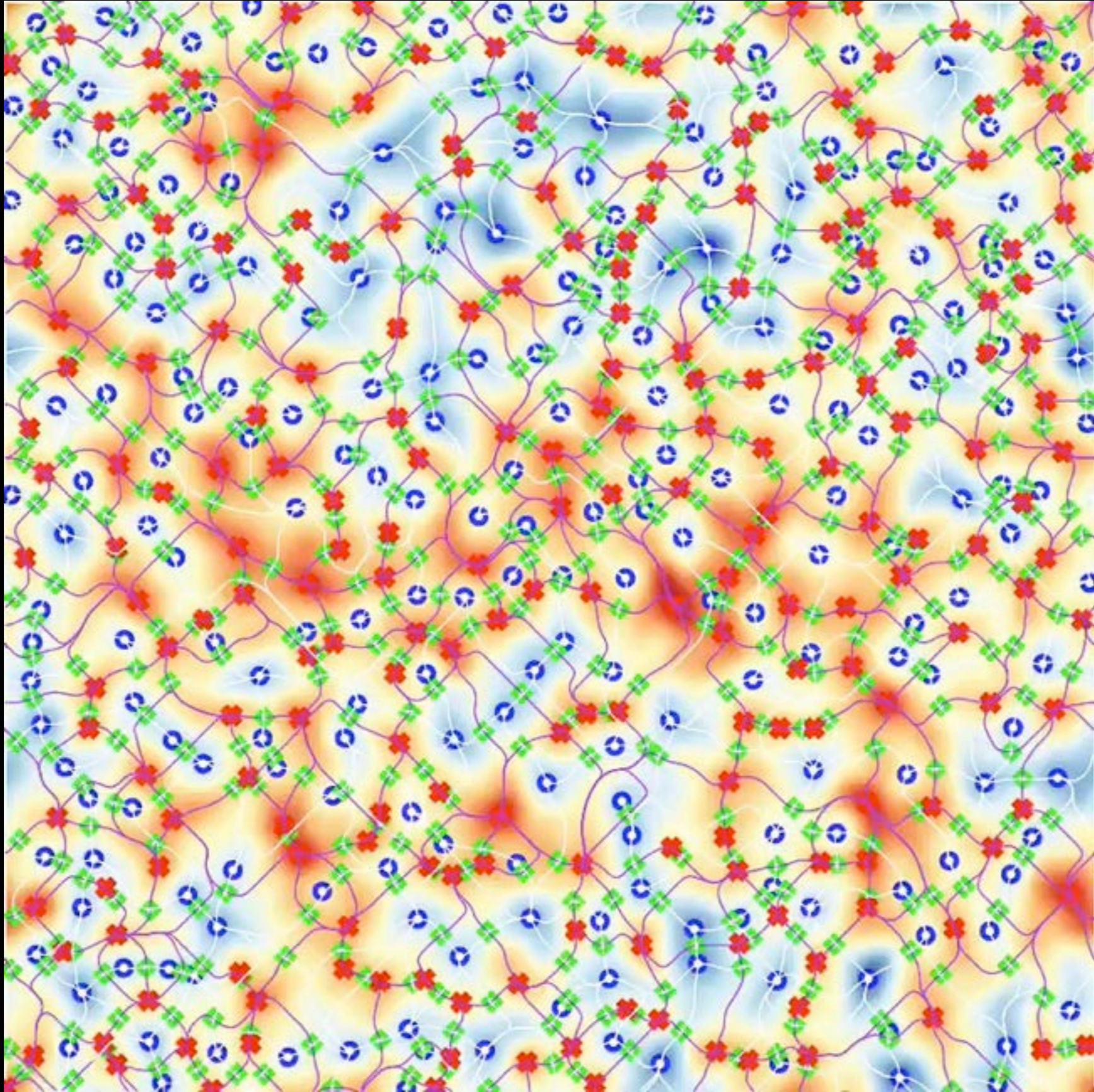


1D outlook



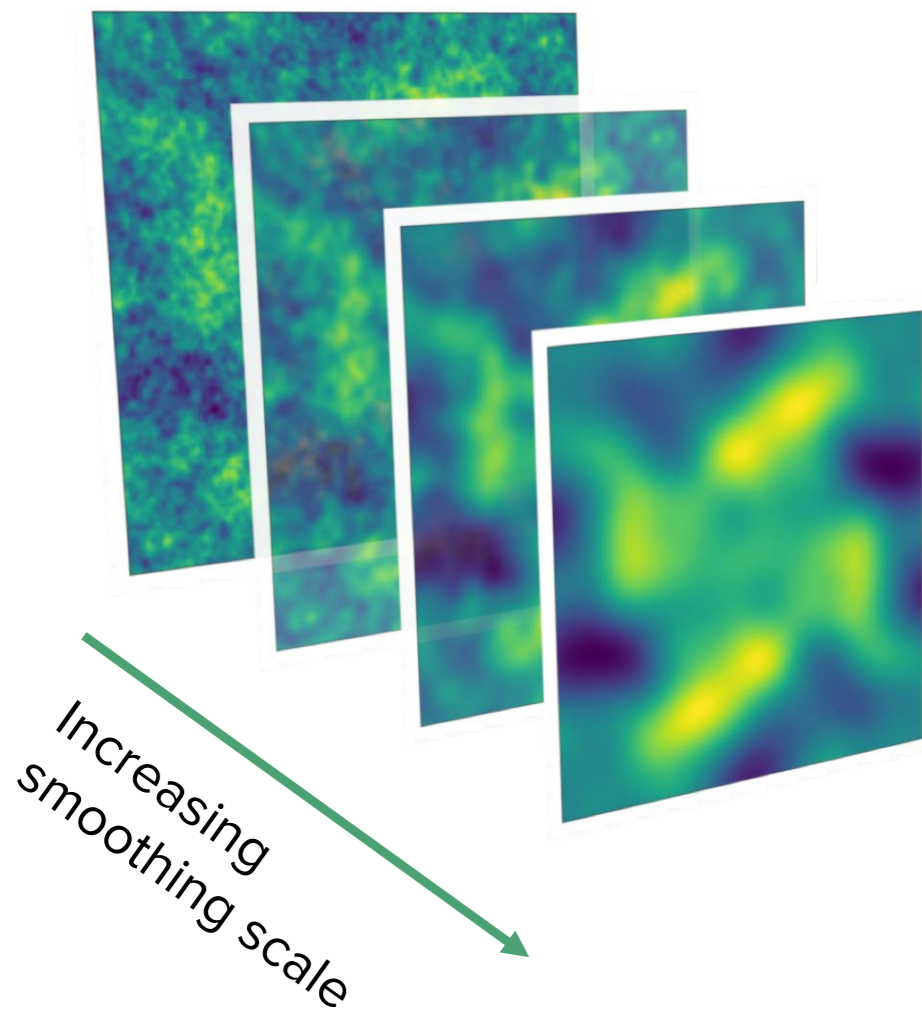
Special event : topology of underlying field changes

2D outlook

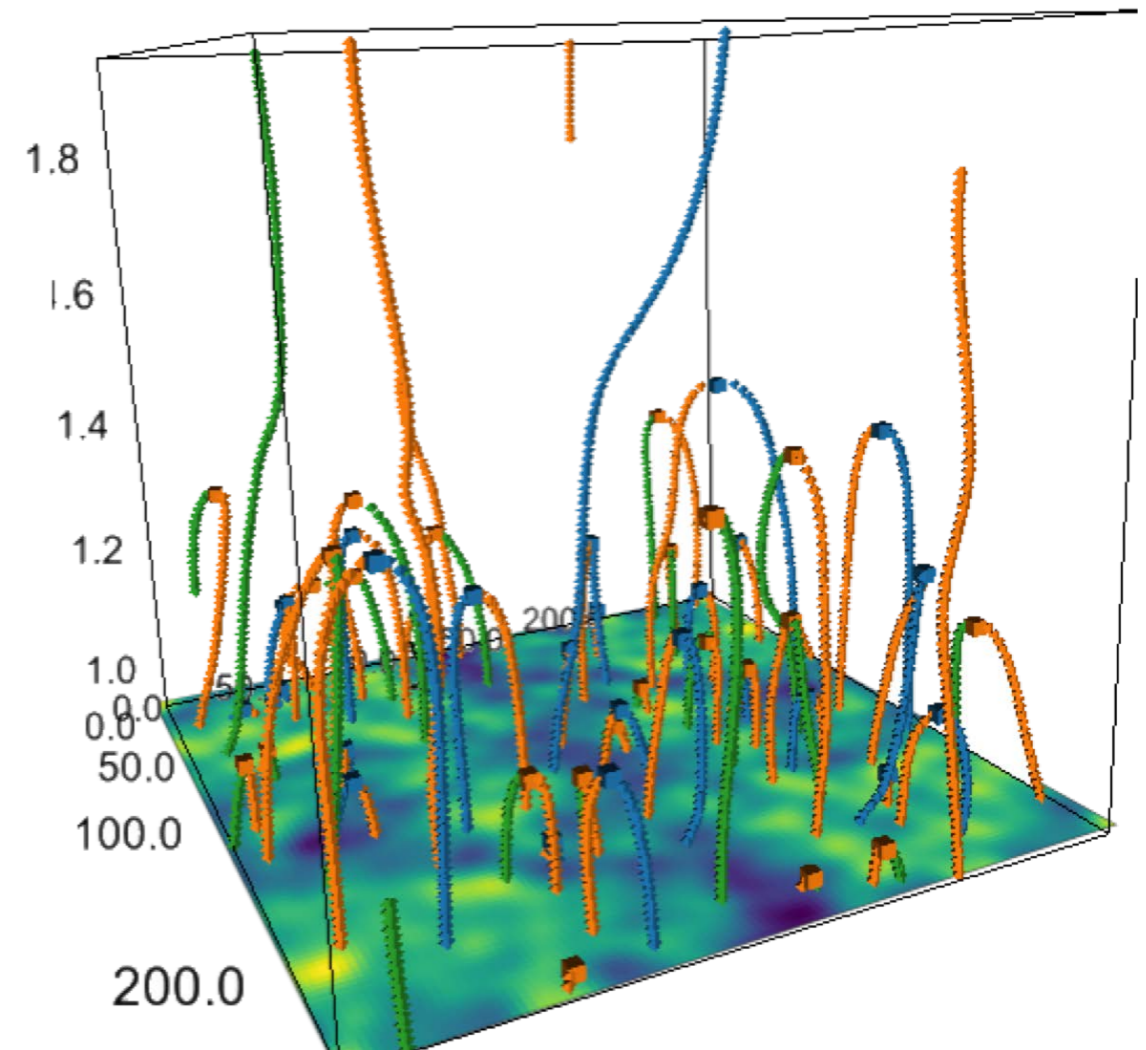


2D outlook

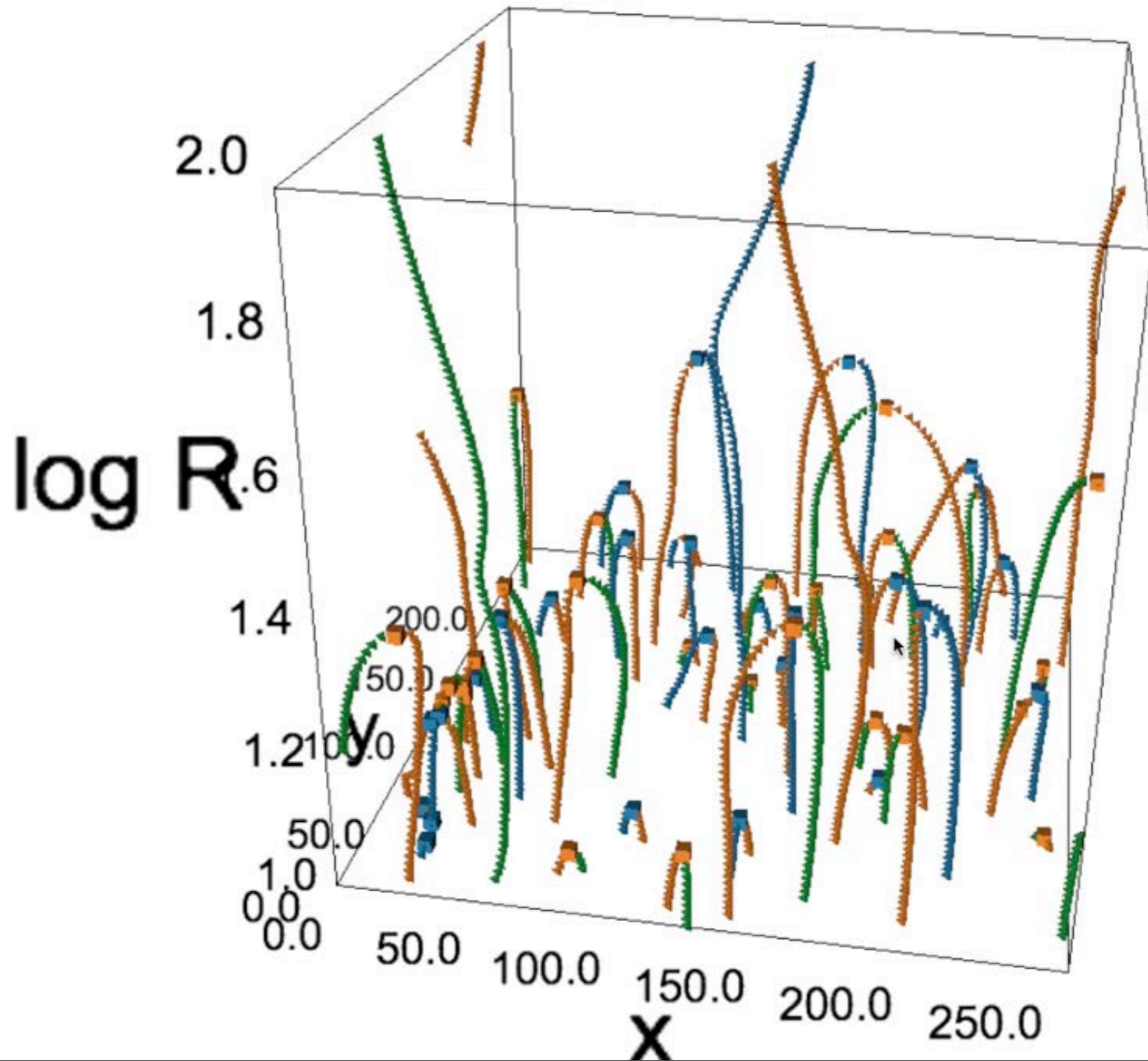
Building the skeleton tree



Increasing smoothing scale

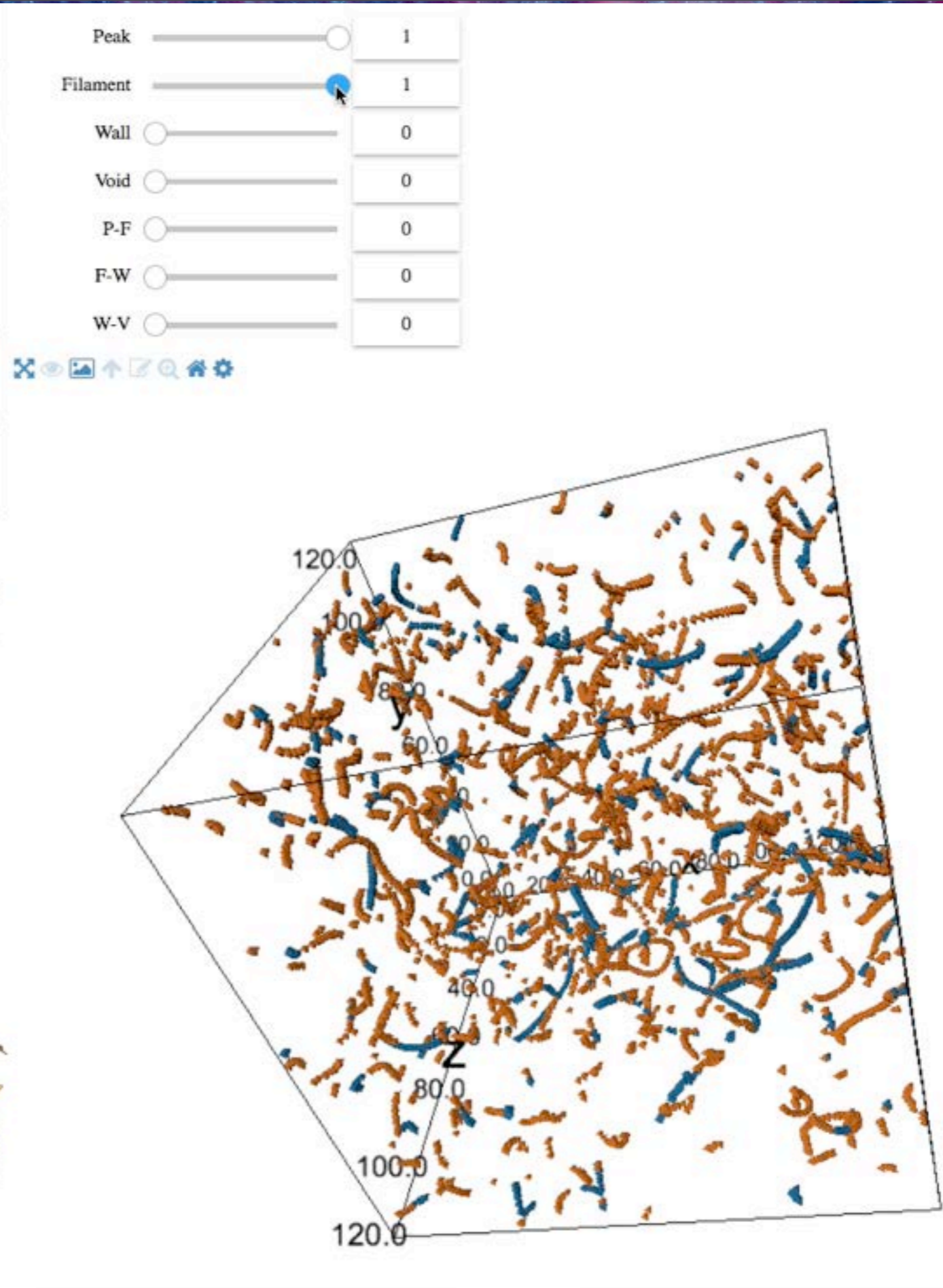
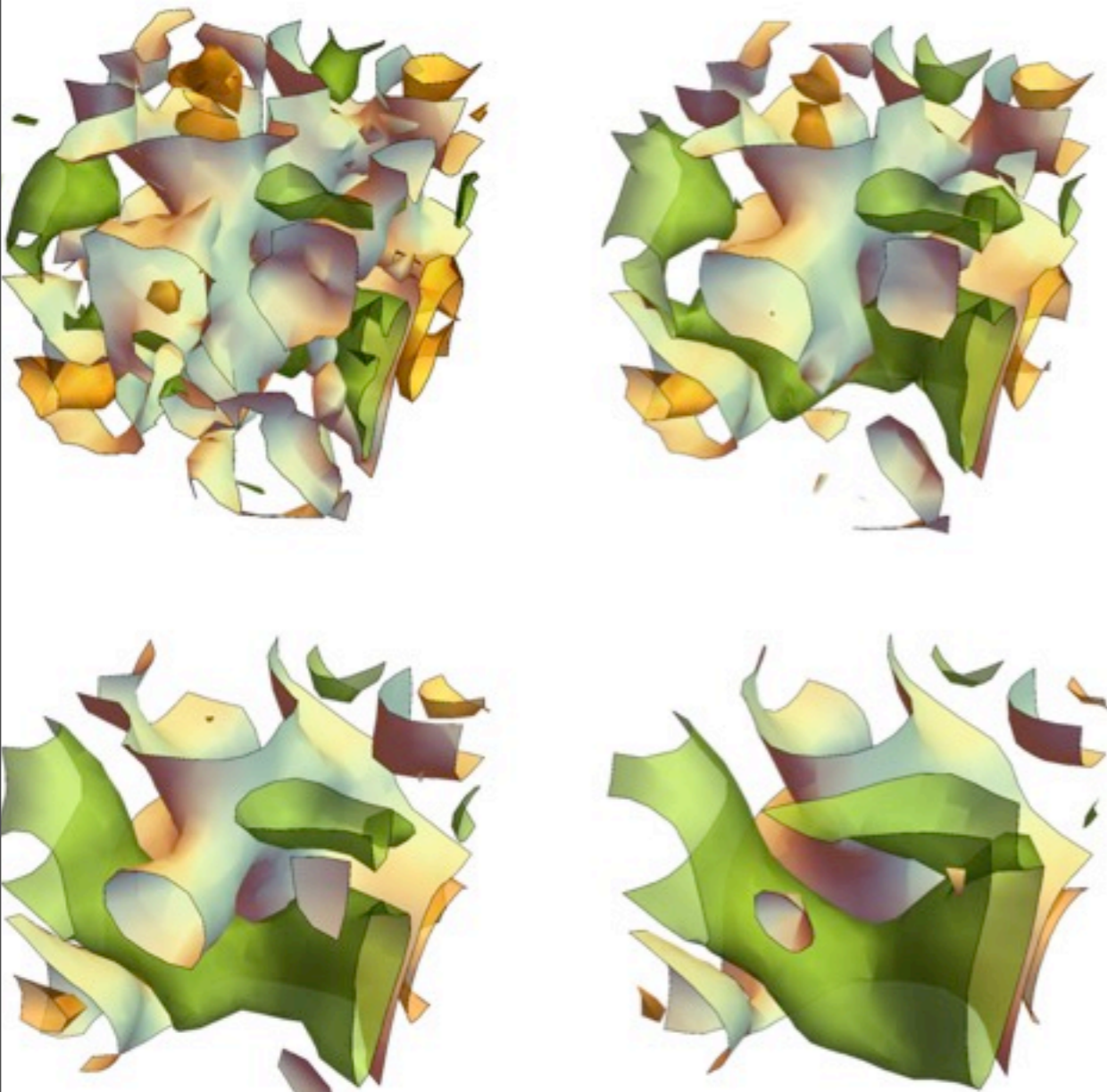


2D outlook

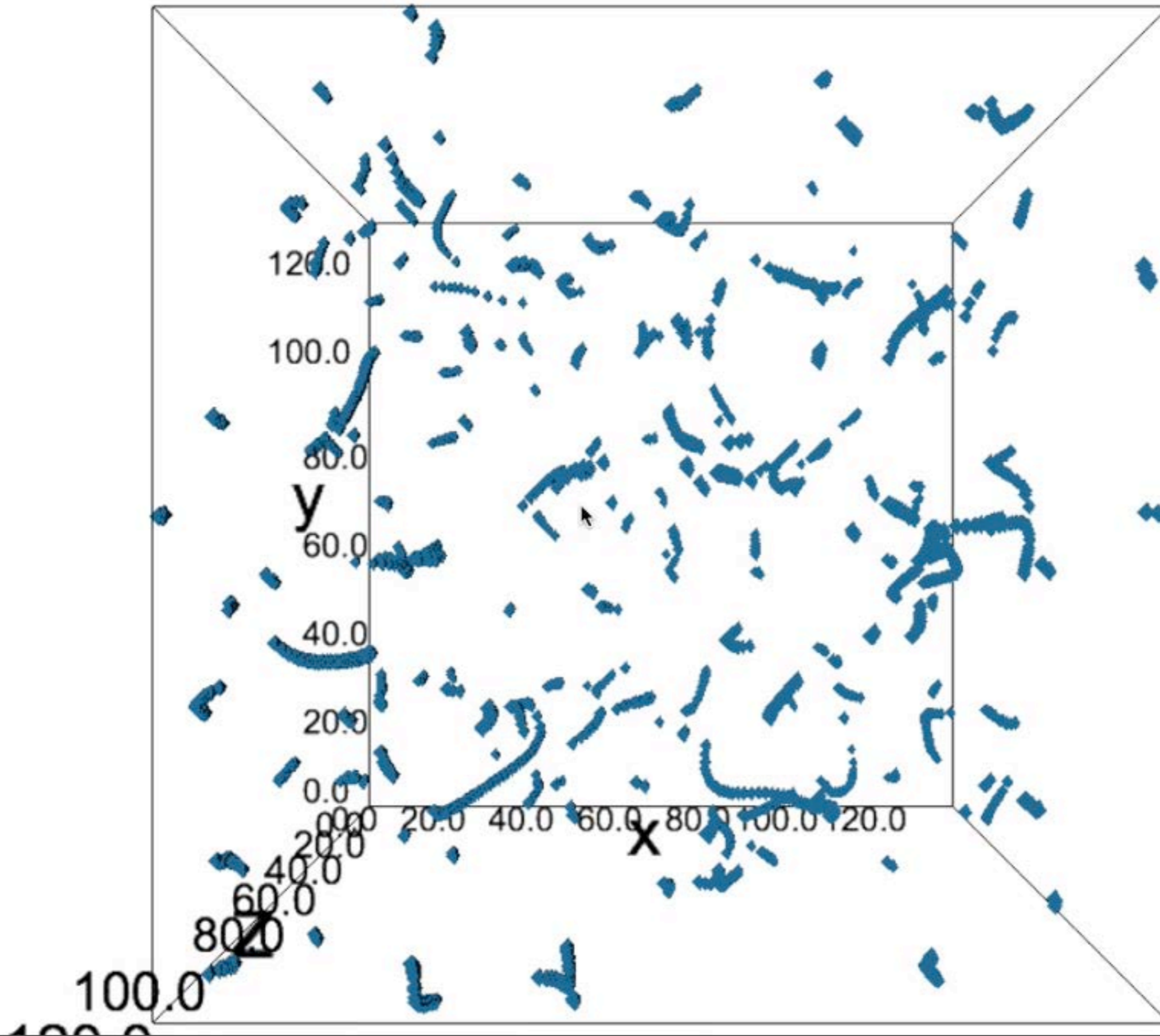


3D outlook

- ▶ GRF smoothed at \neq scales
- ▶ identify critical points
- ▶ build skeleton tree
- ▶ find critical events



3D outlook

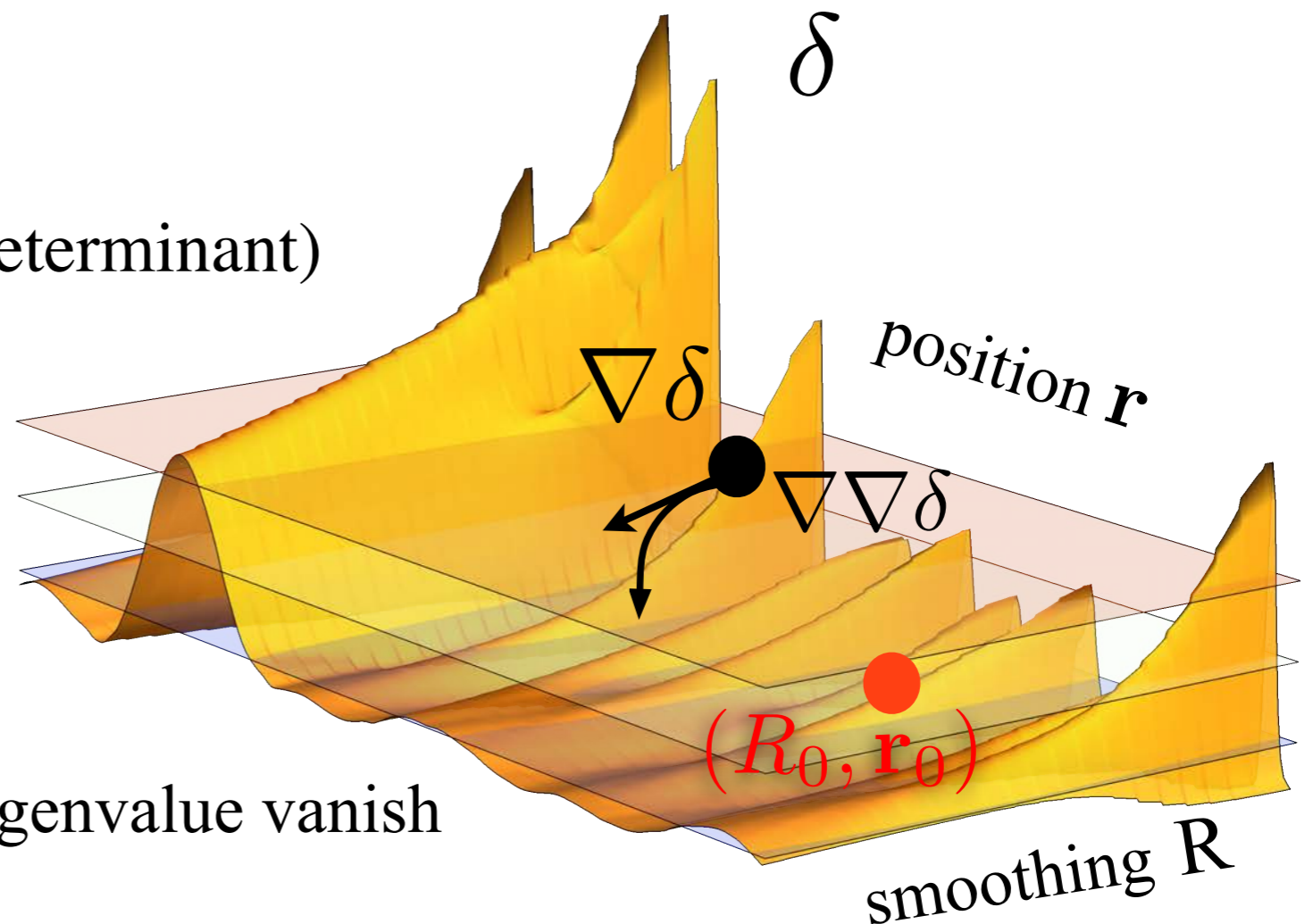


Critical event PDF

$$\frac{\partial^2 \mathcal{N}}{\partial r^3 \partial R} \equiv \langle \delta_D^{(3)}(\mathbf{r} - \mathbf{r}_0) \delta_D(R - R_0) \rangle,$$

where \mathbf{r}_0 is a (double) critical point in real space and R_0 the scale at which the two critical points merge.

- ✓ Invoke ergodicity
- ✓ Change variable to (gradient, determinant)



At (R_0, \mathbf{r}_0) gradient and one eigenvalue vanish

Critical event PDF

$$\frac{\partial^2 \mathcal{N}}{\partial r^3 \partial R} \equiv \langle \delta_{\text{D}}^{(3)}(\mathbf{r} - \mathbf{r}_0) \delta_{\text{D}}(R - R_0) \rangle,$$

where \mathbf{r}_0 is a (double) critical point in real space and R_0 the scale at which the two critical points merge.

$$d(\delta) \equiv \det(\nabla \nabla \delta) = \lambda_1 \lambda_2 \lambda_3$$

$$\frac{\partial^2 \mathcal{N}}{\partial r^3 \partial R} = \left\langle J \delta_{\text{D}}^{(3)}(\nabla \delta) \delta_{\text{D}}(d) \right\rangle$$

$$J(d, \delta) = \begin{vmatrix} \partial_R d & \vec{\nabla} d \\ \partial_R \vec{\nabla} \delta^T & \vec{\nabla} \vec{\nabla} \delta \end{vmatrix}$$

Critical event PDF

$$\frac{\partial^2 \mathcal{N}}{\partial r^3 \partial R} \equiv \langle \delta_D^{(3)}(\mathbf{r} - \mathbf{r}_0) \delta_D(R - R_0) \rangle,$$

where \mathbf{r}_0 is a (double) critical point in real space and R_0 the scale at which the two critical points merge.

$$d(\delta) \equiv \det(\nabla \nabla \delta) = \lambda_1 \lambda_2 \lambda_3$$

$$\frac{\partial^2 \mathcal{N}}{\partial r^3 \partial R} = \left\langle J \delta_D^{(3)}(\nabla \delta) \delta_D(d) \right\rangle$$

$$J(d, \delta) = \begin{vmatrix} \partial_R d & \vec{\nabla} d \\ \partial_R \vec{\nabla} \delta^T & \vec{\nabla} \vec{\nabla} \delta \end{vmatrix} = \begin{vmatrix} \partial_R d & \vec{\nabla} d \\ -R \vec{\nabla} \Delta \delta^T & \vec{\nabla} \vec{\nabla} \delta \end{vmatrix},$$

for a Gaussian filter

$$\partial_R \delta = -R \Delta \delta$$

Critical event PDF

$$\frac{\partial^2 \mathcal{N}}{\partial r^3 \partial R} \equiv \langle \delta_D^{(3)}(\mathbf{r} - \mathbf{r}_0) \rangle$$

where \mathbf{r}_0 is a (double) critical point at which the two critical points meet.

$$d(\delta) \equiv \det(\nabla \nabla \delta)$$

$$\begin{aligned} \frac{J(d, \delta)}{\sigma_1 \sigma_2^4 \sigma_3} &= |x_{11} x_{22}| \begin{vmatrix} \partial_R x_{33} & x_{33i} \\ \partial_R x_i & x_{ij} \end{vmatrix}, \\ &= |x_{11} x_{22}| \begin{vmatrix} \partial_R x_{33} & x_{133} & x_{233} & x_{333} \\ \partial_R x_1 & x_{11} & 0 & 0 \\ \partial_R x_2 & 0 & x_{22} & 0 \\ \partial_R x_3 & 0 & 0 & 0 \end{vmatrix} \\ &= |x_{11} x_{22}|^2 |\partial_R x_3| |x_{333}|, \end{aligned}$$

$$\frac{\partial^2 \mathcal{N}}{\partial r^3 \partial R} = \left\langle J \delta_D^{(3)}(\nabla \delta) \delta_D(d) \right\rangle$$

$$x \equiv \frac{\delta}{\sigma_0}, x_k \equiv \frac{\nabla_k \delta}{\sigma_1}, x_{kl} \equiv \frac{\nabla_k \nabla_l \delta}{\sigma_2}, x_{klm} \equiv \frac{\nabla_m \nabla_l \nabla_k \delta}{\sigma_3}$$

$$J(d, \delta) = \begin{vmatrix} \partial_R d & \vec{\nabla} d \\ \partial_R \vec{\nabla} \delta^T & \vec{\nabla} \vec{\nabla} \delta \end{vmatrix} = \begin{vmatrix} \partial_R d & \vec{\nabla} d \\ -R \vec{\nabla} \Delta \delta^T & \vec{\nabla} \vec{\nabla} \delta \end{vmatrix},$$

for a Gaussian filter

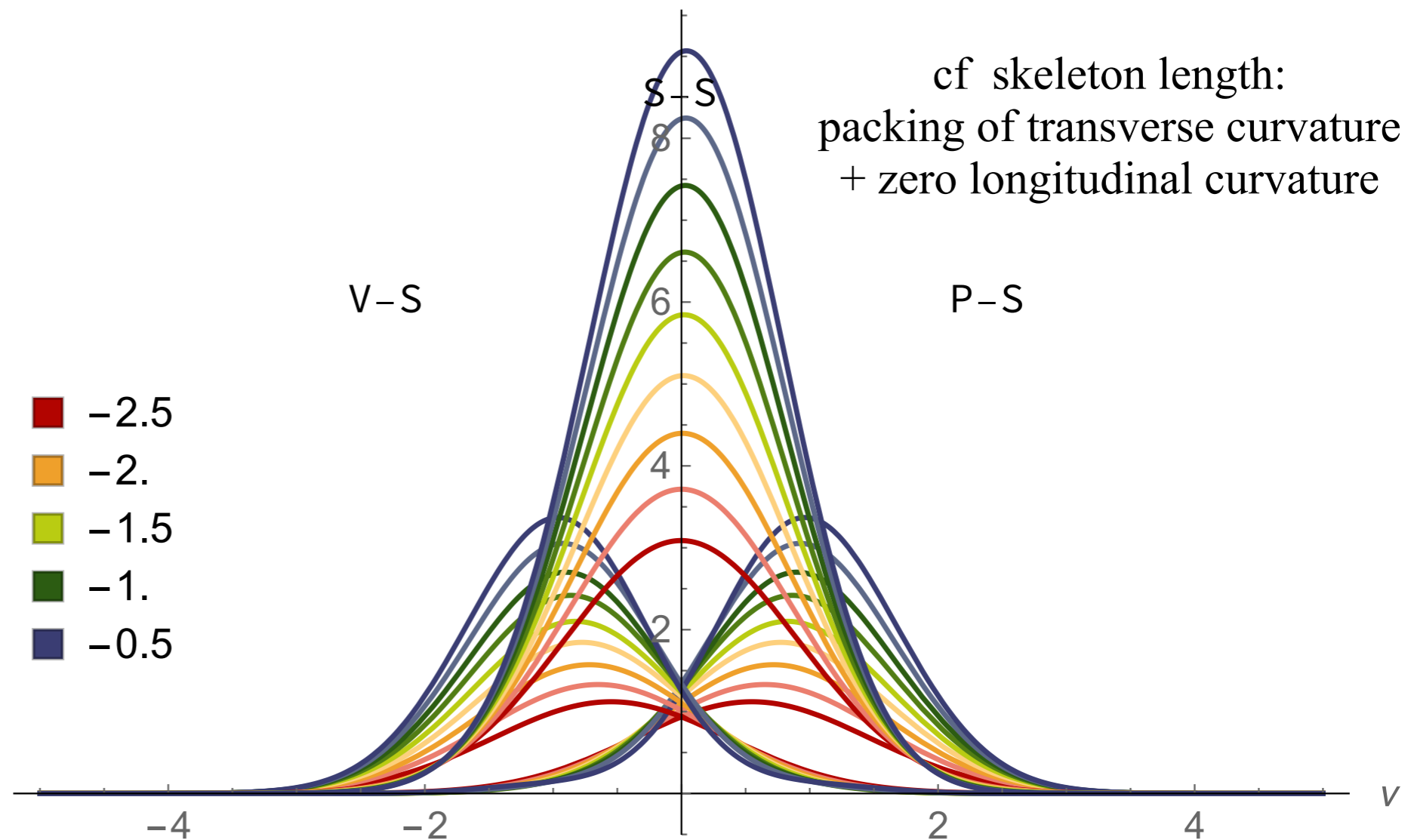
$$\partial_R \delta = -R \Delta \delta$$

Derivation

$$\frac{\partial^2 n}{\partial R \partial \nu} = \frac{\partial^5 \mathcal{N}}{\partial r^3 \partial R \partial \nu},$$

$$= \frac{R \left\langle |x_{11} x_{22} |x_{3ii} |x_{333} | \delta_D^{(3)}(x_i) \delta_D(x_{33}) \delta_D(x - \nu) \right\rangle}{\tilde{R} R_*^3 \tilde{R}},$$

$10^3 \times R^4 \partial^4 \mathcal{N} / \partial r^3 \partial R$



Derivation

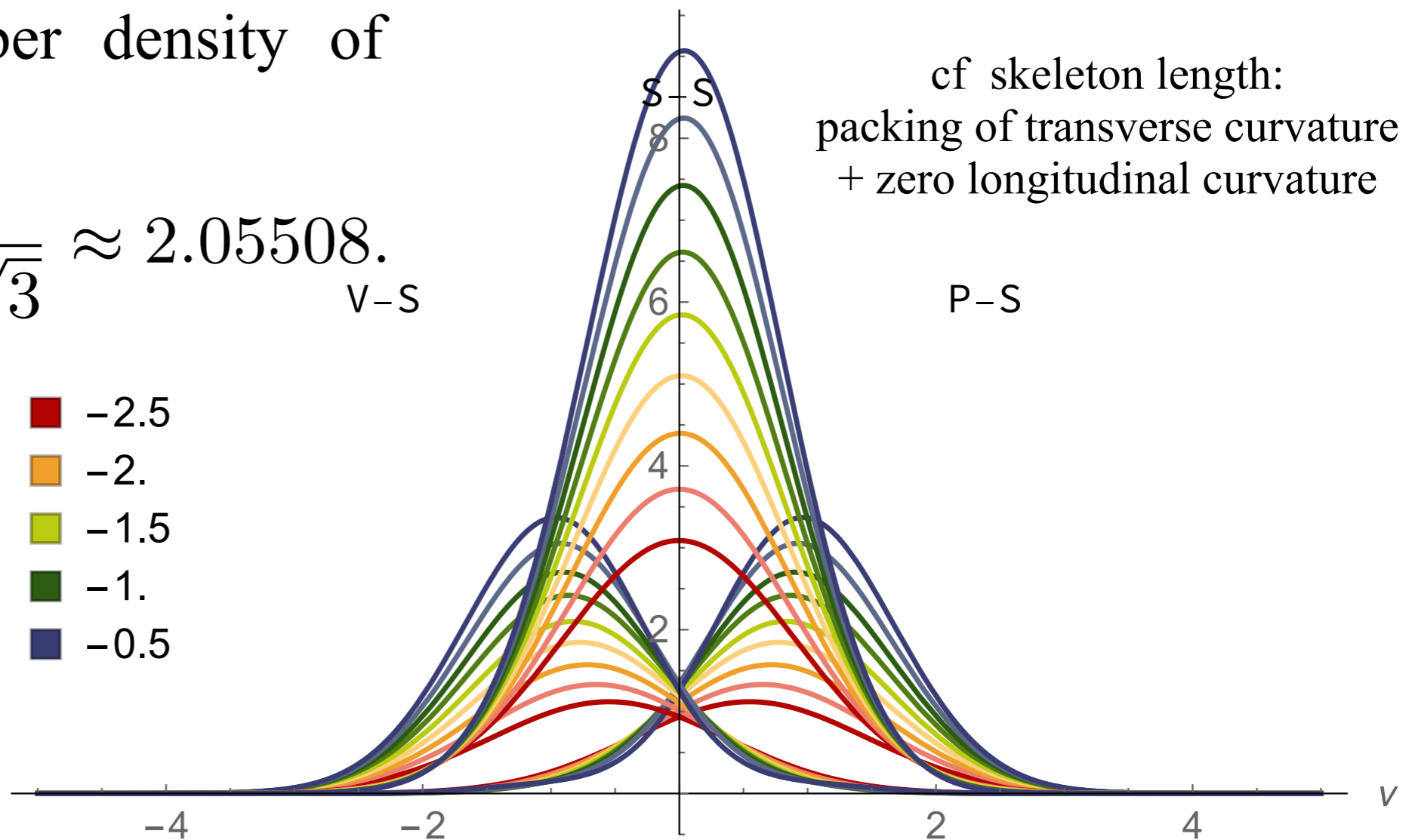
$$\frac{\partial^2 n}{\partial R \partial \nu} = \frac{\partial^5 \mathcal{N}}{\partial r^3 \partial R \partial \nu},$$

$$= \frac{R \left\langle |x_{11} x_{22} |x_{3ii} |x_{333} | \delta_D^{(3)}(x_i) \delta_D(x_{33}) \delta_D(x - \nu) \right\rangle}{\tilde{R} R_*^3 \tilde{R}},$$

E.g. number density of peak-filament mergers to the number density of filament-wall mergers

$$r_{2/1} = \frac{24\sqrt{3}}{29\sqrt{2} - 12\sqrt{3}} \approx 2.05508.$$

- -2.5
- -2.
- -1.5
- -1.
- -0.5



Derivation

$$\frac{\partial^2 n}{\partial R \partial \nu} = \frac{\partial^5 \mathcal{N}}{\partial r^3 \partial R \partial \nu},$$

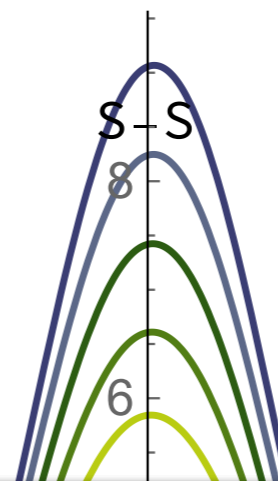
$$= \frac{R \left\langle |x_{11} x_{22} |x_{3ii} |x_{333} | \delta_D^{(3)}(x_i) \delta_D(x_{33}) \delta_D(x - \nu) \right\rangle}{\tilde{R} R_*^3 \tilde{R}},$$

E.g. number density of peak-filament mergers to the number density of filament-wall mergers

$$r_{2/1} = \frac{24\sqrt{3}}{29\sqrt{2} - 12\sqrt{3}} \approx 2.05508.$$

V-S

$10^3 \times R^4 \partial^4 \mathcal{N} / \partial r^3 \partial R$

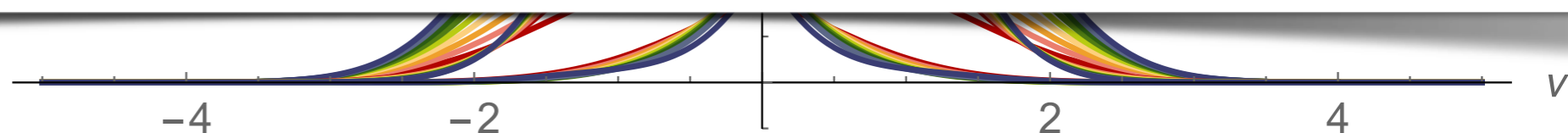


cf skeleton length:
packing of transverse curvature
+ zero longitudinal curvature

$$\frac{1}{8\sqrt{5}\pi^{3/2}(6-5\gamma^2)^4(5\gamma^2-9)^5} e^{2(\gamma^2-1)} \left(-8\sqrt{\pi}(6-5\gamma^2)^{7/2}(5\gamma^2-9)^5 e^{\frac{\gamma^2 v^2}{10\gamma^4-22\gamma^2+12}} + 60\gamma(6-5\gamma^2)^4 \sqrt{2-2\gamma^2}(5\gamma^2-9)v(275\gamma^4+30\gamma^2(2v^2-23)+351) - \right.$$

$$\left. 2\sqrt{\pi}(6-5\gamma^2)^4 \sqrt{9-5\gamma^2} e^{\frac{2\gamma^2 v^2}{5\gamma^4-14\gamma^2+9}} (3600\gamma^4 v^4 + 120\gamma^2(5\gamma^2-9)(35\gamma^2-27)v^2 + (9-5\gamma^2)^2(575\gamma^4-1230\gamma^2+783)) - 8\sqrt{\pi}(6-5\gamma^2)^{7/2}(5\gamma^2-9)^5 e^{\frac{\gamma^2 v^2}{10\gamma^4-22\gamma^2+12}} \operatorname{erf}\left(\frac{\gamma v}{\sqrt{2}\sqrt{5\gamma^4-11\gamma^2+6}}\right) - \right.$$

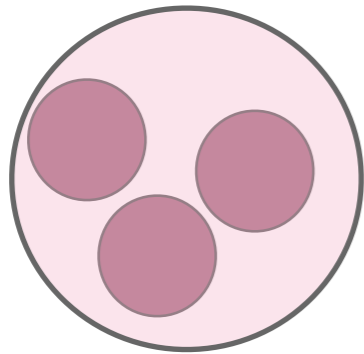
$$\left. 2\sqrt{\pi}(6-5\gamma^2)^4 \sqrt{9-5\gamma^2} e^{\frac{2\gamma^2 v^2}{5\gamma^4-14\gamma^2+9}} (3600\gamma^4 v^4 + 120\gamma^2(5\gamma^2-9)(35\gamma^2-27)v^2 + (9-5\gamma^2)^2(575\gamma^4-1230\gamma^2+783)) \operatorname{erf}\left(\frac{\sqrt{2}\gamma v}{\sqrt{5\gamma^4-14\gamma^2+9}}\right) \right)$$



In (invariant) Hessian frame:

BBKS

extrema

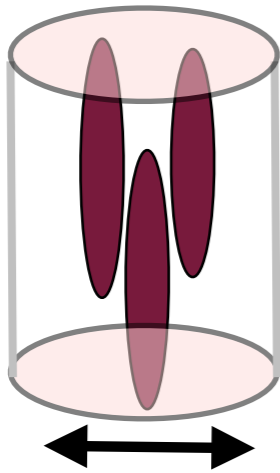


volume $\propto 1/\lambda_1\lambda_2\lambda_3$

packing sphere problem: curvature.

$$n_{\text{ext}} = \int \mathcal{P}(\mathbf{x}) \prod_{1 \leq i \leq 3} \delta_D(x_i) \lambda_i d\mathbf{x}$$

skeleton



section $\propto 1/\lambda_2\lambda_3$

packing tube problem: transverse curvature.

$$n_{\text{skl}} = \int P(\mathbf{x}) \prod_{1 < i \leq 3} \delta_D(x_i) \lambda_i d\mathbf{x} =$$

SPCP

Peak theory: Gaussian predictions

If the field is Gaussian (large scales/early times), the total number density of critical points then reads

2D

$$\langle n_{\max} \rangle = \langle n_{\min} \rangle = \frac{1}{8\sqrt{3}\pi R_{\star}^2}$$

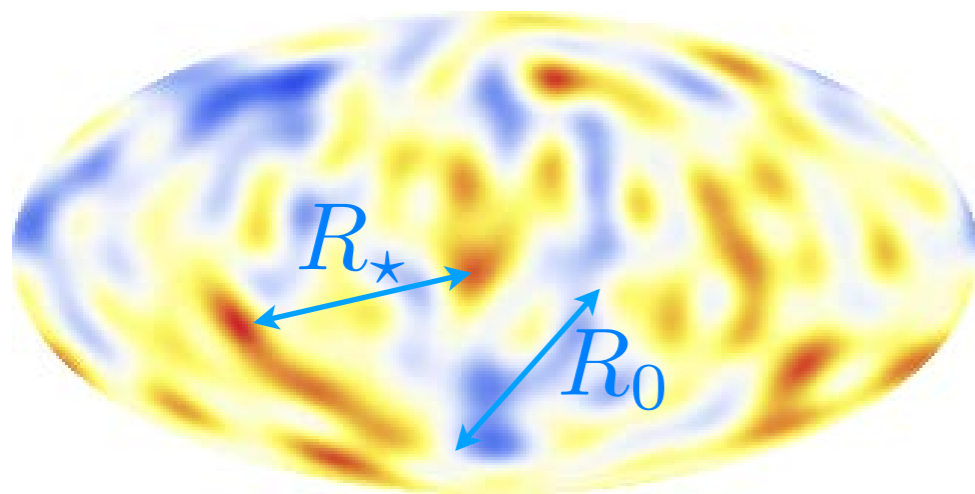
$$\langle n_{\text{sad}} \rangle = \frac{1}{4\sqrt{3}\pi R_{\star}^2}$$

3D

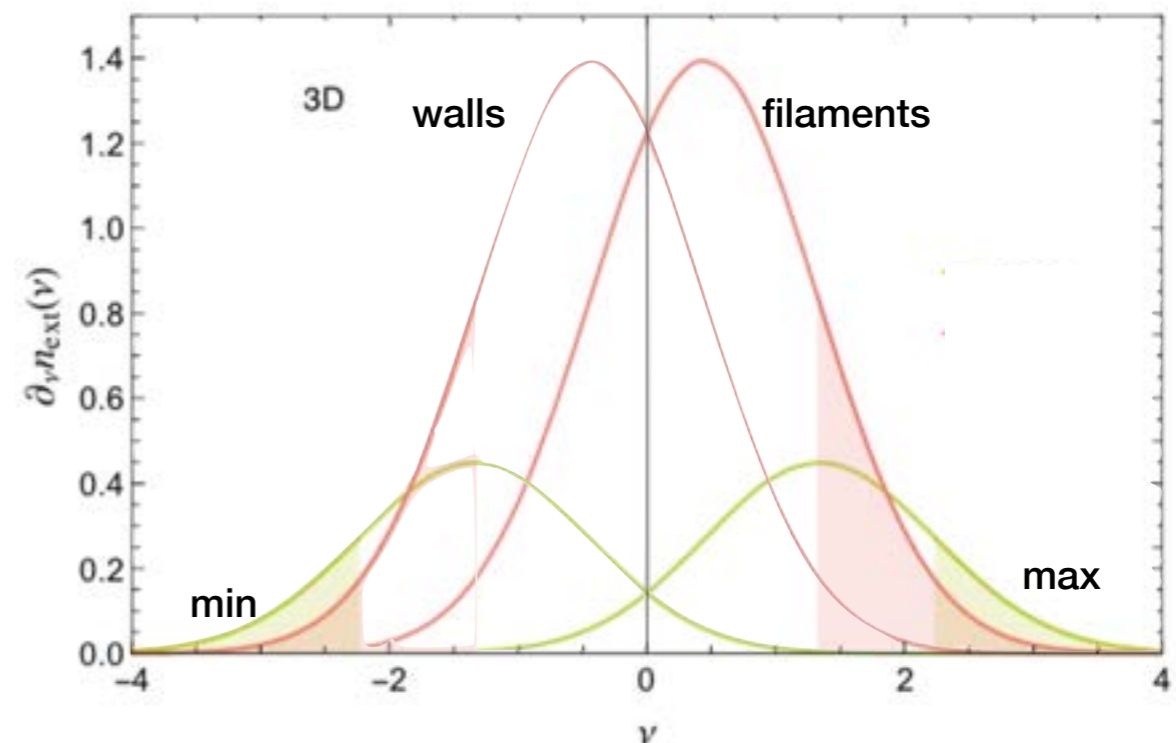
$$\langle n_{\max} \rangle = \langle n_{\min} \rangle = \frac{29\sqrt{15} - 18\sqrt{10}}{1800\pi^2 R_{\star}^3}$$

$$\langle n_{\text{sadf}} \rangle = \langle n_{\text{sadw}} \rangle = \frac{29\sqrt{15} + 18\sqrt{10}}{1800\pi^2 R_{\star}^3},$$

And as a function of peak height (analytical in 2D, not in 3D) :



$R_{\star} = \sigma_1/\sigma_2 =$ distance between peaks



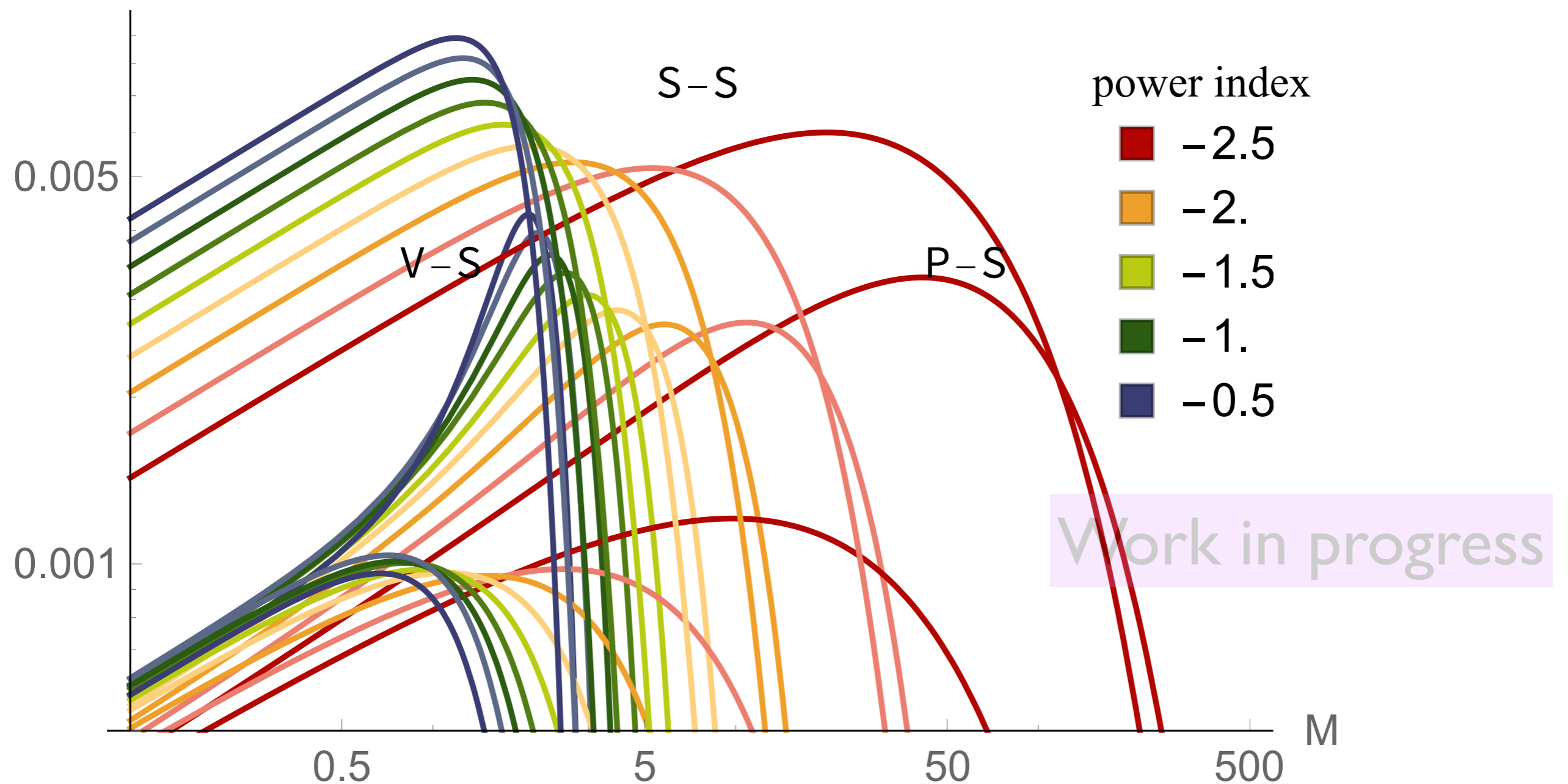
Application: merger rates

Map event count to (z, M)

$$\nu \sigma_0 = \delta_c D(z) \quad \text{where} \quad \delta_c = \frac{3}{20} (12\pi)^{2/3}$$

$\partial^2 n / \partial \log M \partial z$

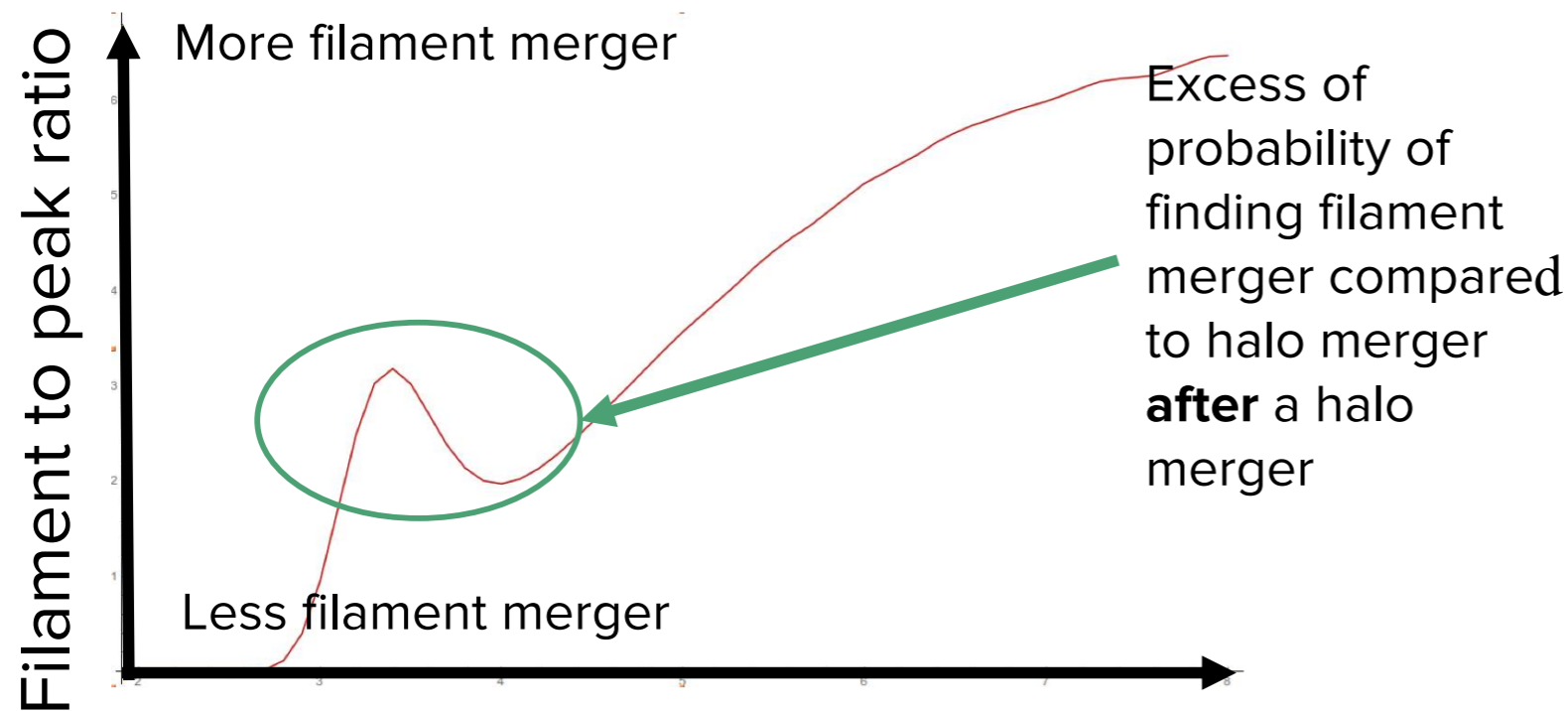
$$\left. \frac{\partial^2 n}{\partial \log M \partial z} \right|_c = \left. \frac{\partial^2 n}{\partial R \partial \nu} \right|_c \delta_c \frac{dD}{dz} \frac{R}{3}$$



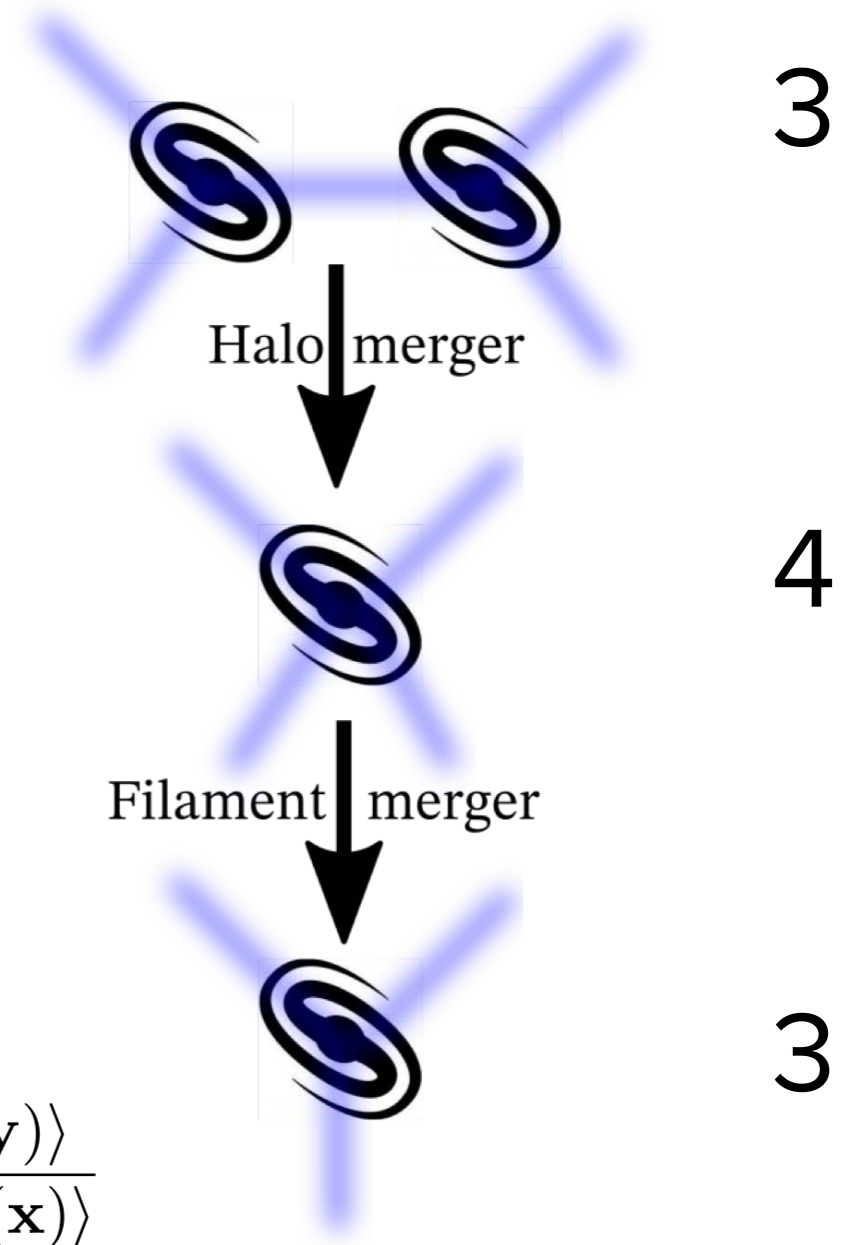
Application: preserving cosmic connectivity

On the connectivity of halos

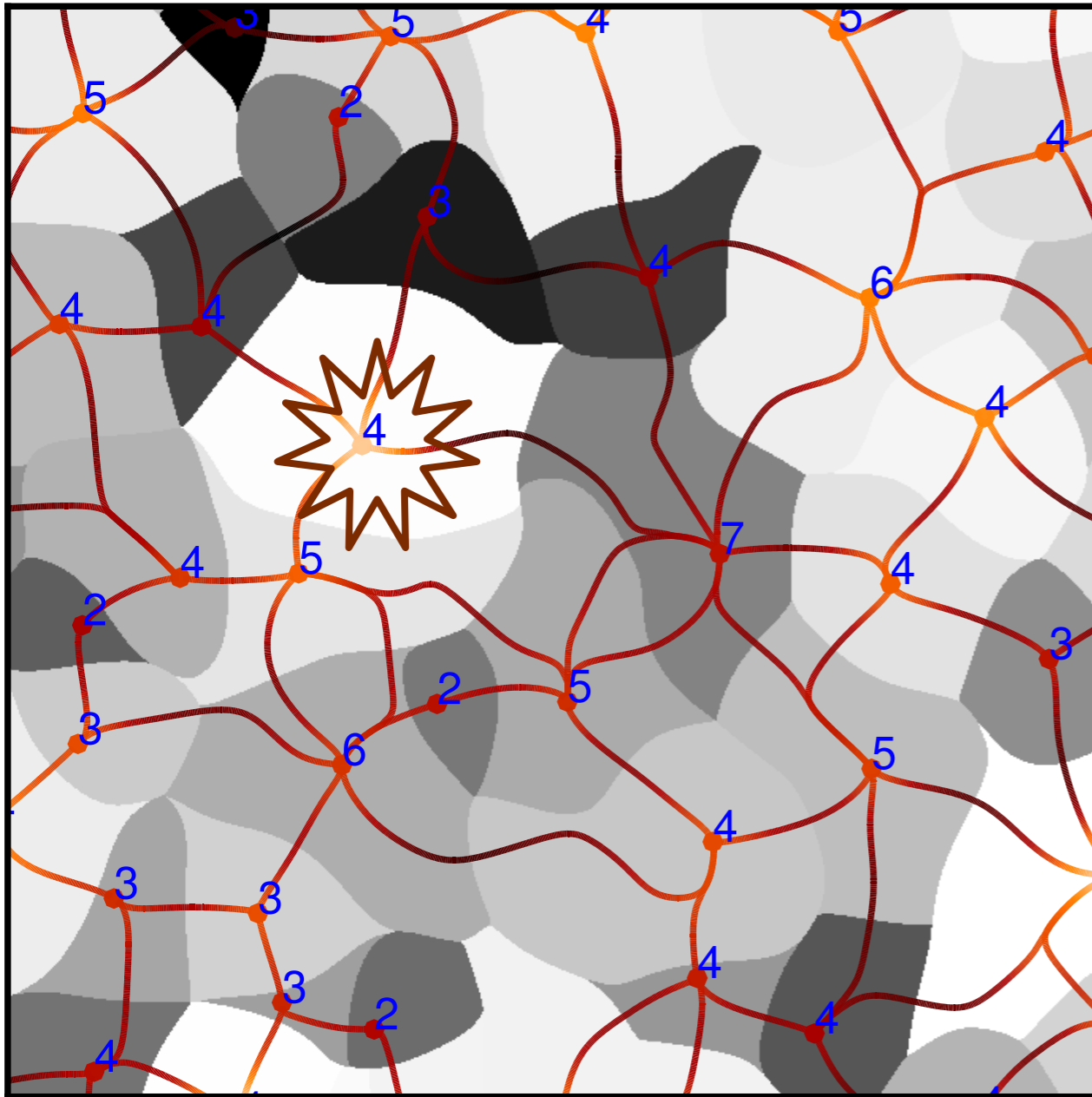
Compute frequency of filament merger compared to halo merger in the vicinity of a halo merger event $\xi_{hf}(r)/\xi_{hh}(r)$.



$$1 + \xi_p = \frac{\langle \text{cond}_p(\mathbf{x}) \text{cond}_p(\mathbf{y}) \rangle}{\langle \text{cond}_p(\mathbf{x}) \rangle^2}, \quad 1 + \xi_f = \frac{\langle \text{cond}_f(\mathbf{x}) \text{cond}_p(\mathbf{y}) \rangle}{\langle \text{cond}_f(\mathbf{x}) \rangle \langle \text{cond}_p(\mathbf{x}) \rangle}$$

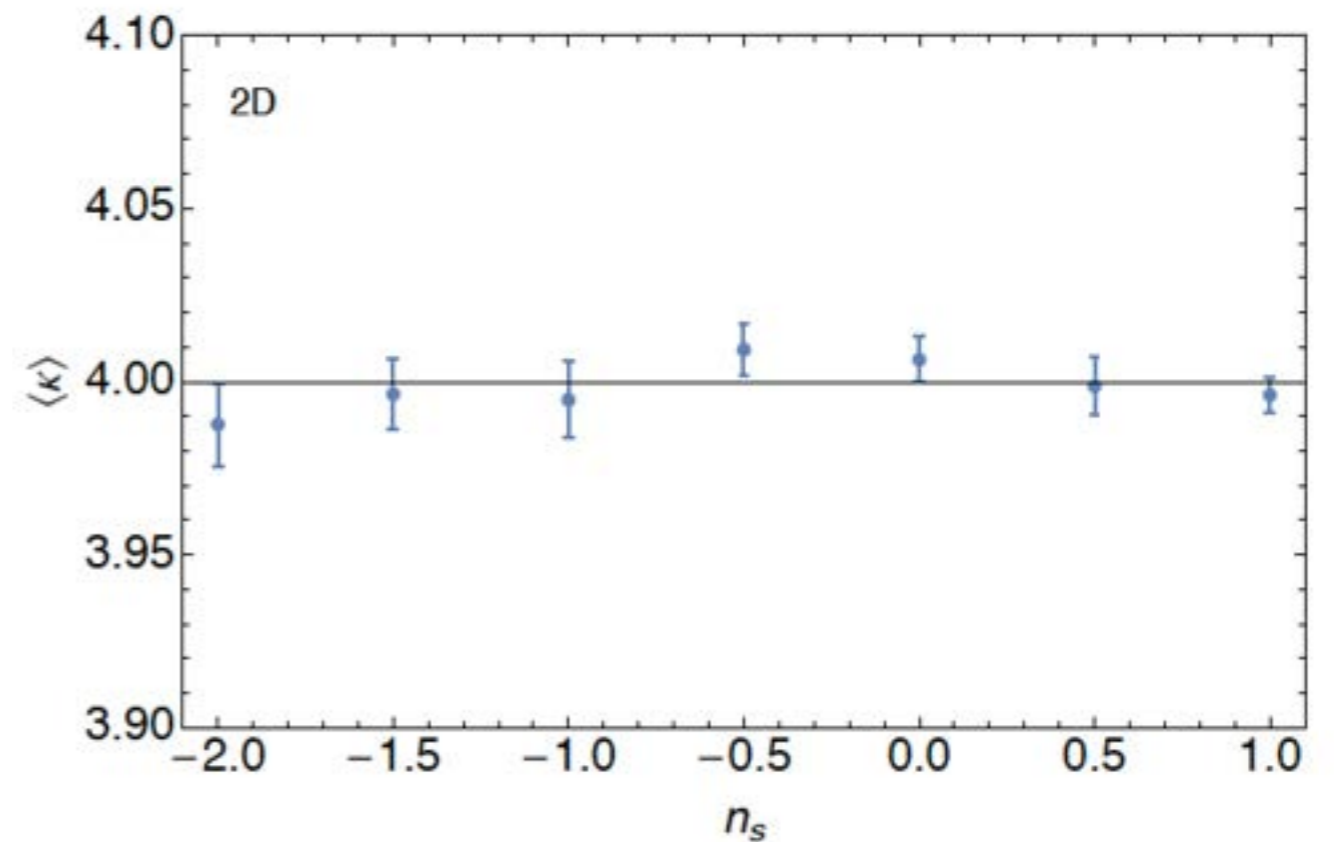


Global connectivity for GRF



How many filaments connect to a node?

Number of connected saddles are measured using the **Disperse** skeleton algorithm (Sousbie +11) in GRF realisations.

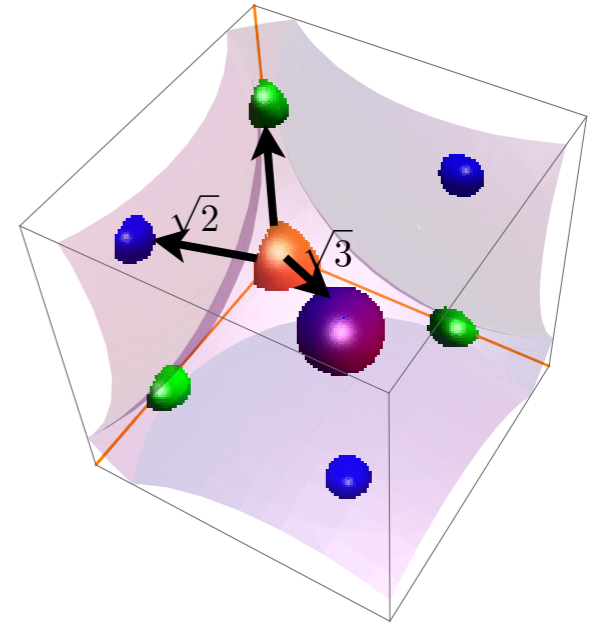


Can we predict the mean connectivity?

Global connectivity for GRF: theory

Because each filament goes through one and only one saddle pt, on average:

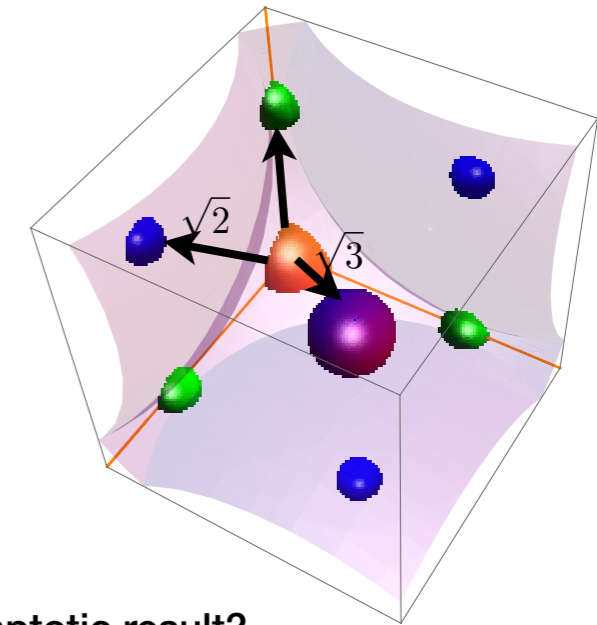
$$\begin{aligned}\langle \kappa \rangle &= \frac{2\bar{n}_{\text{sad}}}{\bar{n}_{\text{max}}} \\ &= 4 \quad \text{in 2D GRF} \\ &= \frac{2(1057 + 348\sqrt{6})}{625} \approx 6.11 \text{ in 3D GRF}\end{aligned}$$



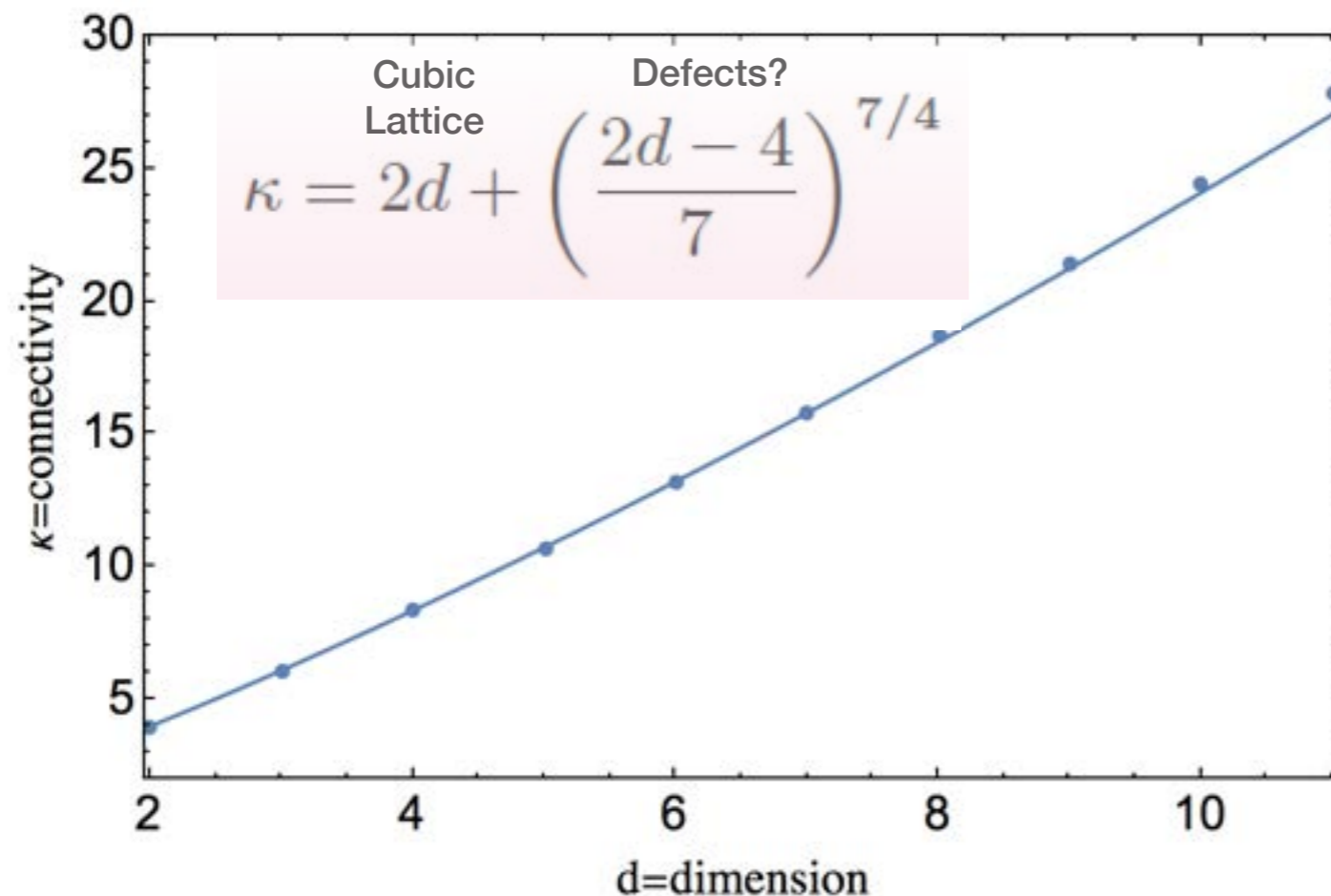
Global connectivity for GRF: theory

Because each filament goes through one and only one saddle pt, on average:

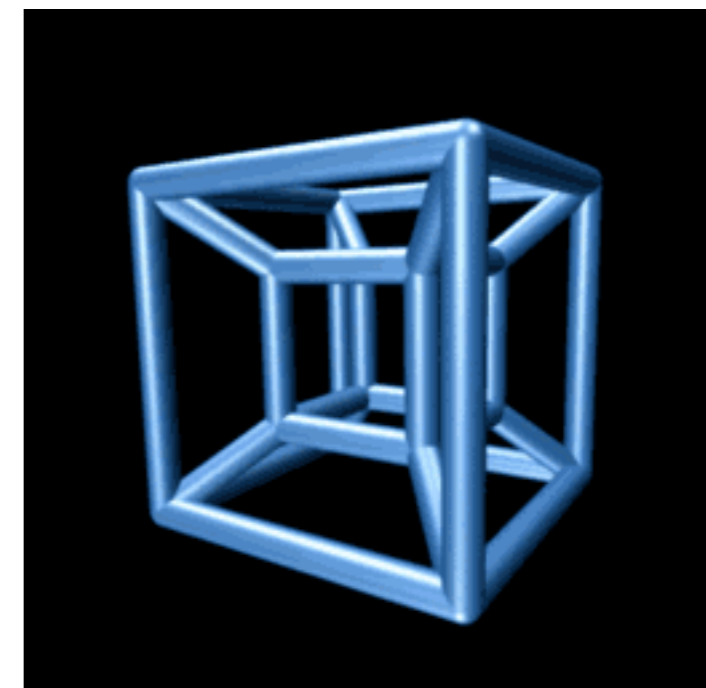
$$\begin{aligned} \langle \kappa \rangle &= \frac{2\bar{n}_{\text{sad}}}{\bar{n}_{\text{max}}} \\ &= 4 \quad \text{in 2D GRF} \\ &= \frac{2(1057 + 348\sqrt{6})}{625} \approx 6.11 \quad \text{in 3D GRF} \end{aligned}$$



In **d dimensions**, (relying on numerical integrations):



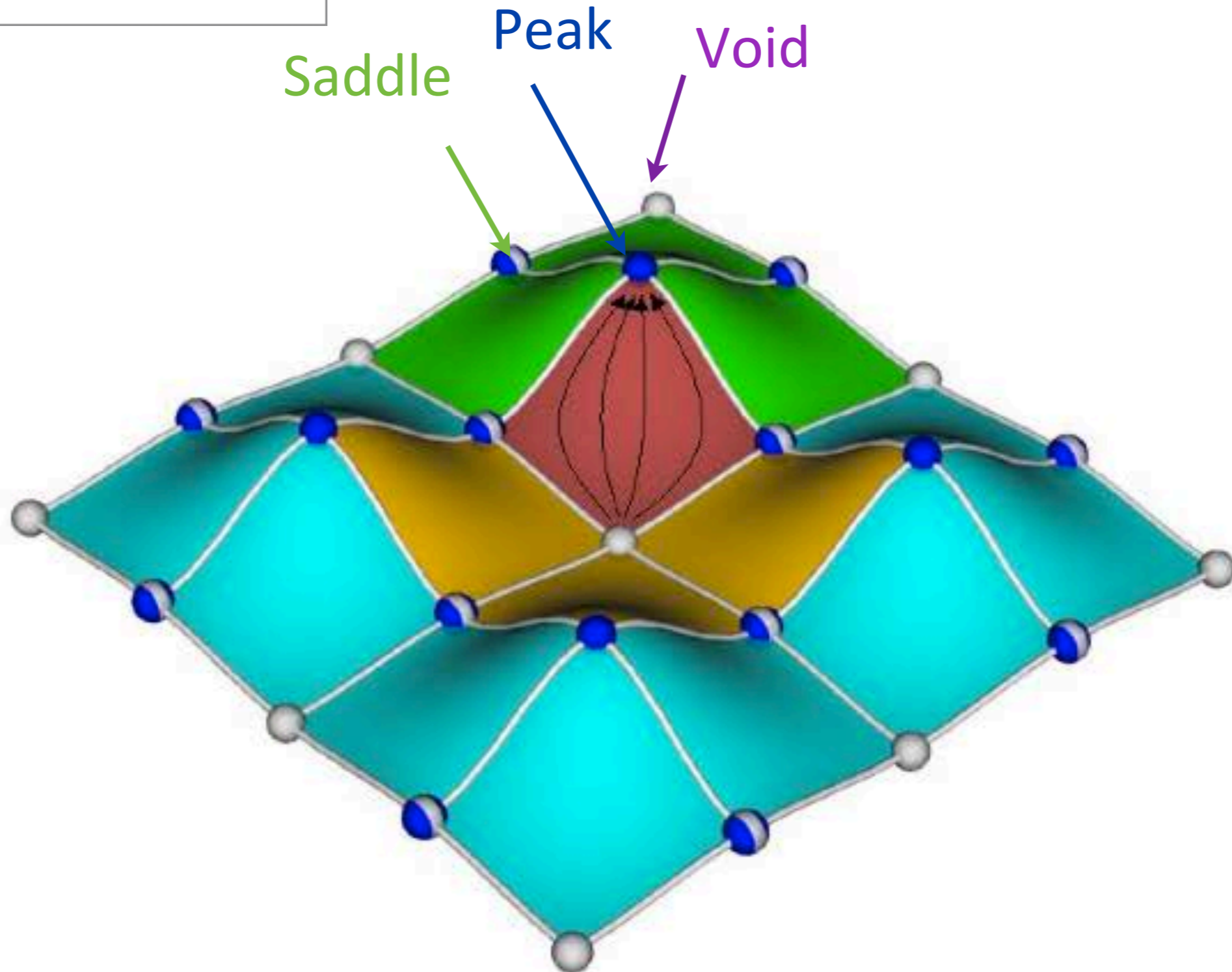
Asymptotic result?



2D connectivity: topology

2D "ideal" cosmic environment :

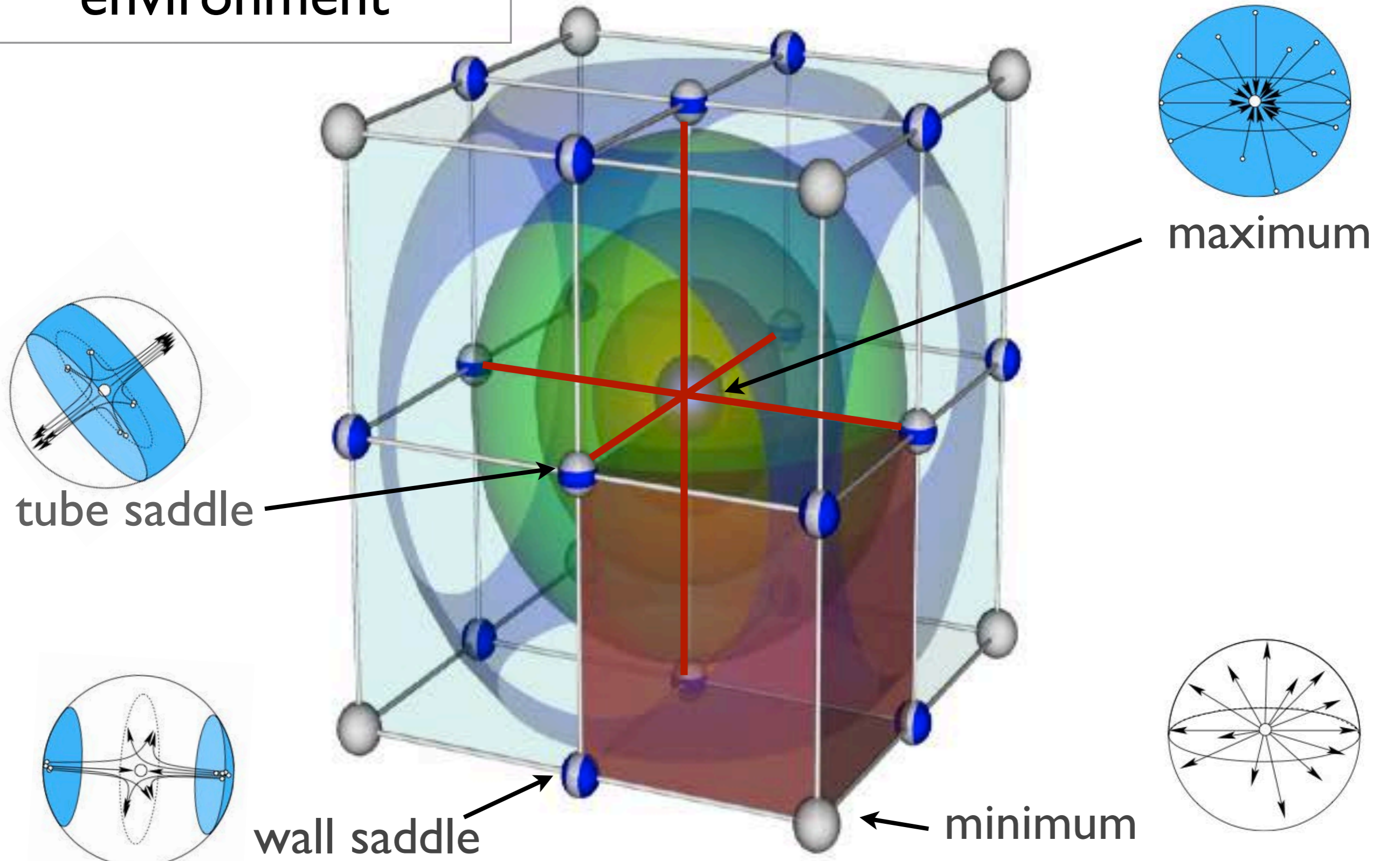
Mean local cosmic initial condition
homeomorphic to such crystal



3D connectivity: topology

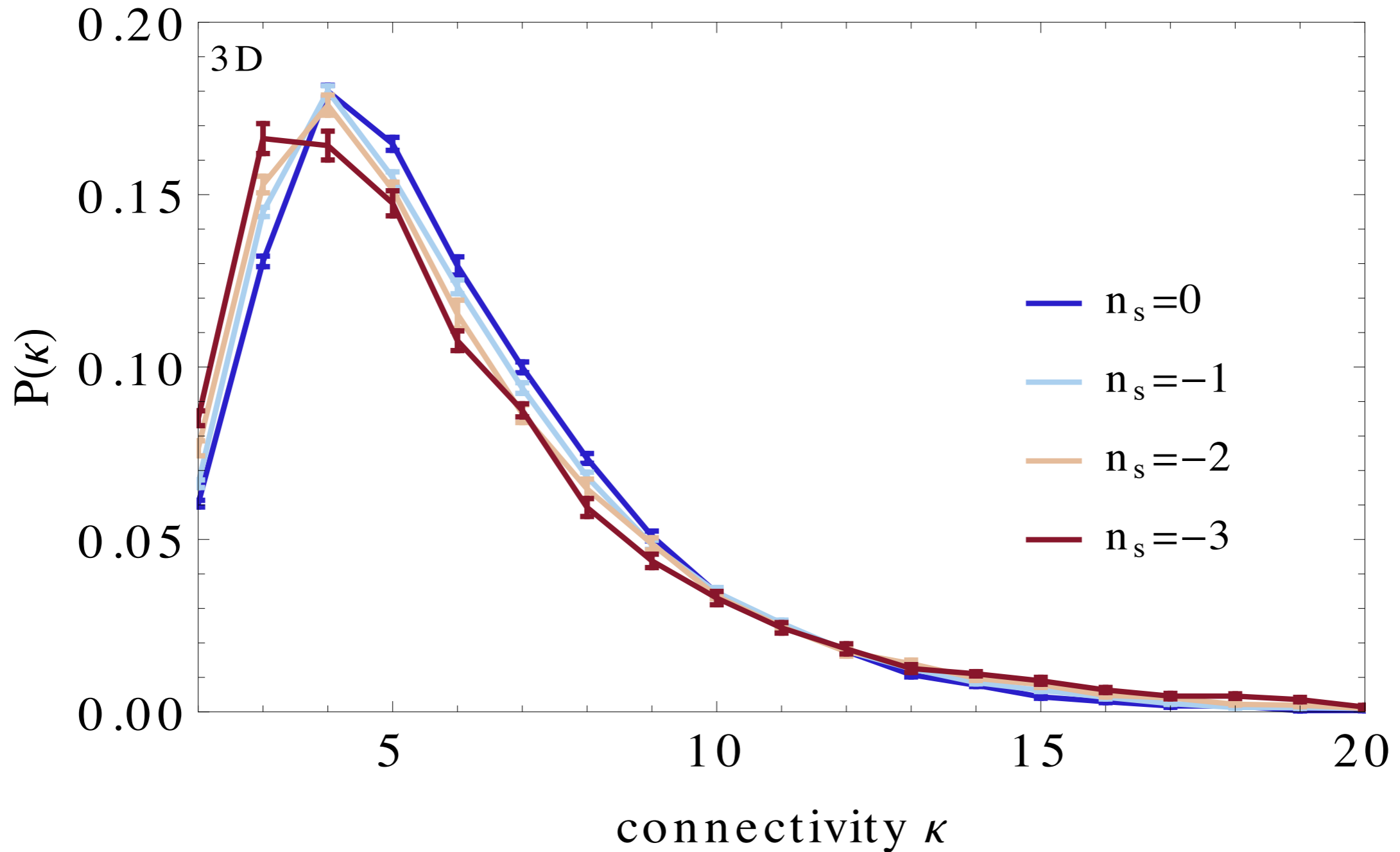
3D "ideal" cosmic environment

Mean local cosmic field **quasi homeomorphic** to such crystal



GRF connectivity PDF: dependence with scale/ n_s

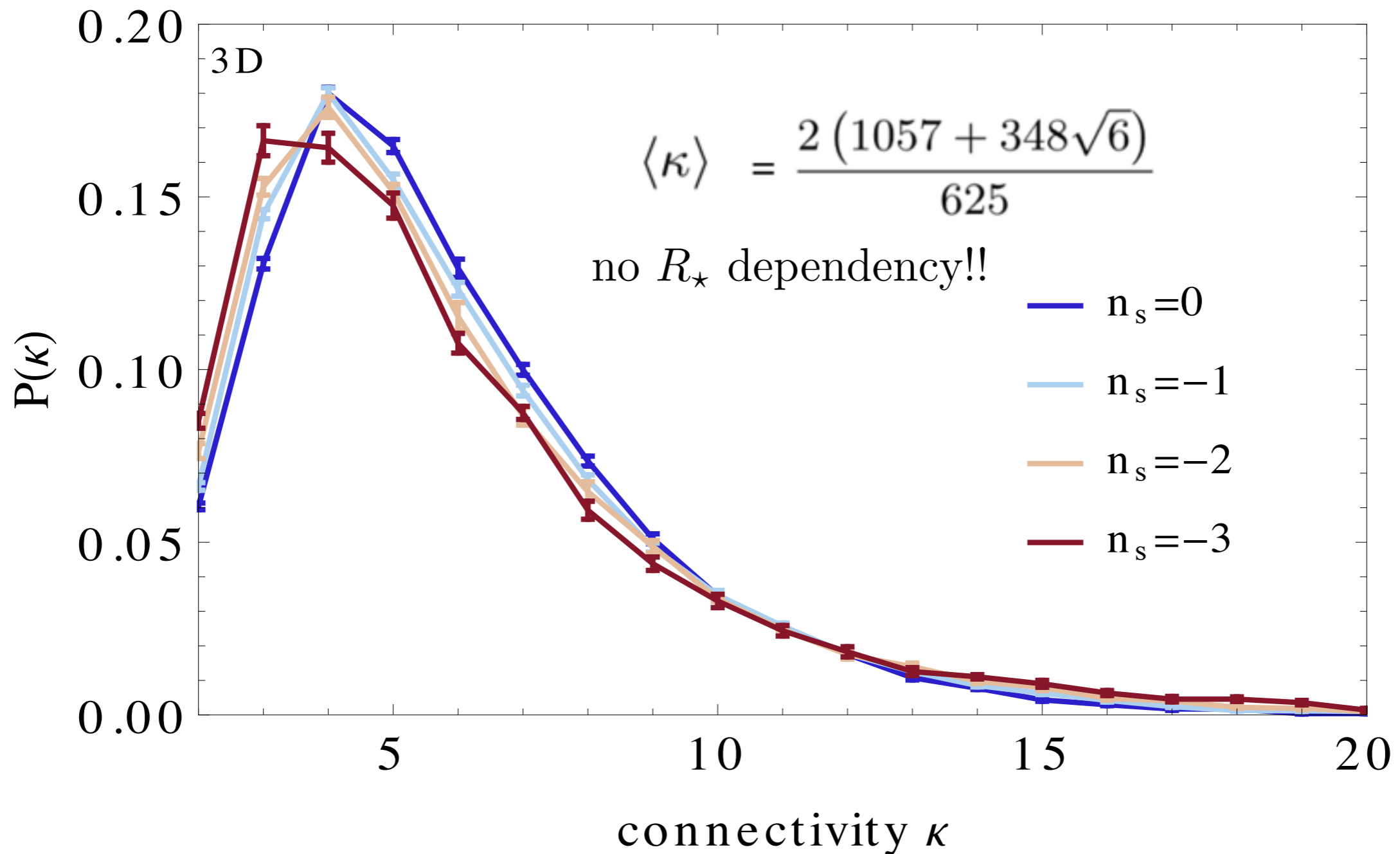
Full distribution of connectivity:



Weak dependency on n_s

GRF connectivity PDF: dependence with scale/ n_s

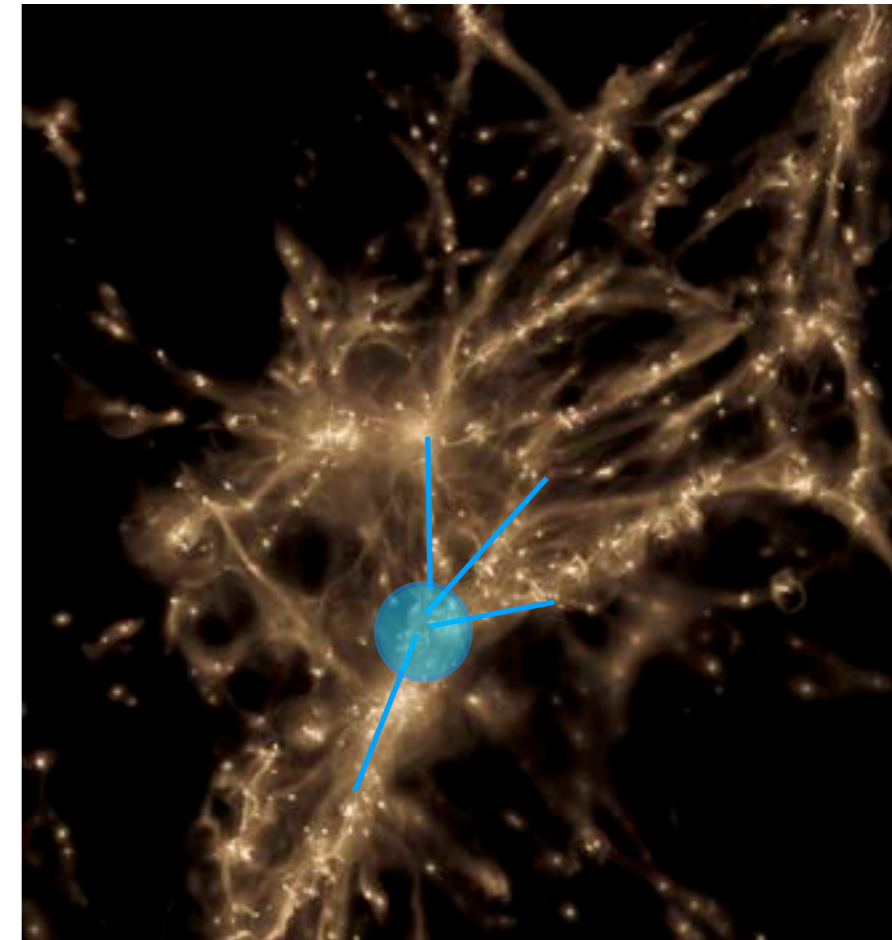
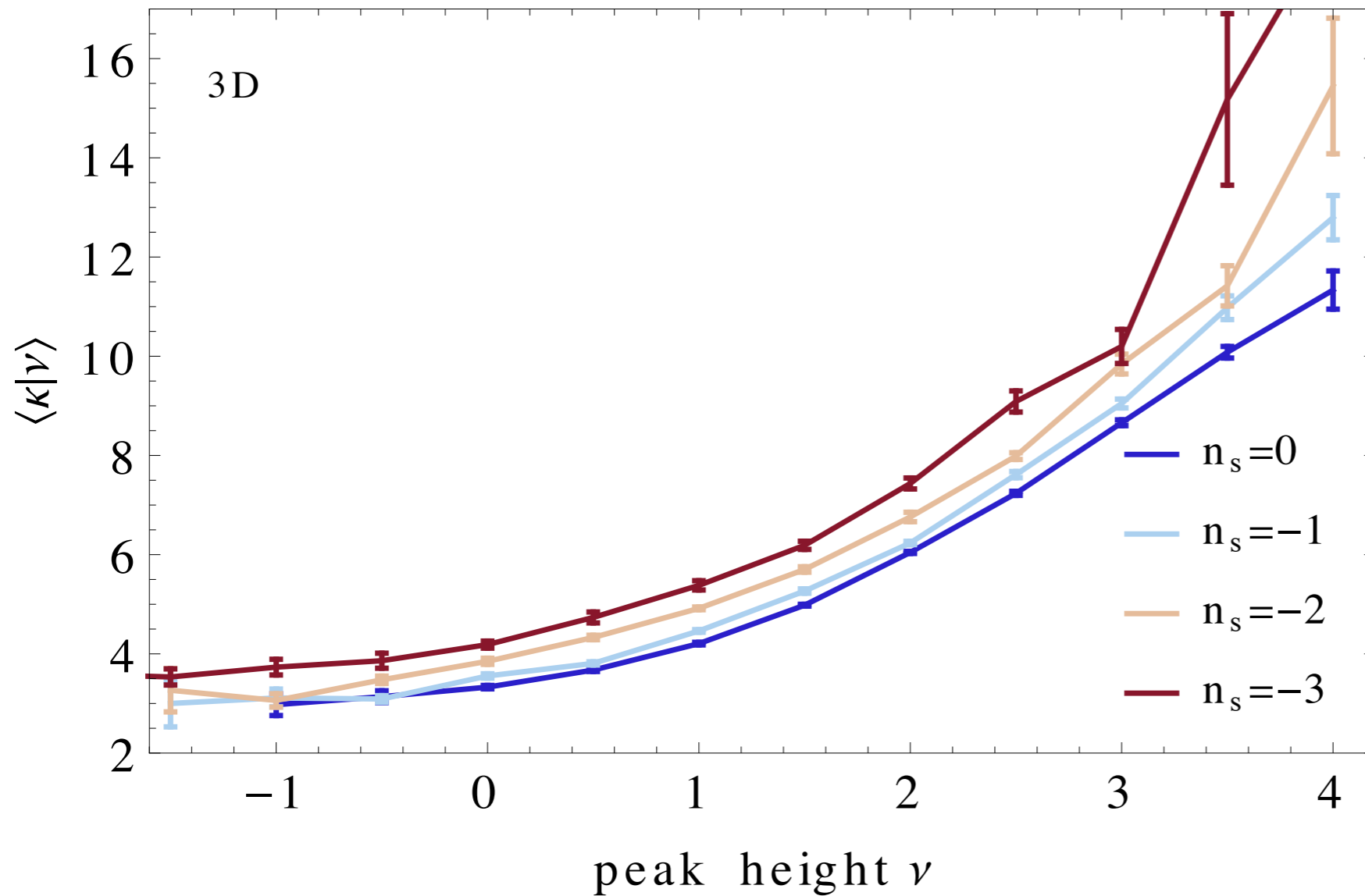
Full distribution of connectivity:



Weak dependency on n_s

GRF connectivity: dependence with peak height

Dependence with peak height:

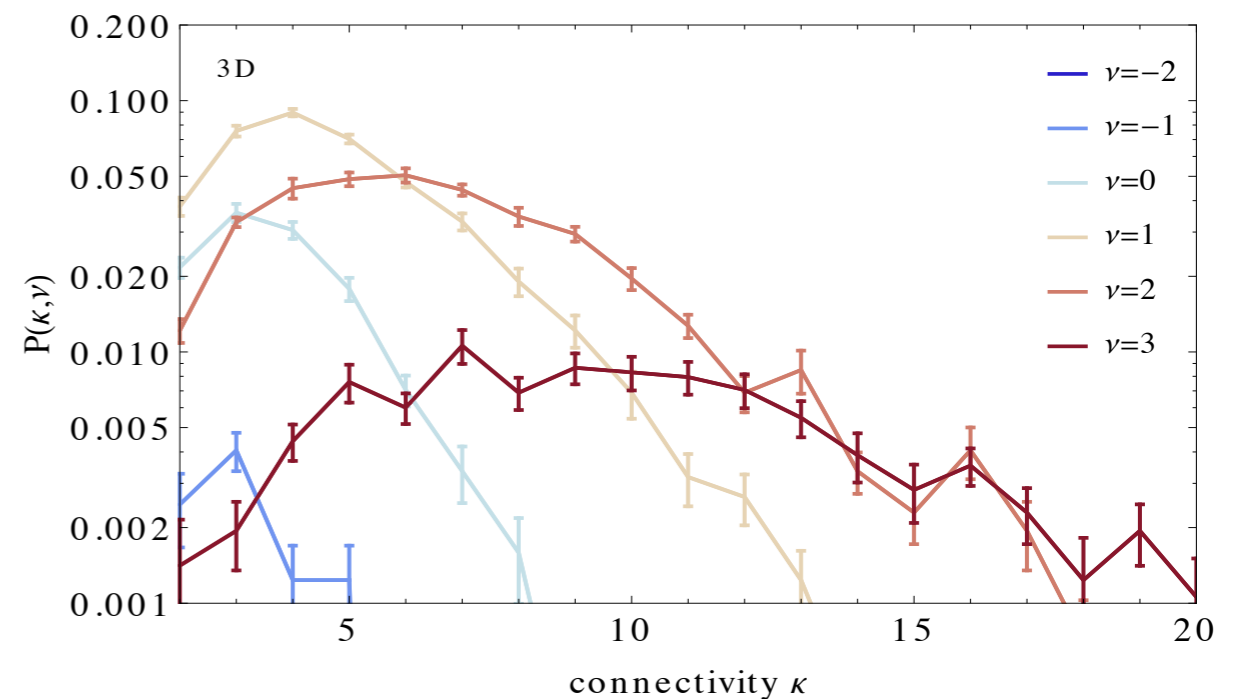
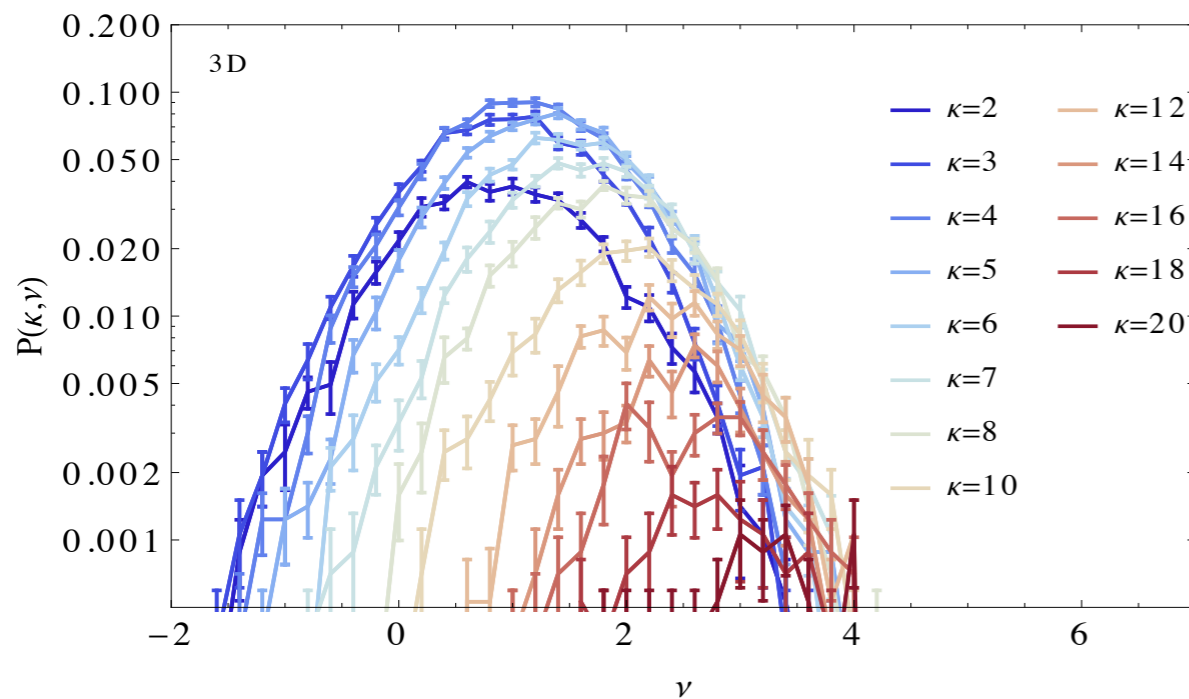


$$\nu = \delta / \sigma$$

The rarer the peak, the more connected

GRF connectivity: dependence with peak height

Joint PDF of κ and ν in 3D

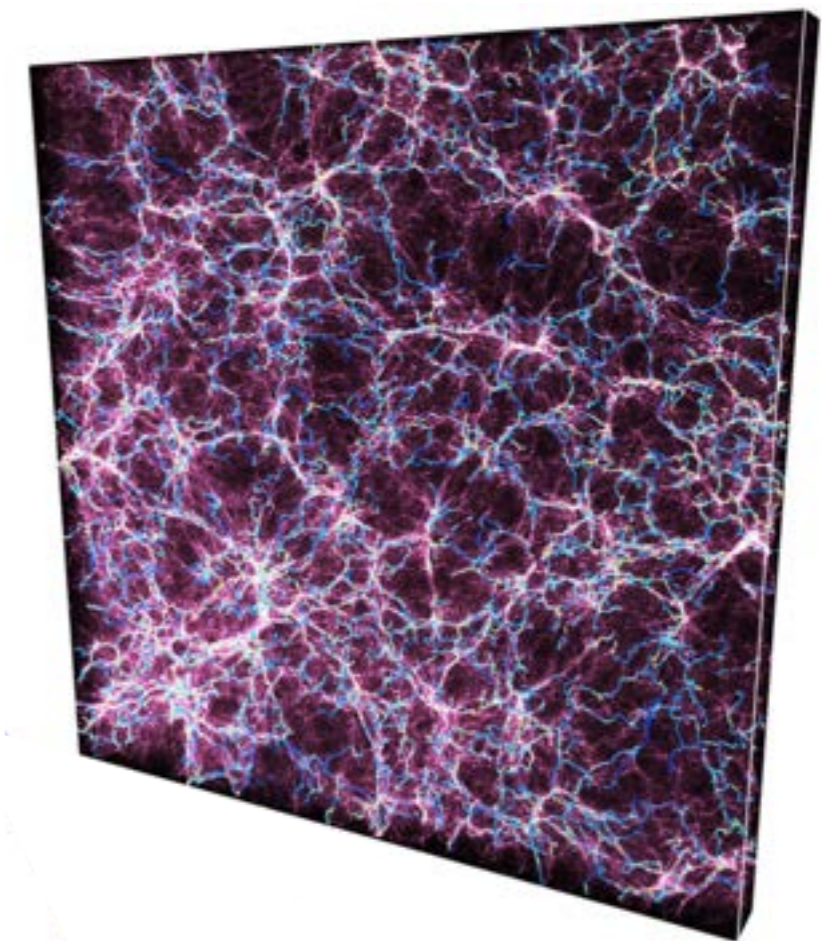
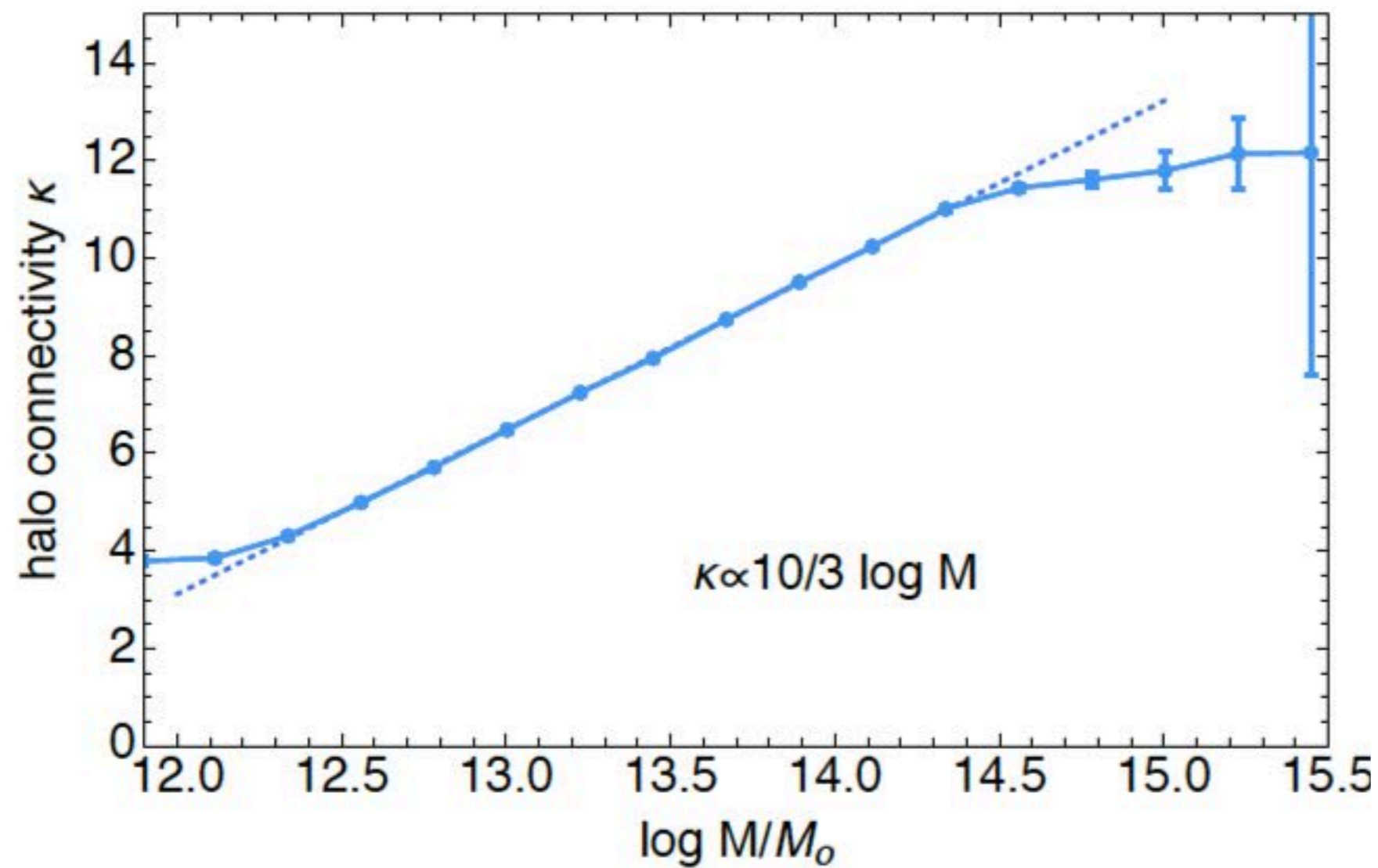


Notable Result:

- High peaks tend to have more connections
- Peaks with large number of connections are predominantly high
- mean $\langle \kappa | \nu \rangle$, **6.5 ($\nu=2$)**, **10 ($\nu=3$)**

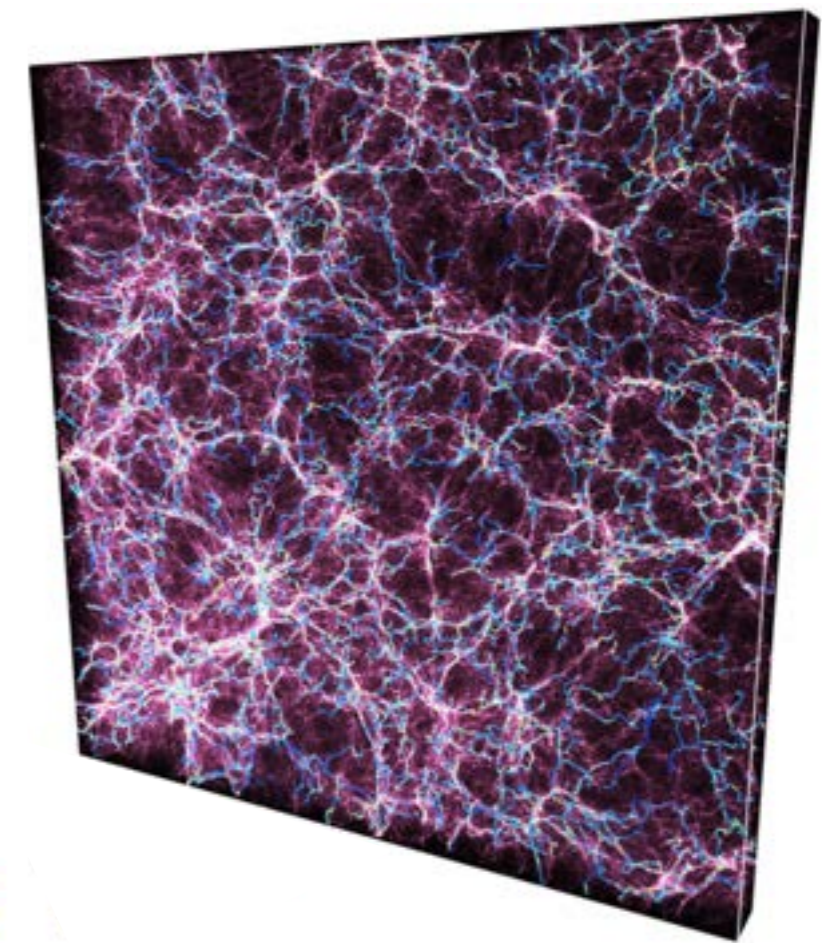
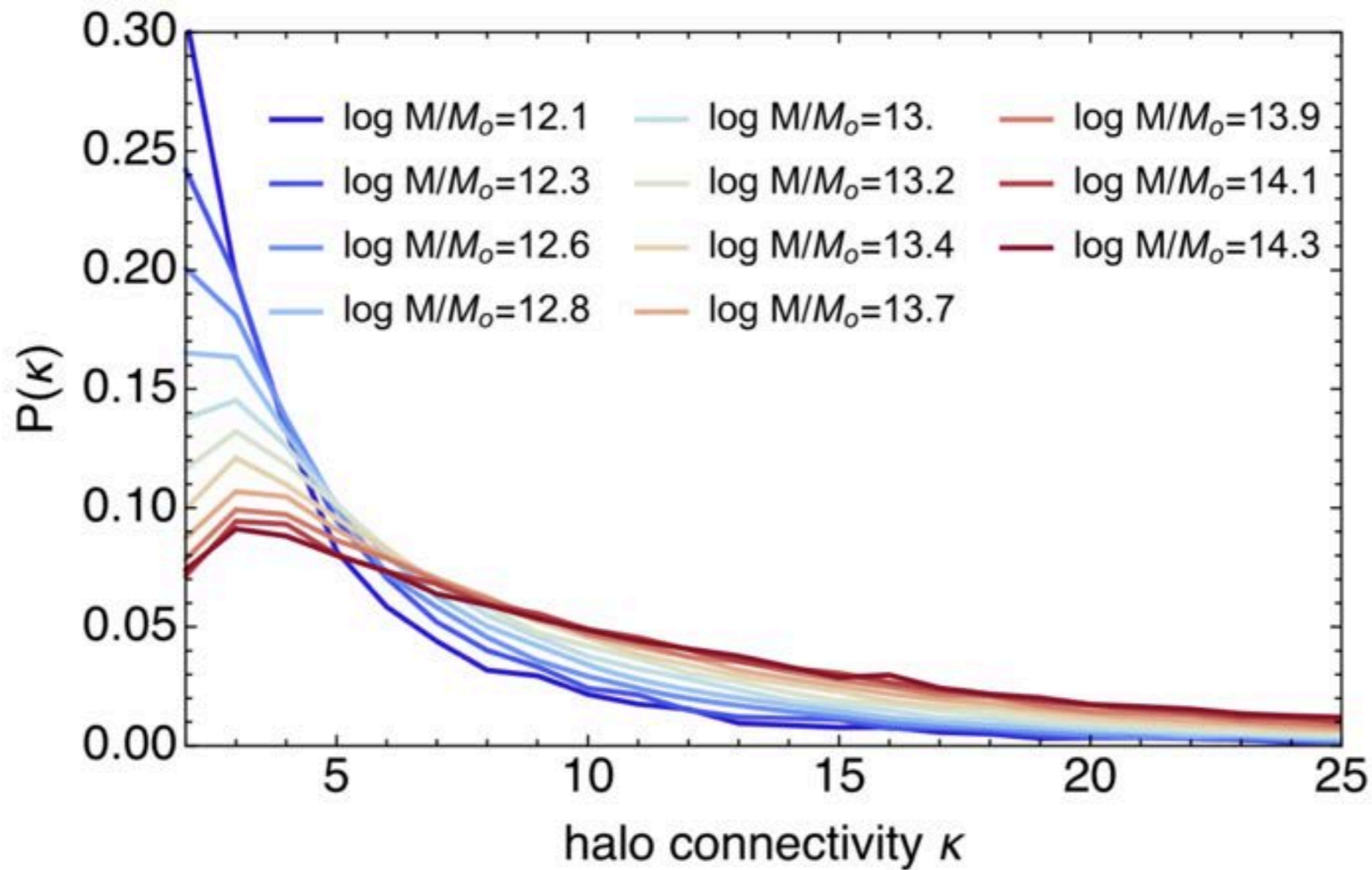
Connectivity versus Mass in LCDM

Connectivity as a function of Mass in Horizon- 4π : 1 000 000 halos.



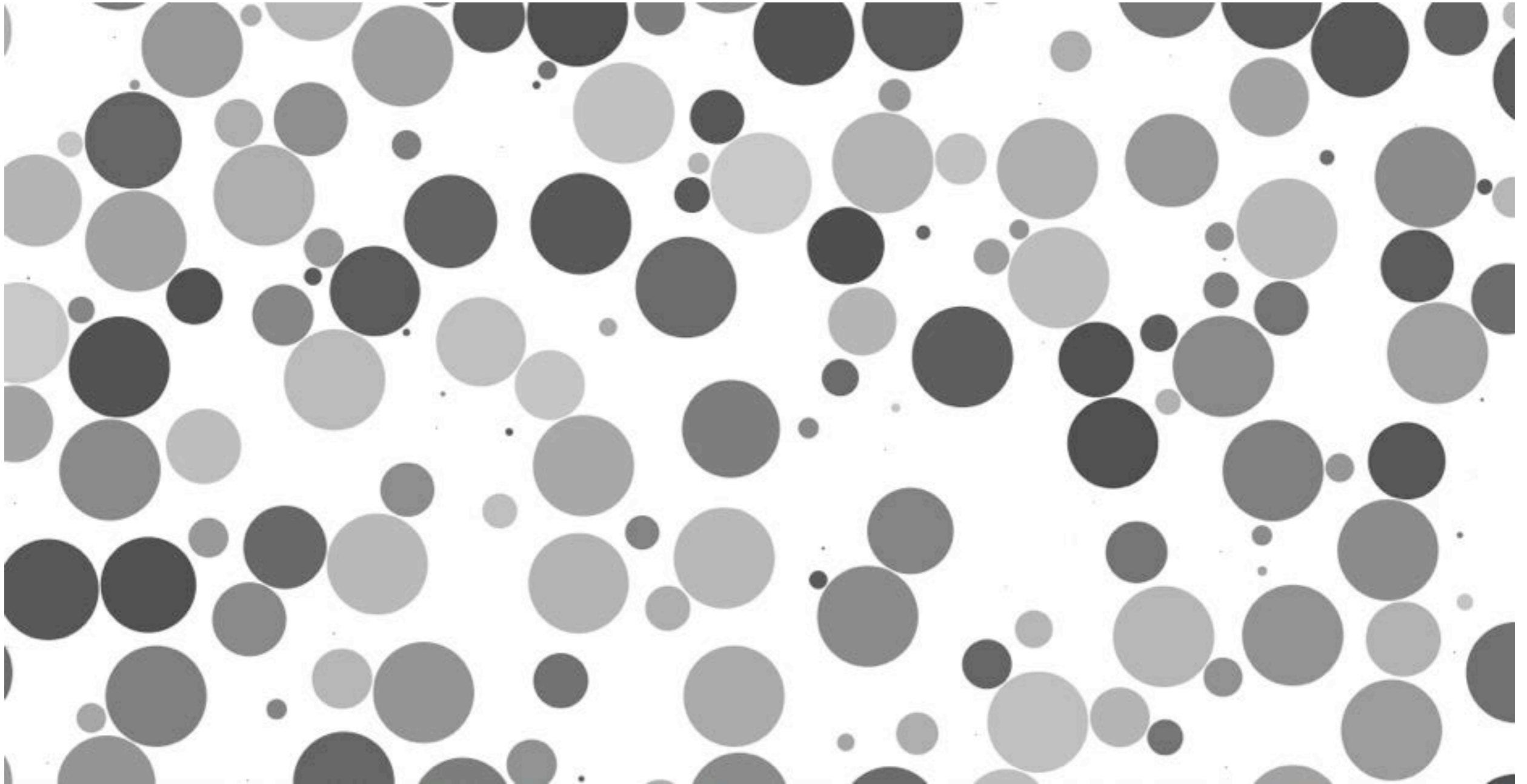
Connectivity versus Mass in LCDM

Connectivity as a function of Mass in Horizon- 4π : 1 000 000 halos.



Global connectivity for GRF: IDEA?

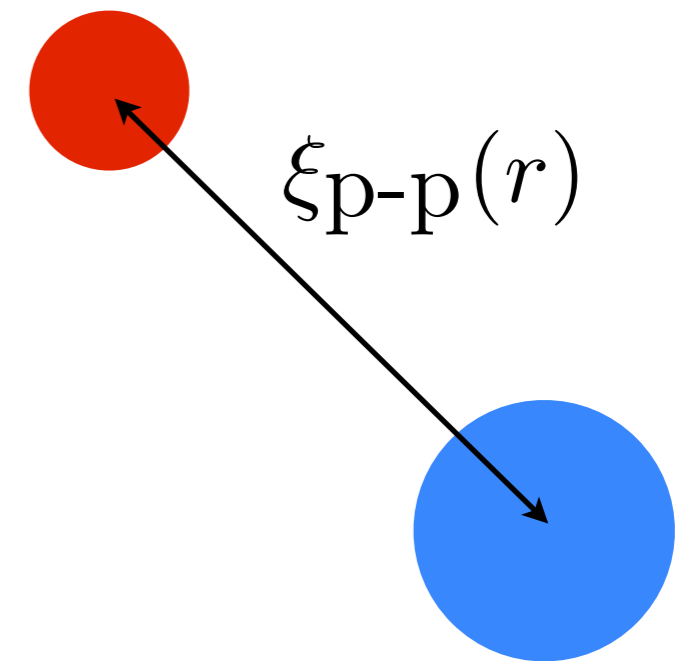
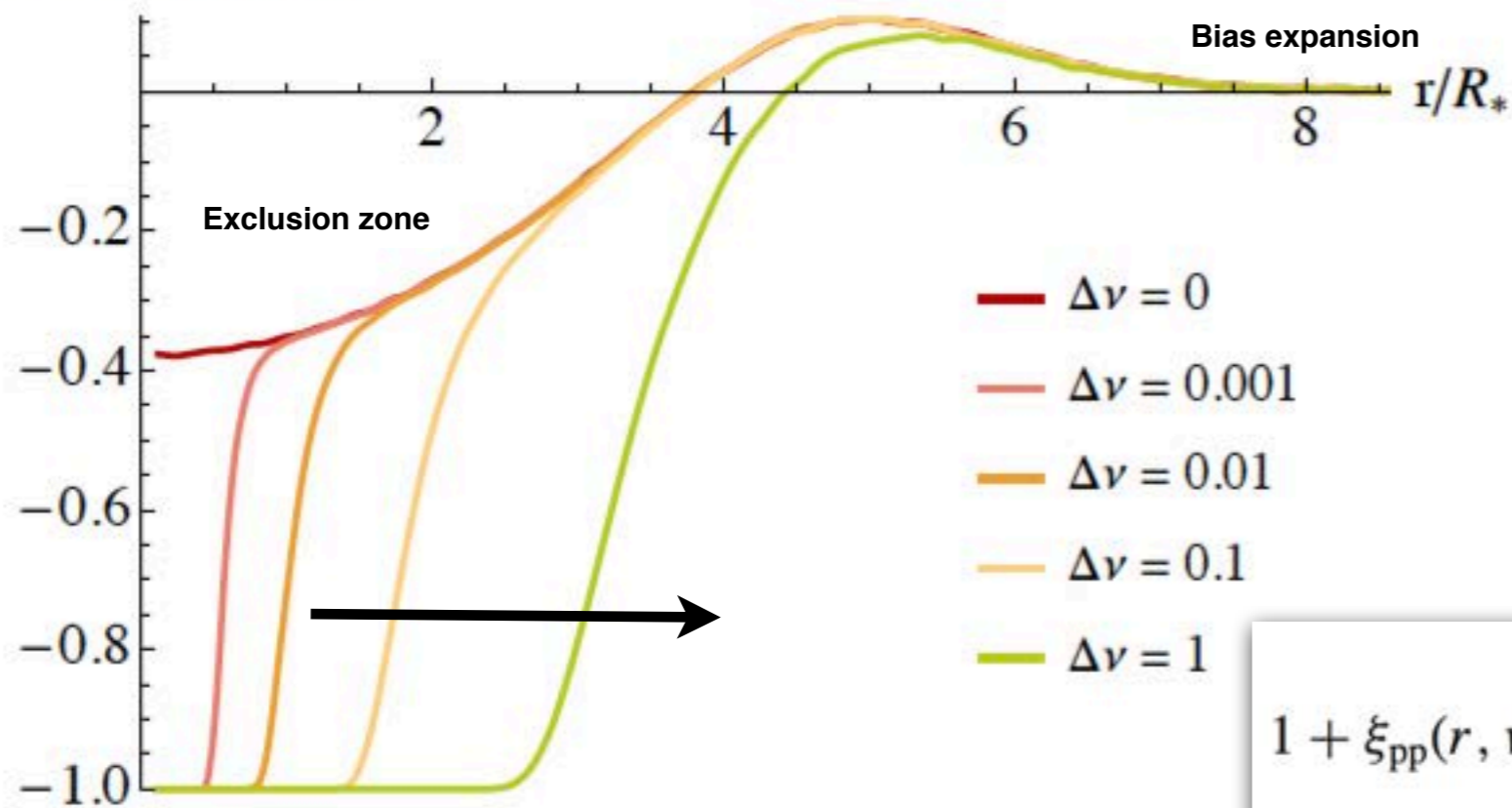
Analogy with sphere packing pb



Peak theory: Clustering (2 point statistics)

Same ideas can be used to also predict the **clustering of peaks** by means of their 2 point correlation function (also applies to peak saddle etc.):

$$\xi_{\text{pk}}(r, \bar{\nu}=1, \Delta\nu, n=0)$$



$$1 + \xi_{\text{pp}}(r, \nu) = \frac{\langle \rho_{\text{pk}}(\mathbf{X}) \rho_{\text{pk}}(\mathbf{Y}) \rangle}{\langle \rho_{\text{pk}}(\mathbf{X}) \rangle^2}.$$

where the localized peak number density $\rho_{\text{pk}}(\mathbf{X})$,

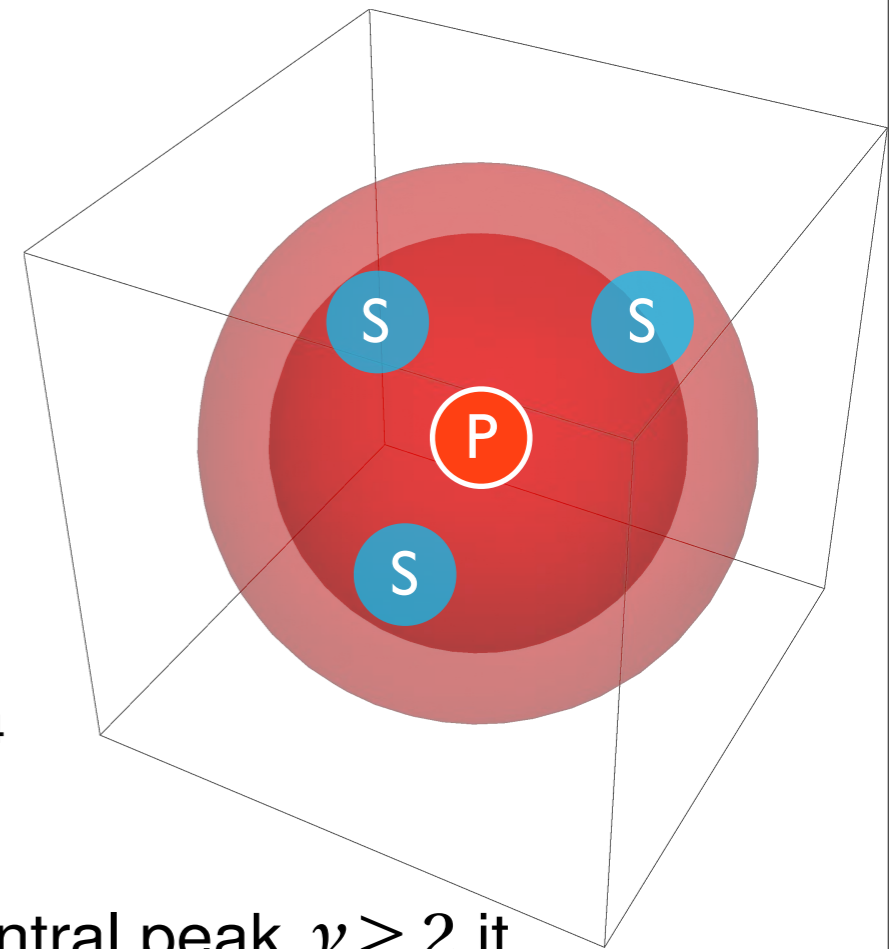
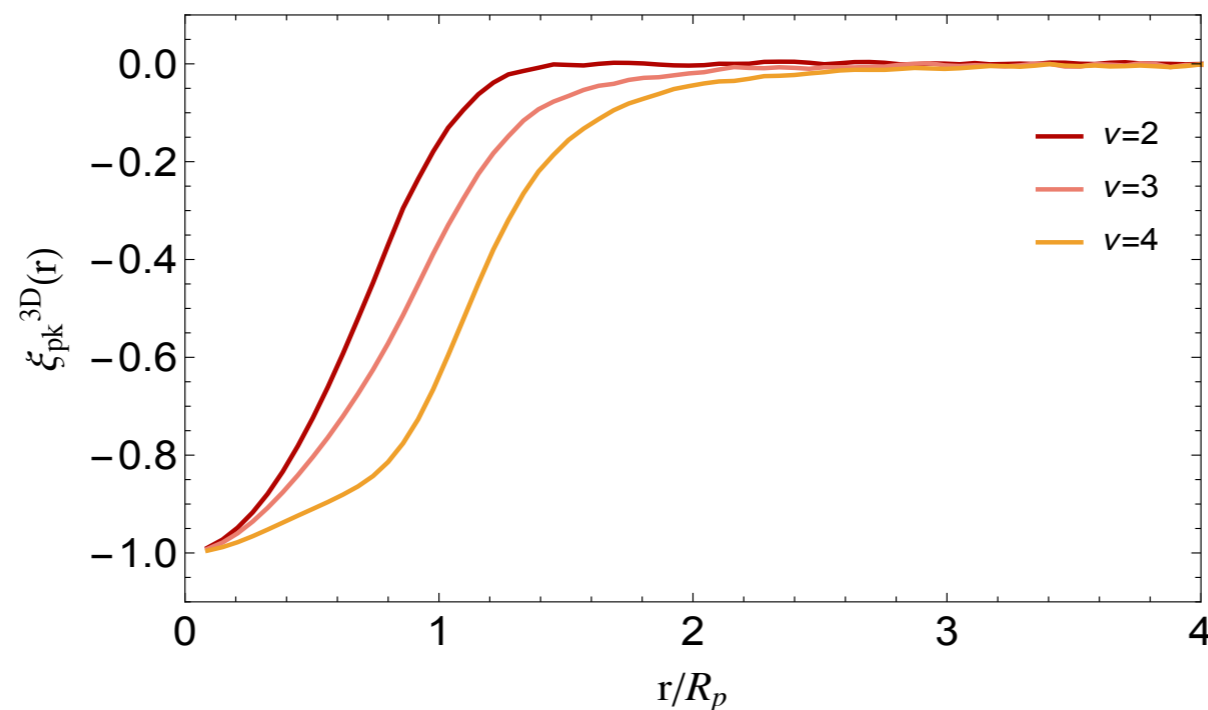
$$\rho_{\text{pk}}(\mathbf{X}) = \frac{1}{R_{\star}^d} |\det(x_{ij})| \delta_D(x_i) \Theta_H(-\lambda_i) \delta_D(x - \nu),$$

exclusion is essential to understand connectivity

Global connectivity for GRF: theory

Towards connectivity theory

Idea: Count the number of saddles up to R_{\max} . . . , conditional on the properties of the peak. But what is R_{\max} ? Some characteristic size of a peak-patch around the peak. Let us look (in 3D) where the neighbouring peaks are using peak-peak correlation function



They are at the **end of the exclusion zone**, which for high central peak $\nu \geq 2$ it increases with ν roughly linearly

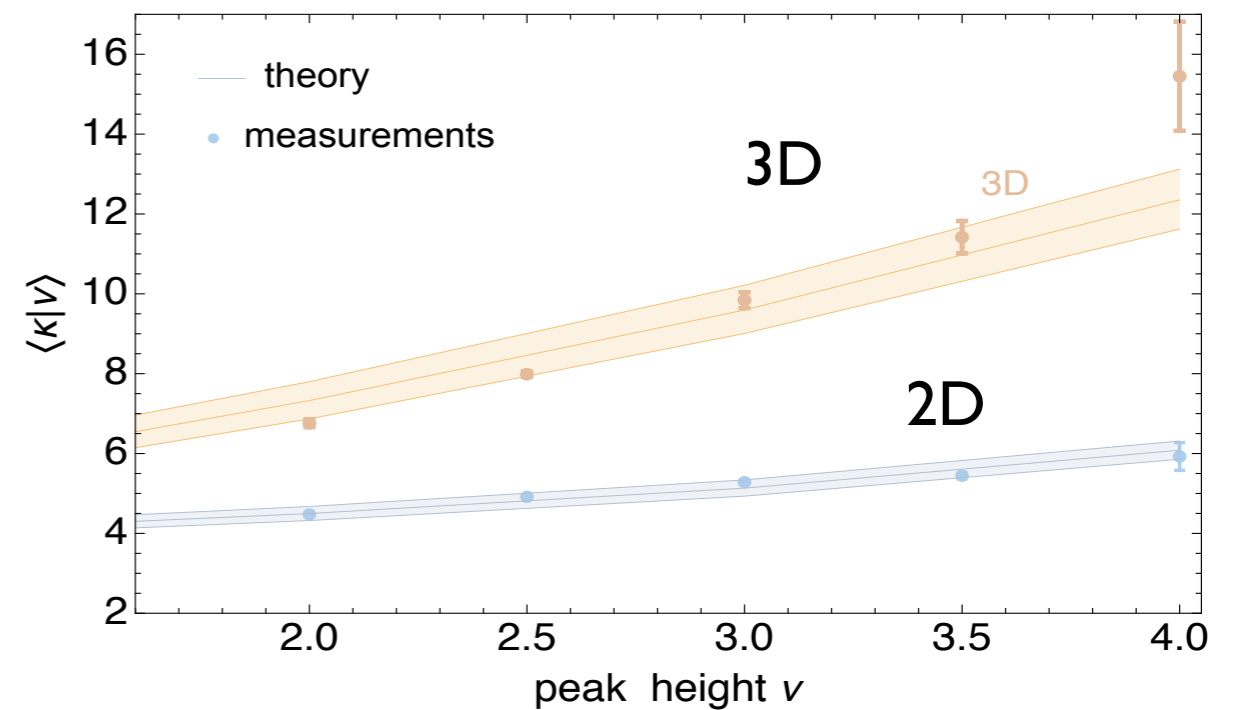
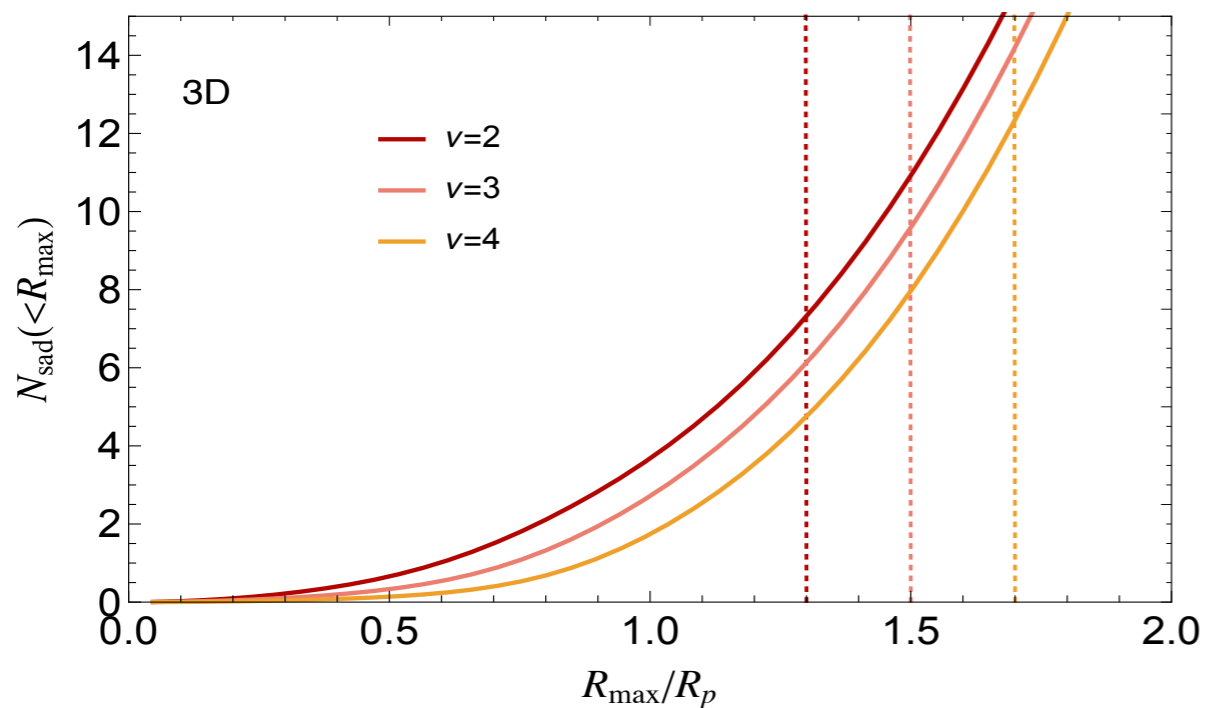
$$R_{\max} \approx (0.9 + \nu/5)R_p \quad R_{\max} = 1.2, 1.5, 1.8 R_p, \quad \nu = 2, 3, 4$$

Global connectivity for GRF: theory

Estimating κ by counting saddles to the next peak

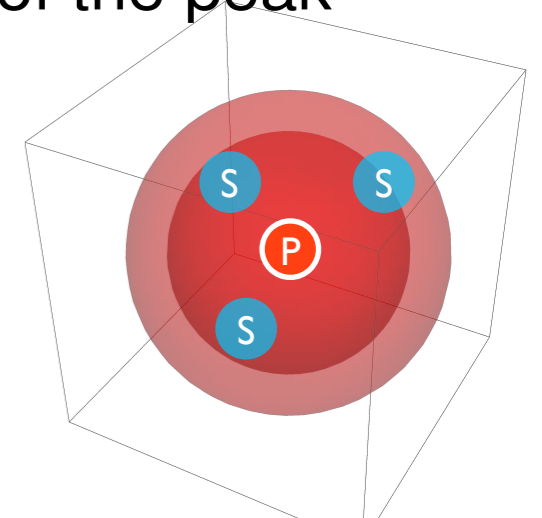
From the Peak-Saddle correlation function

$$\kappa(\nu) = \bar{n}_{\text{sad}} \int_0^{R_{\text{pp}}} d^D r (1 + \xi_{\text{pk-sad}}(r, \nu))$$



Number of saddles to distance R_{max} conditional on the height ν of the peak translates to peak connectivity $\langle \kappa | \nu \rangle$

Subtle interplay between clustering of saddles and zone of influence of peak.

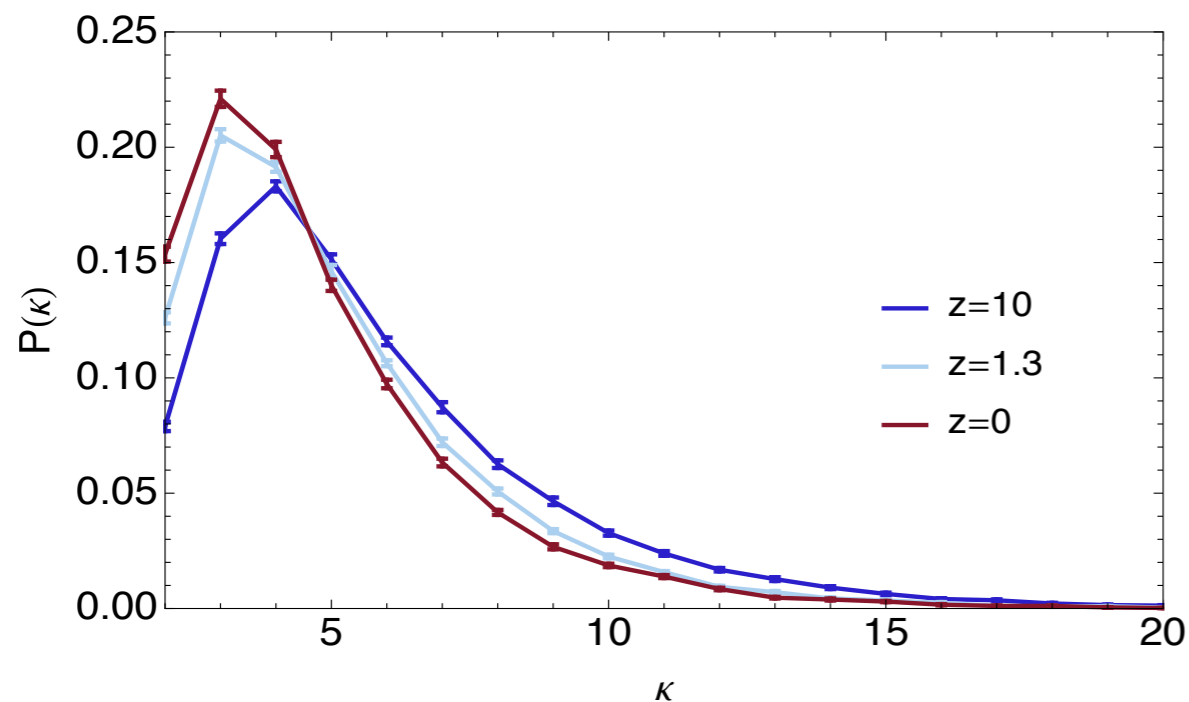


Connectivity: evolution with cosmic time

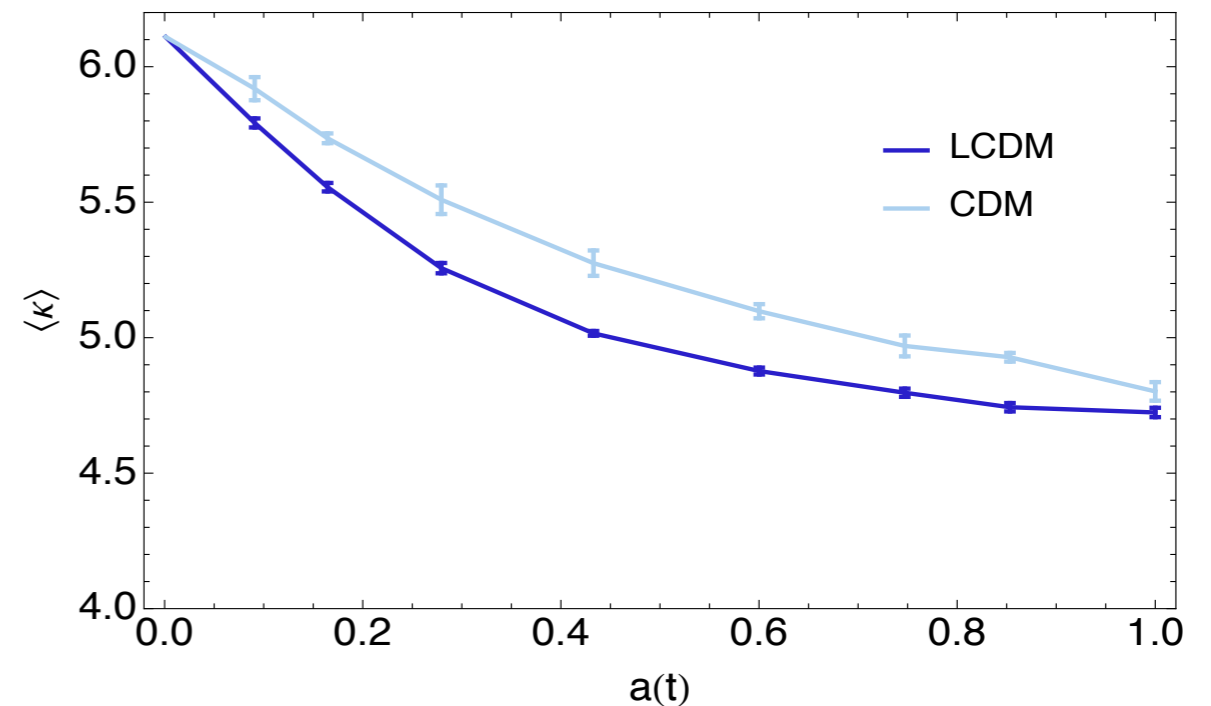
Connectivity of a non-Gaussian field differ from the Gaussian

- In cosmological simulations, as density becomes more non-Gaussian, connectivity of the Cosmic Web decreases
- This leads to model dependent history of the connectivity at different redshifts.

$P(\kappa)$



$\langle \kappa \rangle$



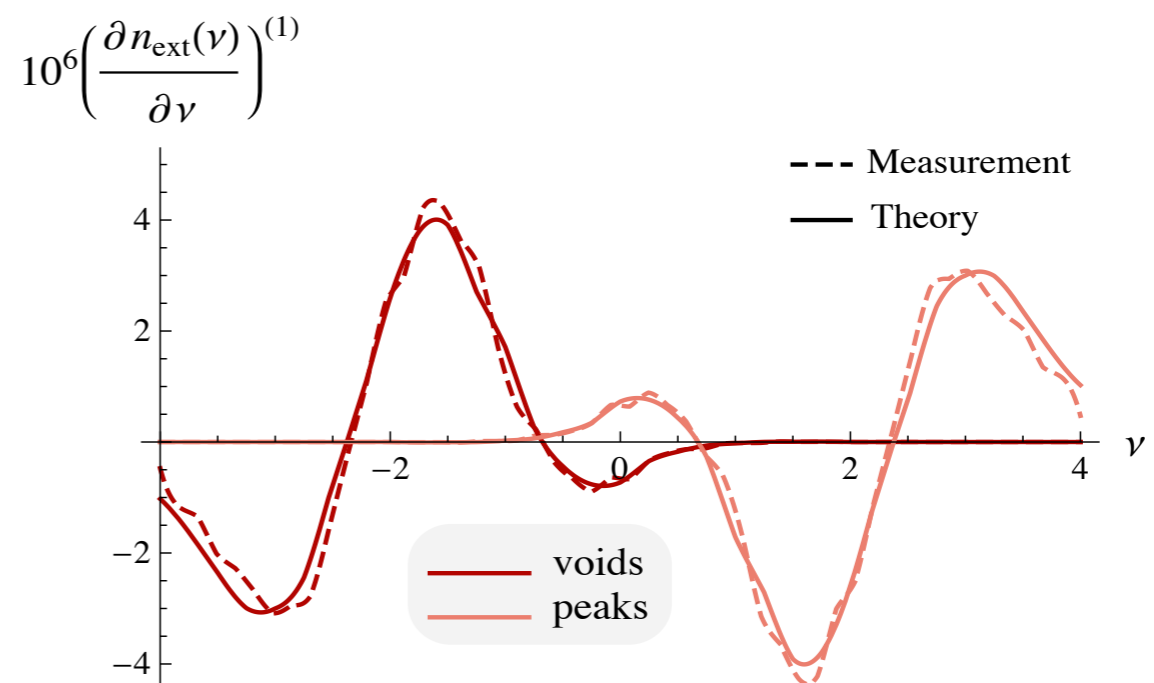
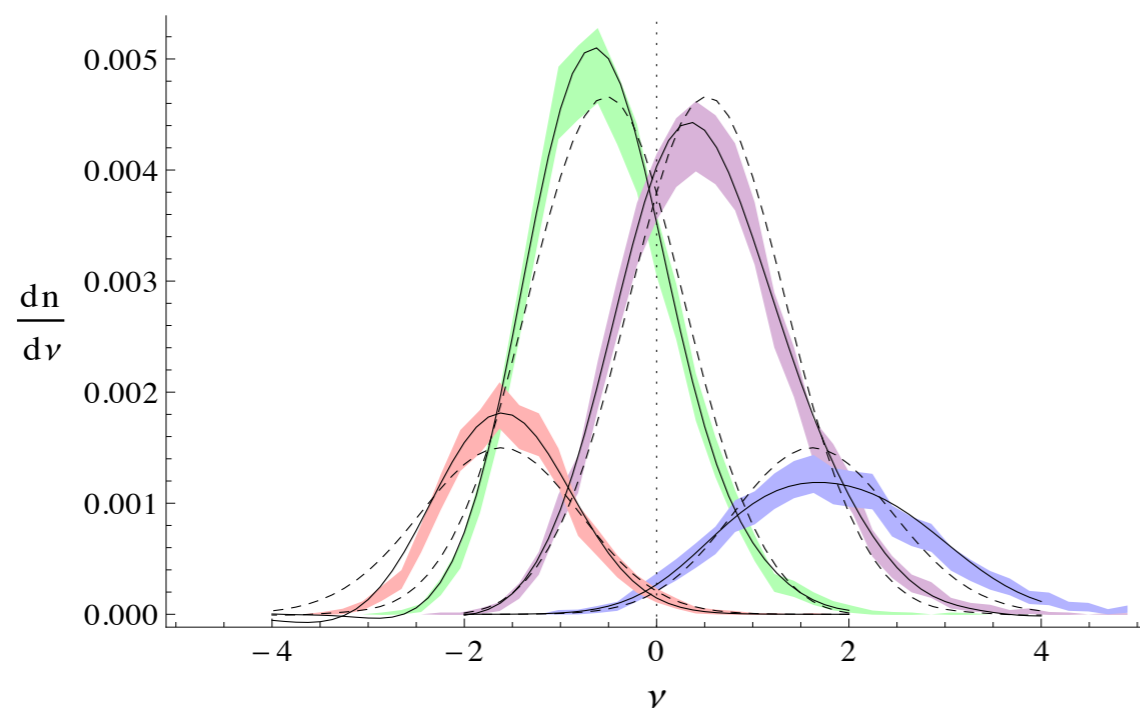
Filaments merge in a cosmology-dependent way!

Theory: evolution with cosmic time

Non-Gaussian 3D Extrema Counts (Gay et al, 2011)

scales like $D(z) \times \text{a number}$

$$\langle n_{\mp} \rangle = \frac{29\sqrt{15} \mp 18\sqrt{10}}{1800\pi^2 R_*^3} + \frac{5\sqrt{5}}{24\pi^2 \sqrt{6\pi} R_*^3} \left(\langle q^2 J_1 \rangle - \frac{8}{21} \langle J_1^3 \rangle + \frac{10}{21} \langle J_1 J_2 \rangle \right)$$



$$\langle \kappa \rangle = \kappa^G \left(1 + \sum_{i \geq 1} \kappa^{(i)} \sigma_0^i \right)$$

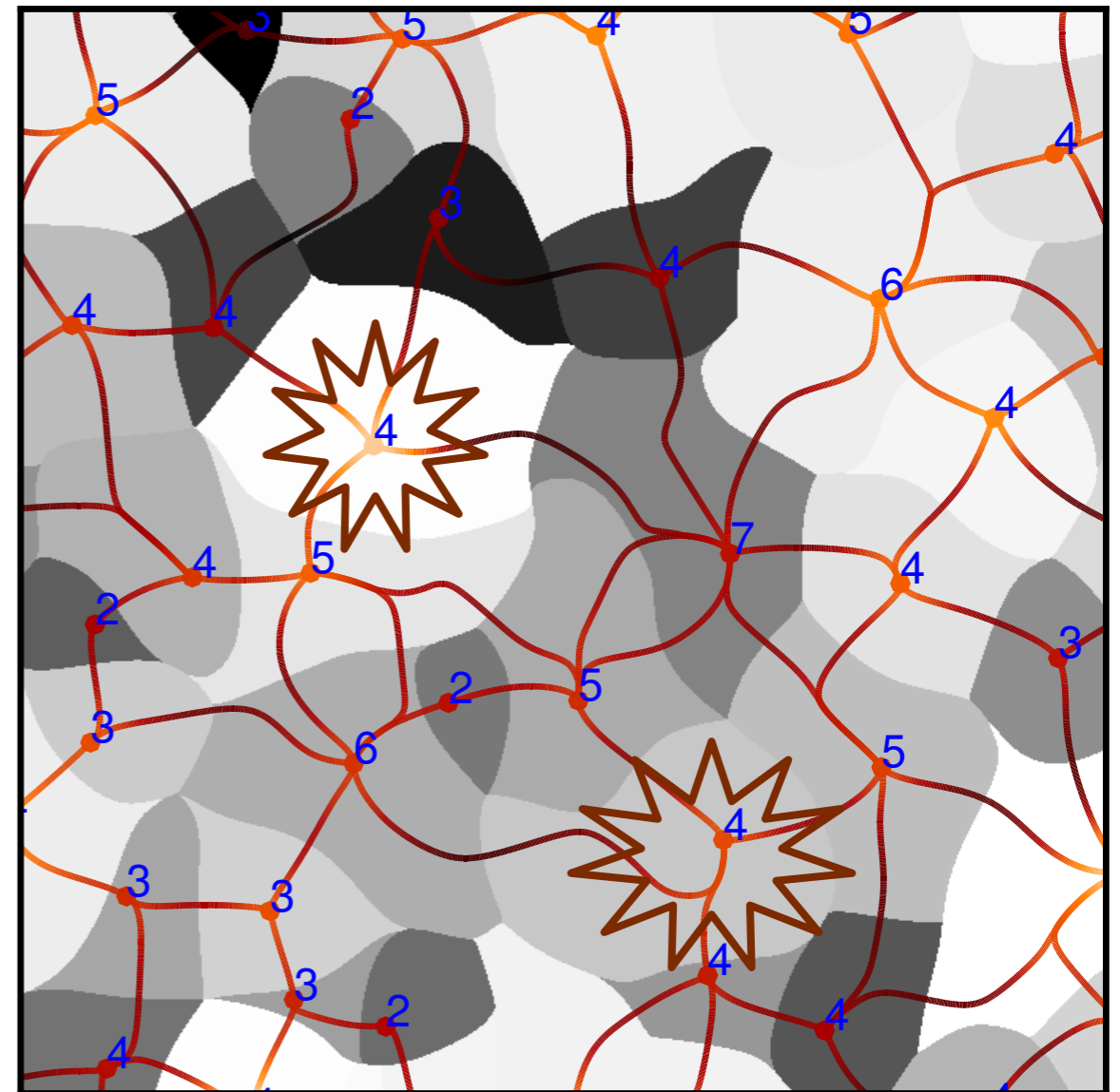
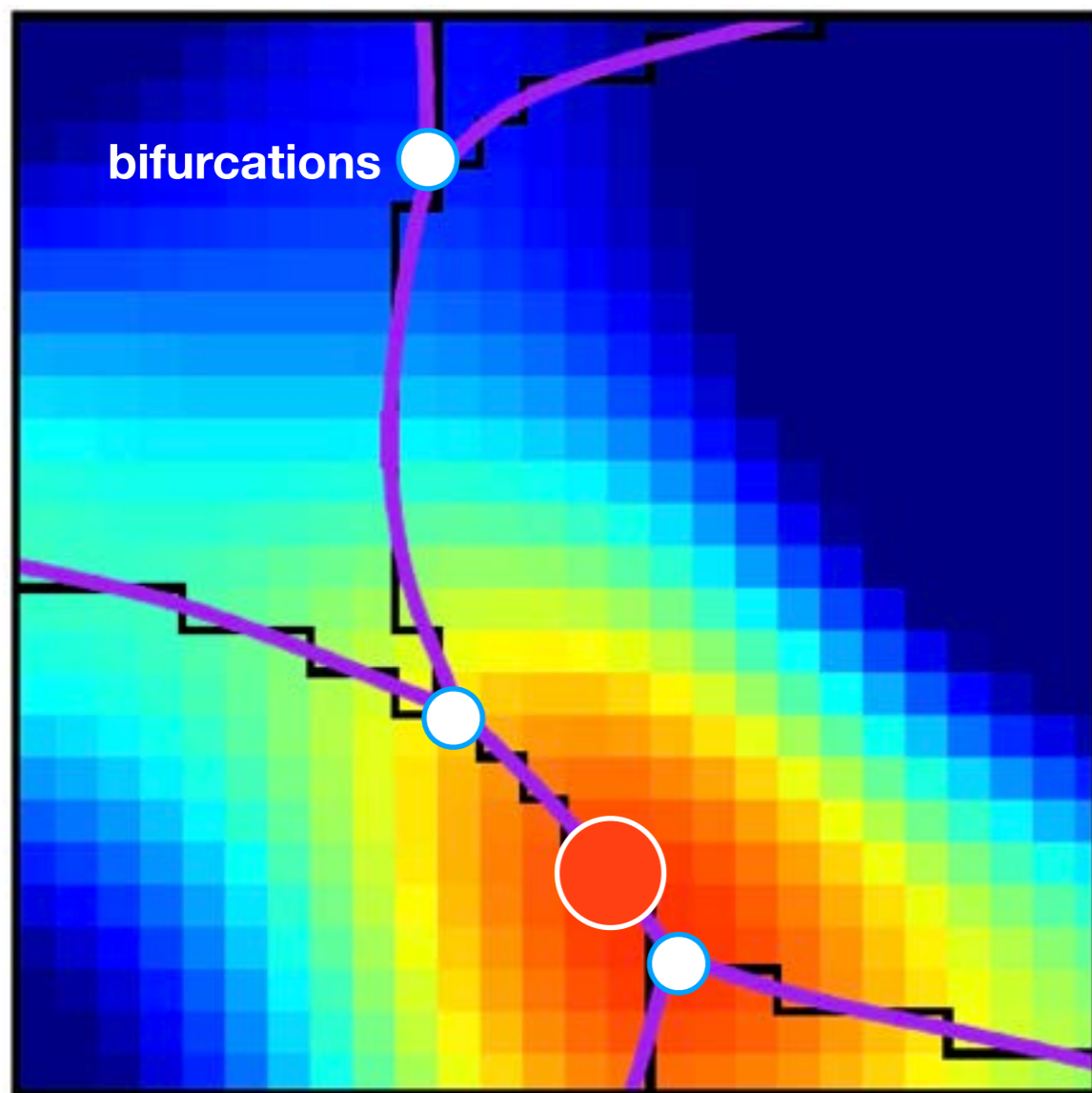
With Gram Charlier expansion, prediction at arbitrary order

At $\sigma \approx 0.2$

$$\frac{\langle n_{\text{saddle}} \rangle}{\langle n_{\text{peak}} \rangle} \approx 2.8 \Rightarrow \langle \kappa \rangle \approx 5.6$$

Local multiplicity and bifurcation points

For galaxy formation, what matters most is how many filament connect **locally** onto a galaxy. At small enough scale, a peak is always **ellipsoidal** so that only two branches of filament stick out. Then those branches **bifurcate**. Some bifurcations appear so close to the peak that they are physically irrelevant. Hence we will define the **multiplicity** as the local number of filaments.



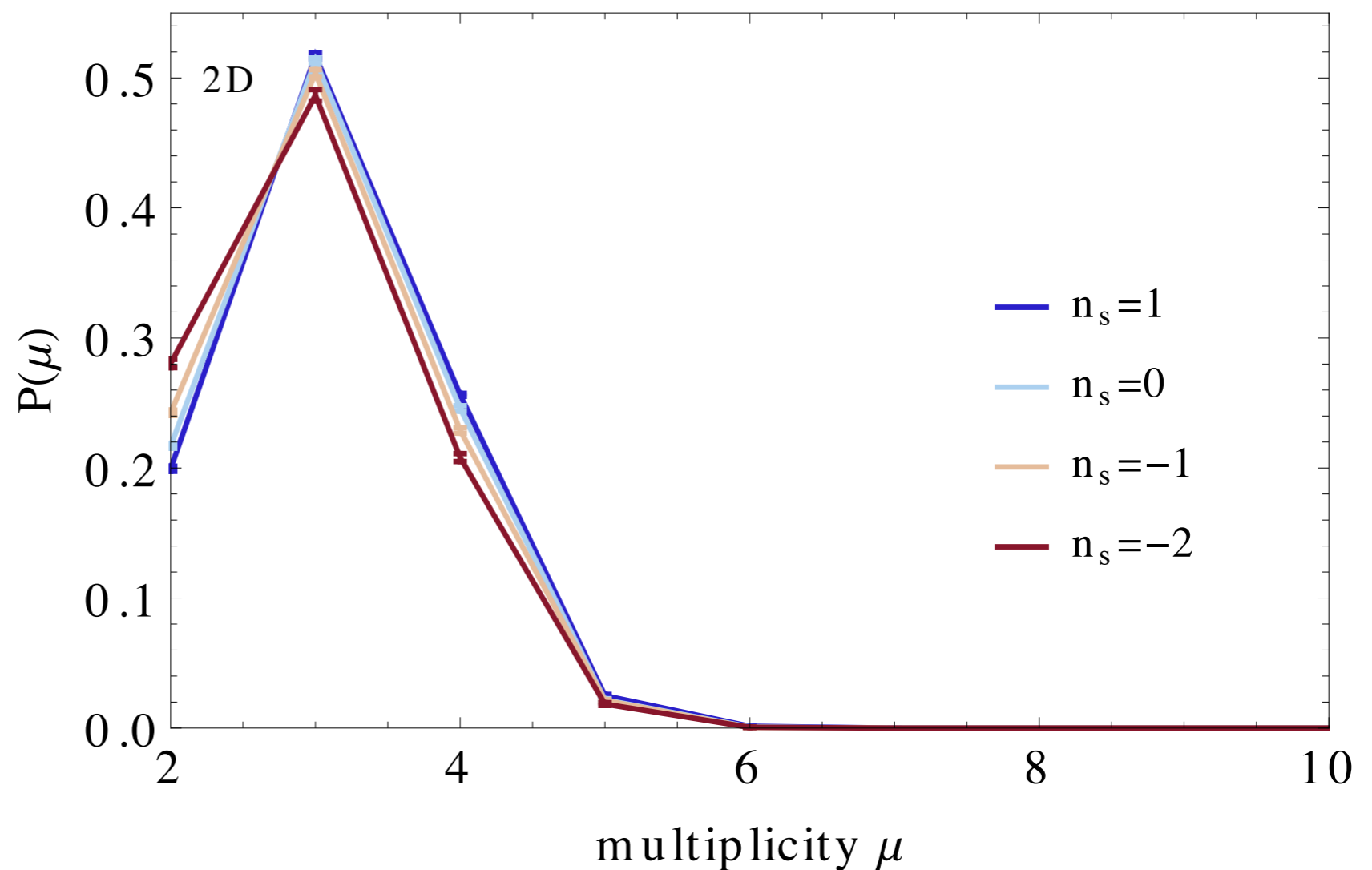
Local multiplicity and bifurcation points

For galaxy formation, what matters most is how many filament connect **locally** onto a galaxy. At small enough scale, a peak is always **ellipsoidal** so that only two branches of filament stick out. Then those branches **bifurcate**. Some bifurcations appear so close to the peak that they are physically irrelevant. Hence we will define the **multiplicity** as the local number of filaments.

$$\mu = \kappa - n_{\text{bifurcations}}$$

$$\mu \approx 3 \quad \text{in 2D}$$

$$\mu \approx 4 \quad \text{in 3D}$$



$$2\text{D}: \langle \mu \rangle = 3$$

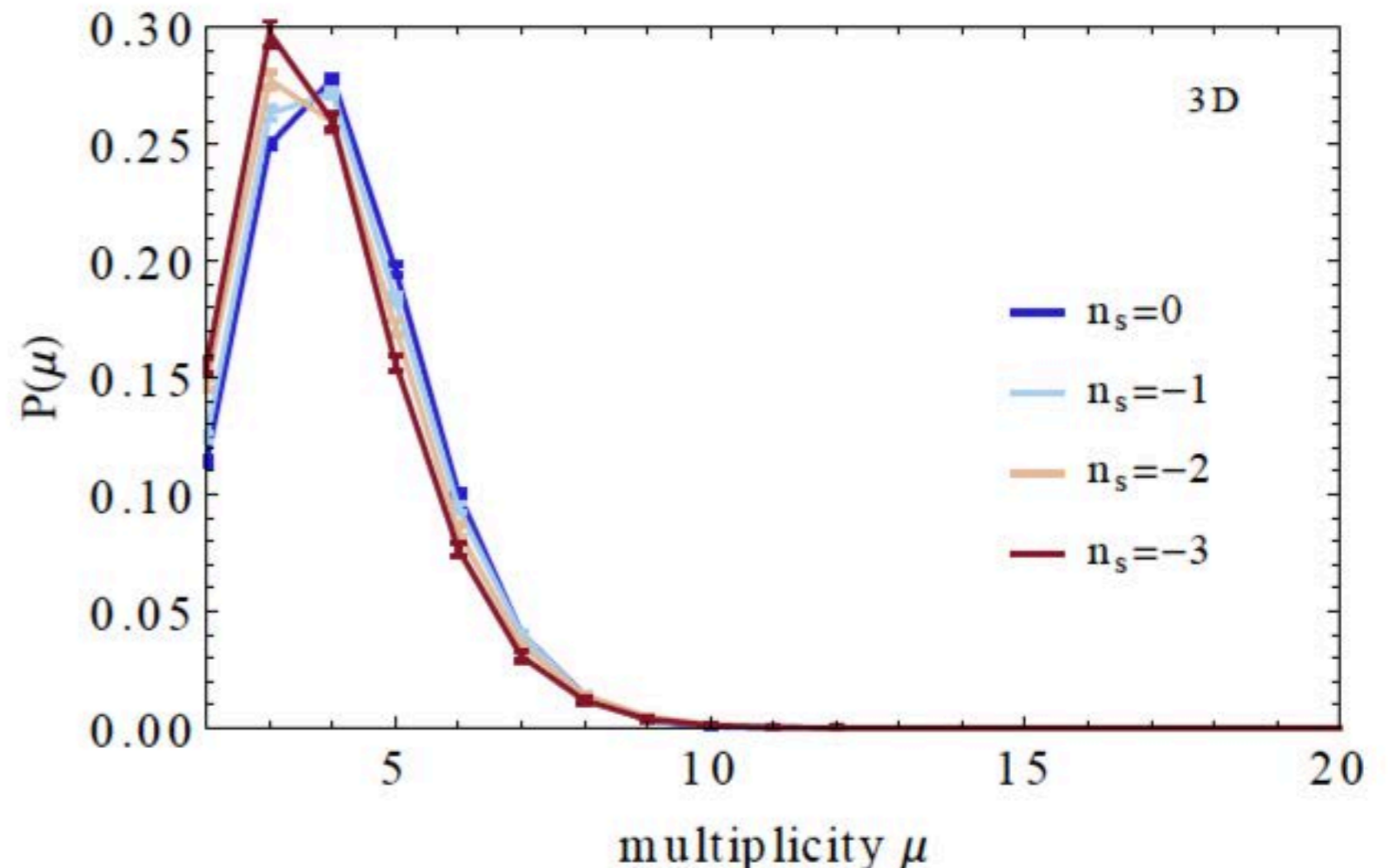
Local multiplicity and bifurcation points

For galaxy formation, what matters most is how many filament connect **locally** onto a galaxy. At small enough scale, a peak is always **ellipsoidal** so that only two branches of filament stick out. Then those branches **bifurcate**. Some bifurcations appear so close to the peak that they are physically irrelevant. Hence we will define the **multiplicity** as the local number of filaments.

$$\mu = \kappa - n_{\text{bifurcations}}$$

$$\mu \approx 3 \quad \text{in 2D}$$

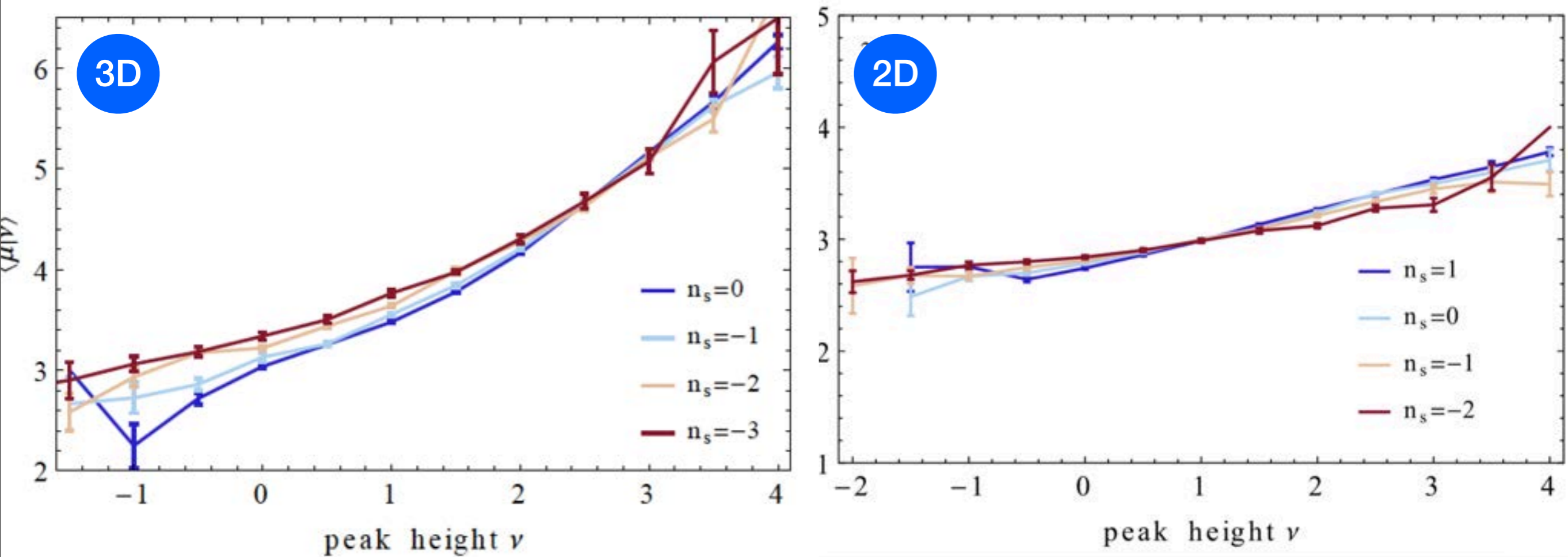
$$\mu \approx 4 \quad \text{in 3D}$$



$$3\text{D: } \langle \mu \rangle = 4$$

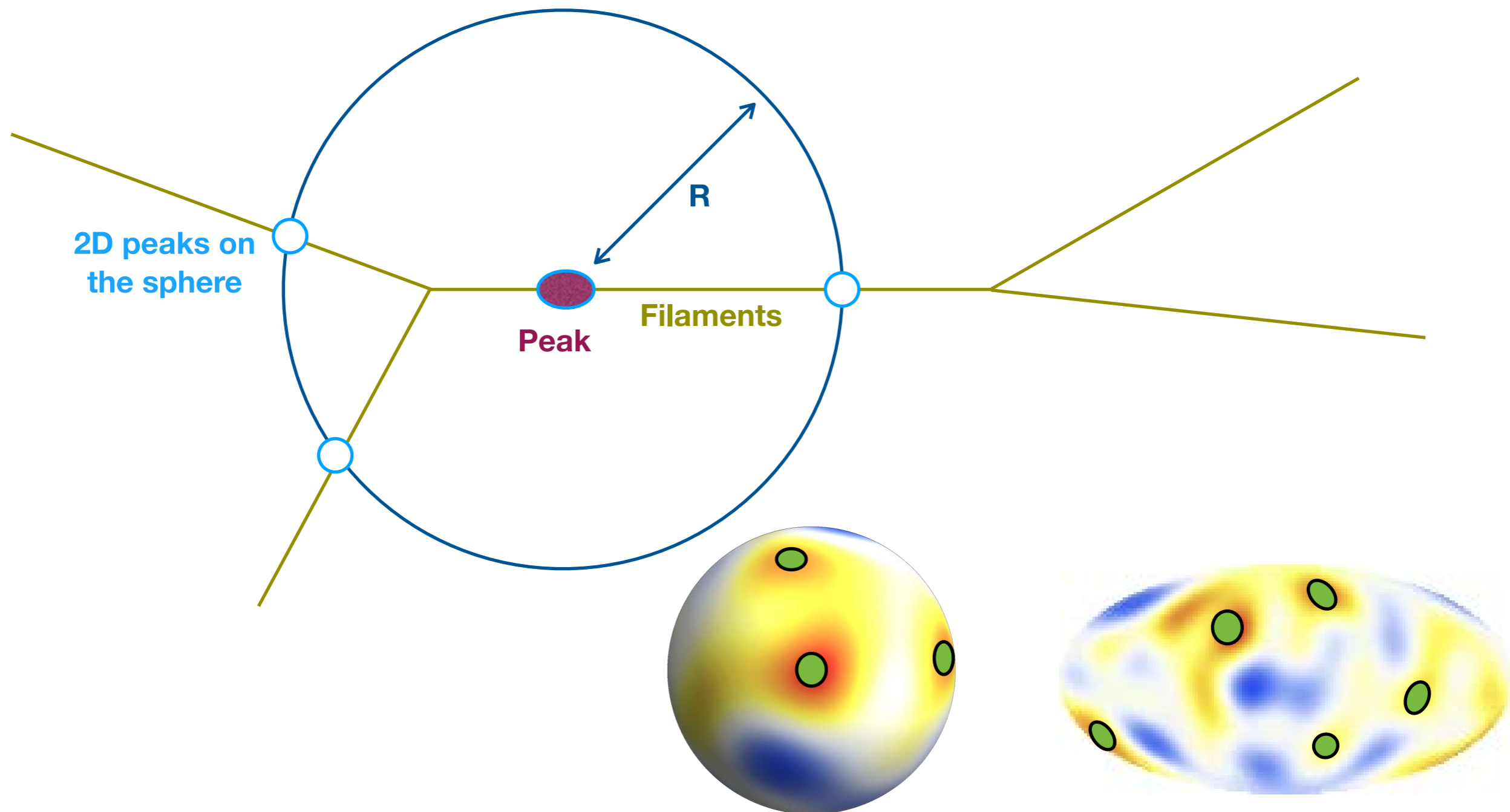
Local multiplicity

The denser the environment, the higher the multiplicity
(e.g. bringing less coherent angular momentum and generating more ellipsoidal galaxies)

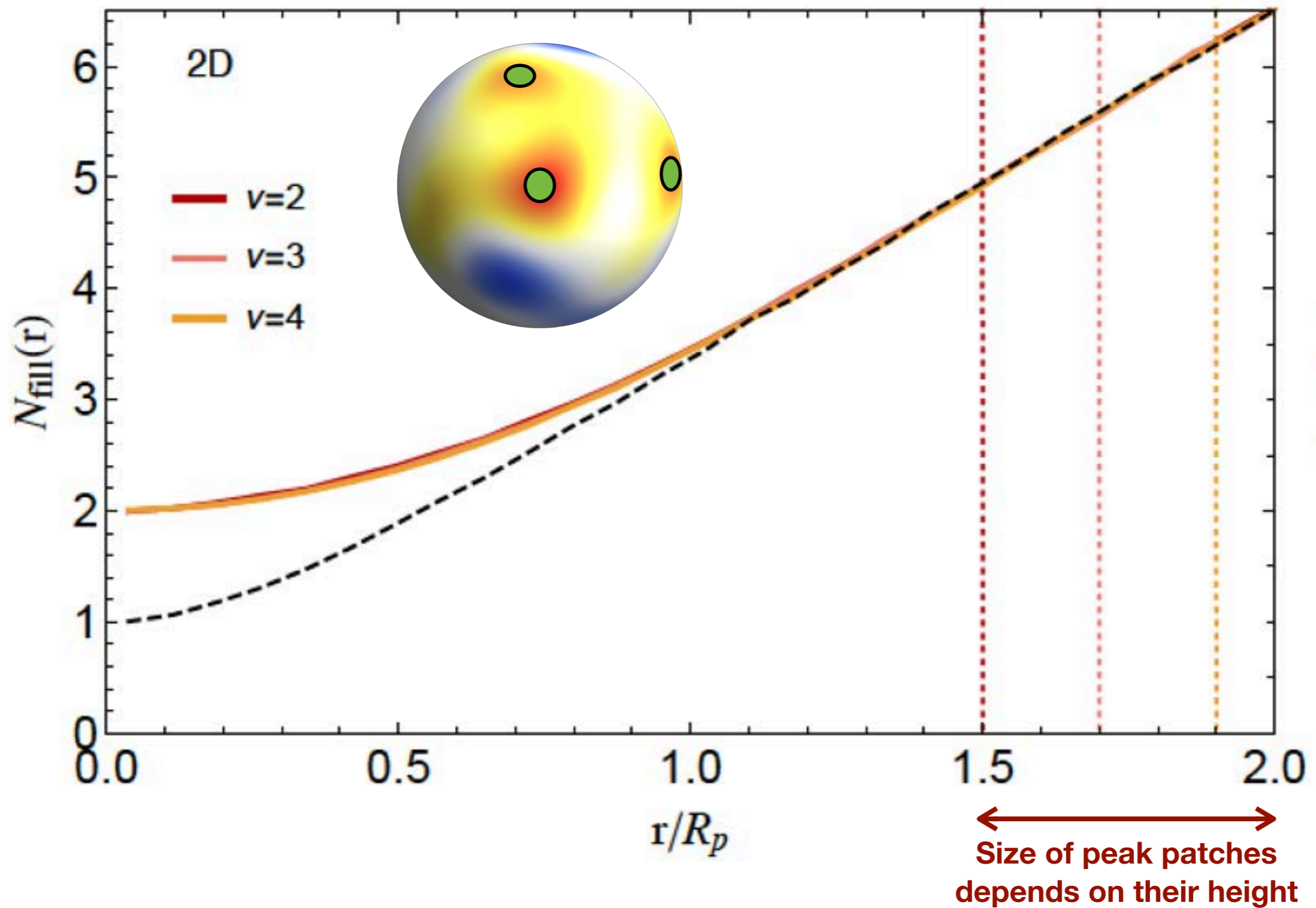


Local multiplicity: towards a theoretical prediction

Let us count filament crossings at a **sphere** of radius R around the central peak...

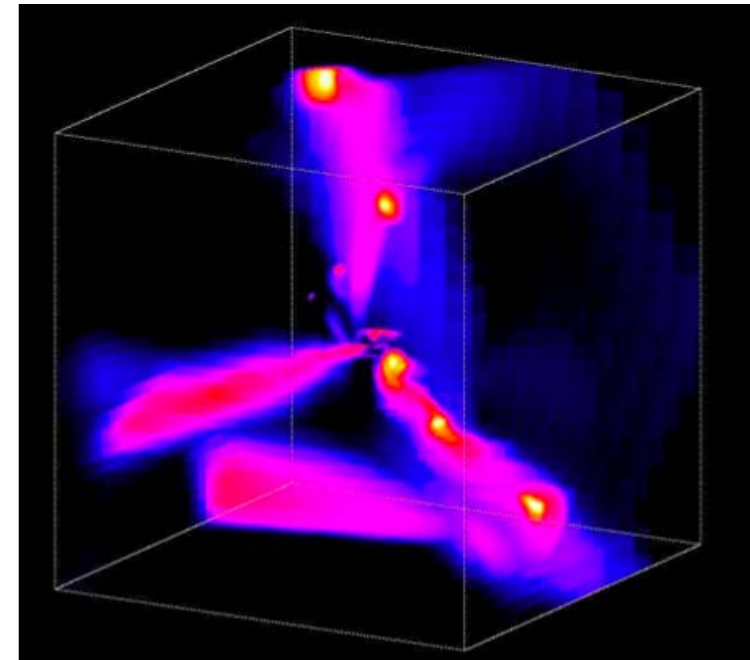
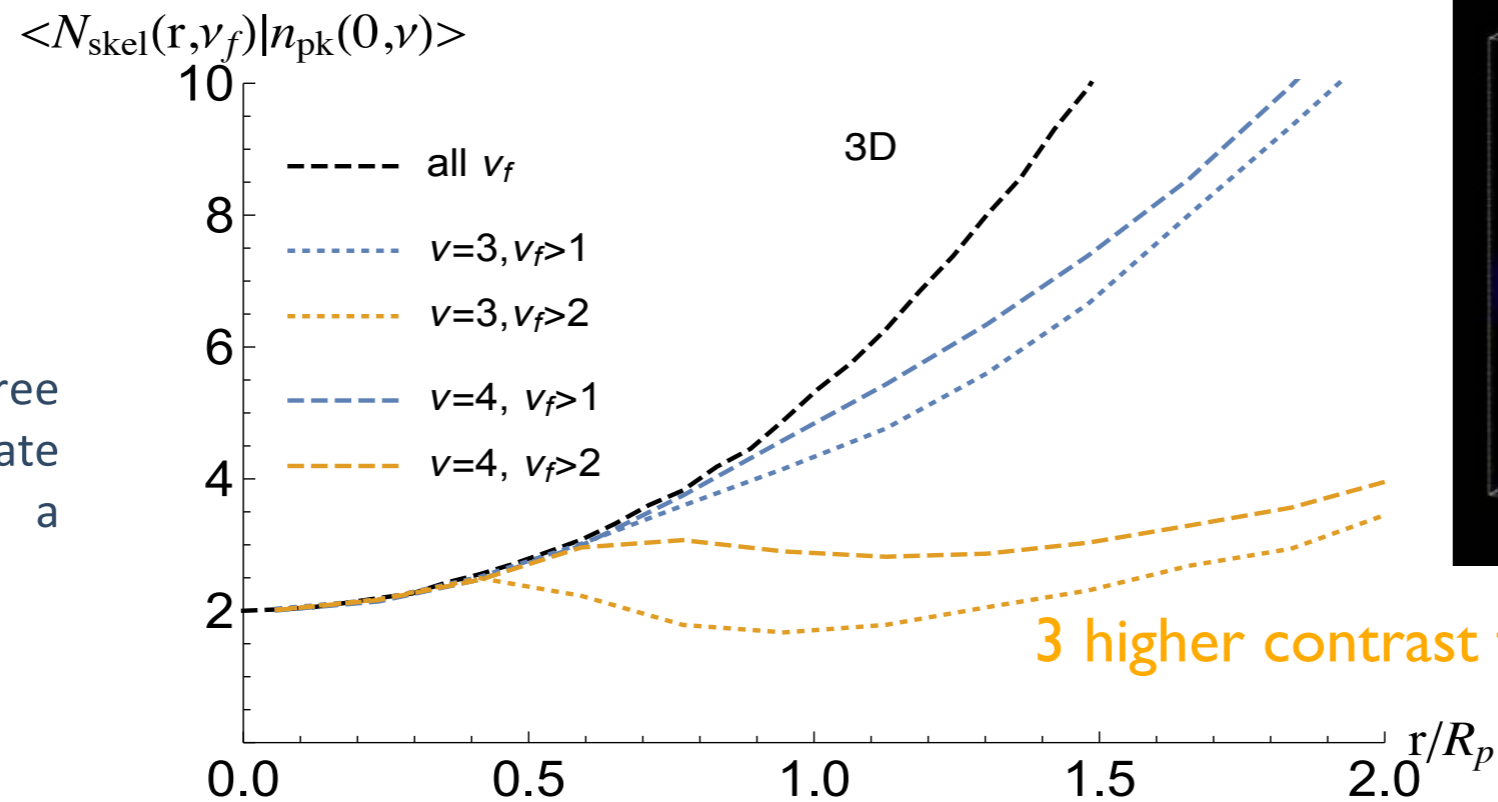


Local multiplicity: towards a theoretical prediction



Local multiplicity: towards a theoretical prediction

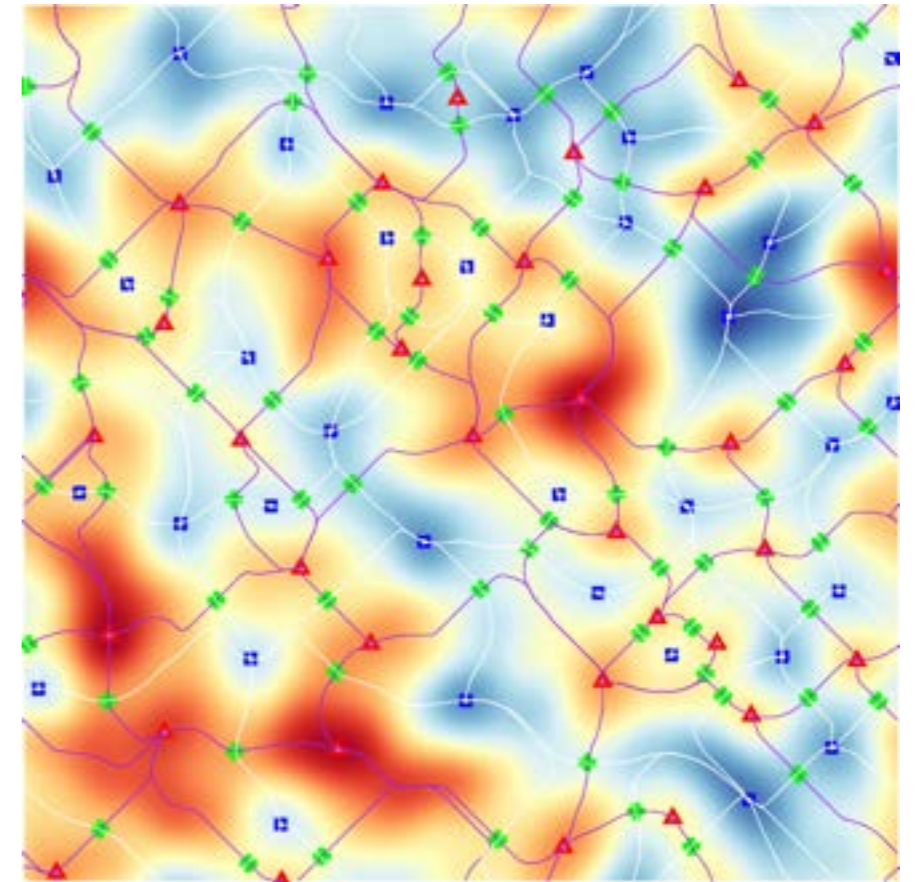
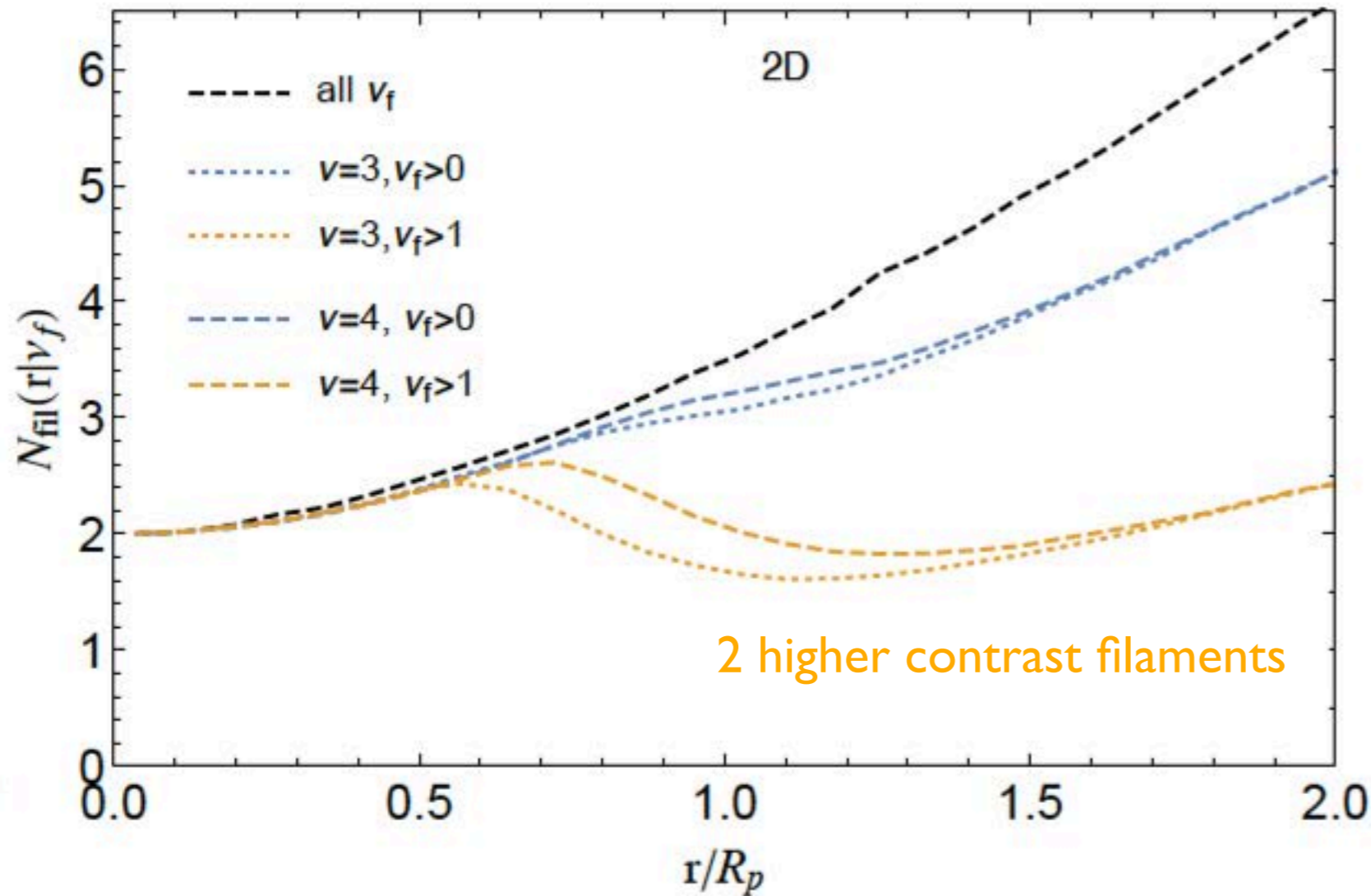
Not all filaments are equally prominent. Counting important ones



Typically, two to three dense filaments dominate and therefore define a plane of accretion....

- Number of dense $\nu_f > 2$ elementary bridges is increasing with the height of the central peak
- Not very rare $\nu = 3$ central peak has two (branches of) dense filaments, i.e. it sits in one dominant filament on average
- Rare $\nu = 4$ peak is at intersection of three prominent branches.

Local multiplicity: towards a theoretical prediction

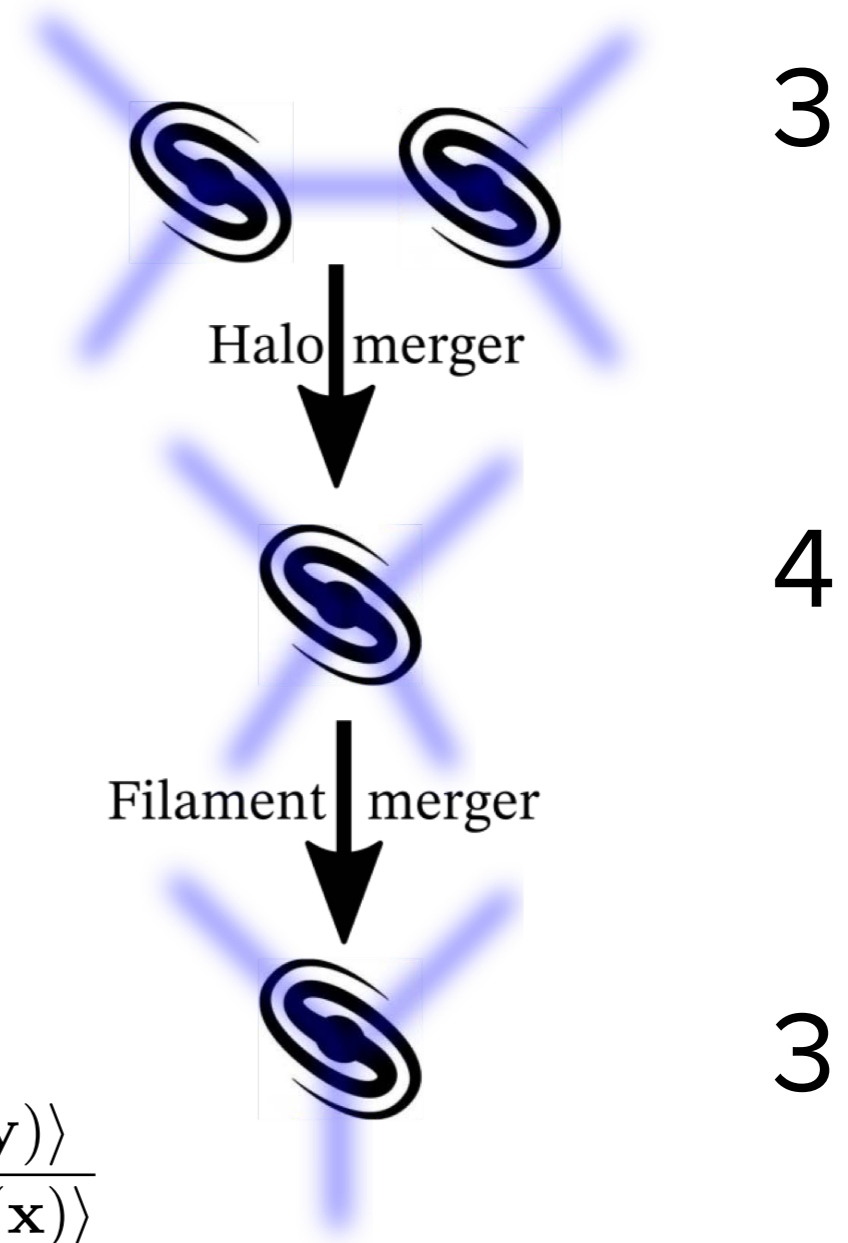
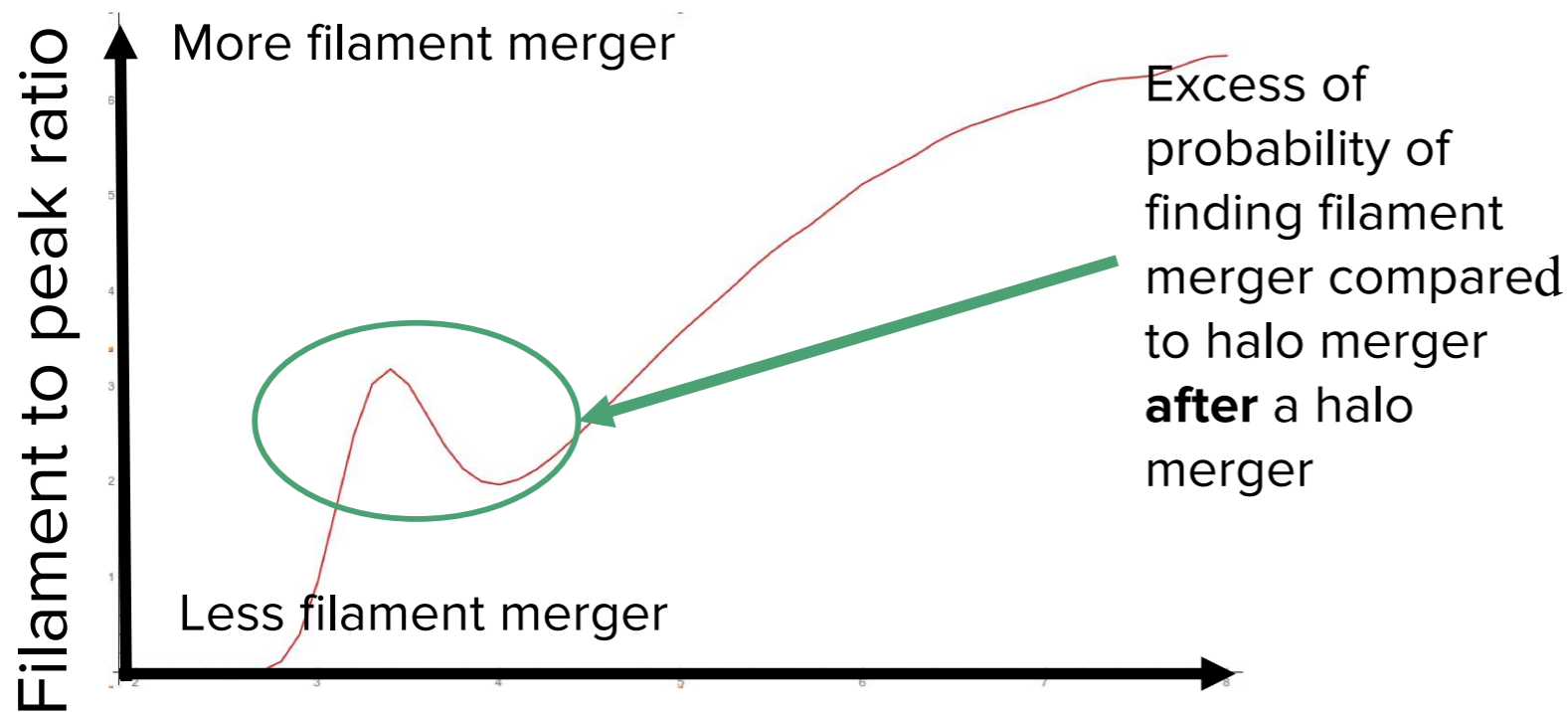


Typically, two to three dense filaments dominate and therefore define a plane of accretion... in agreement with numerical simulation (Danovich+12) and observations of plane of satellites around galaxies.

Application: preserving cosmic connectivity

On the connectivity of halos

Compute frequency of filament merger compared to halo merger in the vicinity of a halo merger event $\xi_{hf}(r)/\xi_{hh}(r)$.



$$1 + \xi_p = \frac{\langle \text{cond}_p(\mathbf{x}) \text{cond}_p(\mathbf{y}) \rangle}{\langle \text{cond}_p(\mathbf{x}) \rangle^2}, \quad 1 + \xi_f = \frac{\langle \text{cond}_f(\mathbf{x}) \text{cond}_p(\mathbf{y}) \rangle}{\langle \text{cond}_f(\mathbf{x}) \rangle \langle \text{cond}_p(\mathbf{x}) \rangle}$$

Upshot

Connectivity is a packaging pb because of exclusion

- ▶ Connectivity = number of filament connected
 - ▶ $\kappa = 4$ in 2D $\kappa = 6.11$ in 3D (for GRF)
- ▶ Multiplicity = number of *local* filament connected
 - ▶ $\mu \sim 3$ in 2D $\mu \sim 4$ in 3D
- ▶ Both can be predicted *from first principle*
- ▶ Hence useful for cosmology & galaxy formation

Upshot

- ▶ Set of critical events = useful topological compression of ICs
 - impacts 'dressed' mergers: ML on morphology?
(i.e. cosmic evolution of peaks and their filaments and walls).
- ▶ Clustering of filament disappearance is consistent with *preserving connectivity* of peaks as they merge:
 - the rarer the peak the higher the rate of filaments merging.
- ▶ Rate of wall disappearance = dark energy probe, depend on the growth rate of structure and $\sigma_2/\sigma_1\sigma_3$.

Conclusion

- ▶ Peak and constrained random field theories are paramount to understand the birth and growth of the cosmic web
- ▶ Many analytical results can be obtained in the weakly non-linear regime
- ▶ The topology and geometry of the cosmic web carries important cosmological information and is key for galaxy evolution.
- ▶ In particular, we now have a precise understanding of the connectivity of the cosmic web (the cosmic crystal) and its evolution through statistics of critical events.

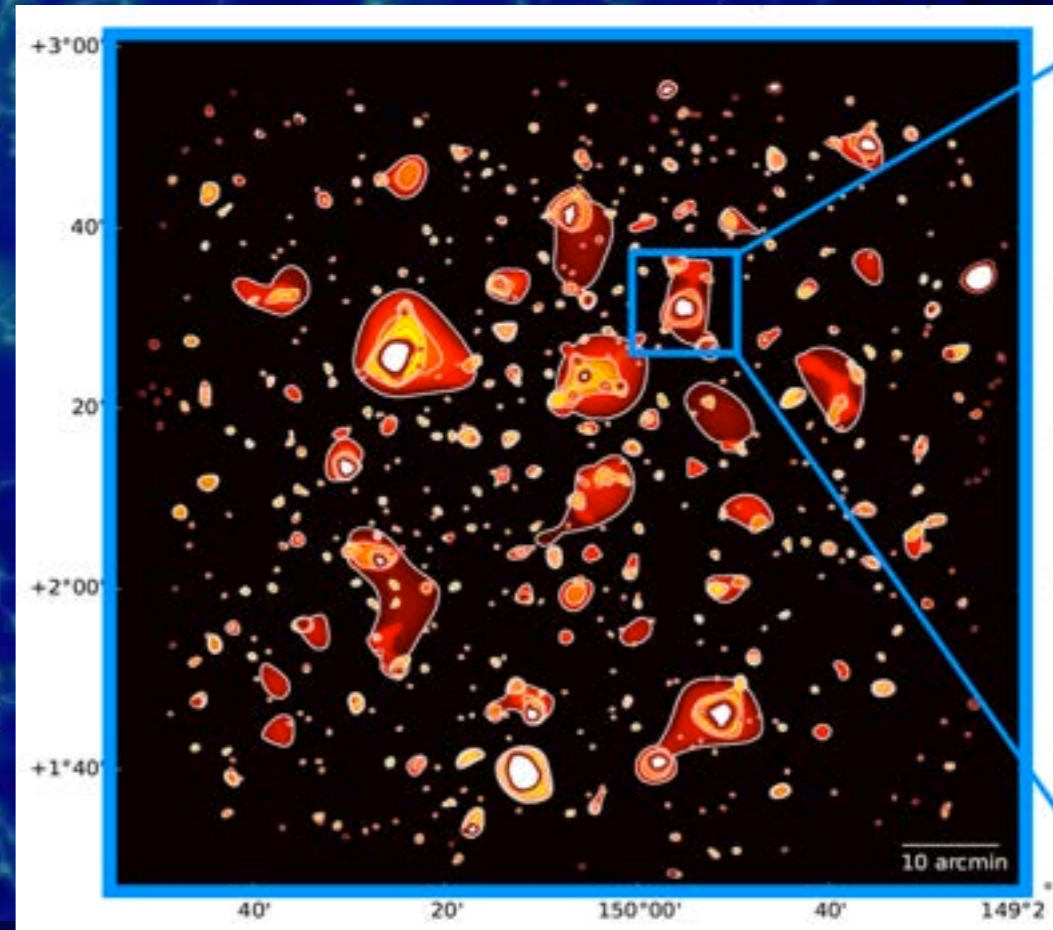
IMHO of interest beyond cosmology

Application: impact of AGN feedback?

X-Ray detected groups

filaments from galaxy distribution

Elise Darragh-Ford
Laigle, Gozaliasl, Pichon, Devriendt, Slyz et al.



Filament extraction in 2D around groups

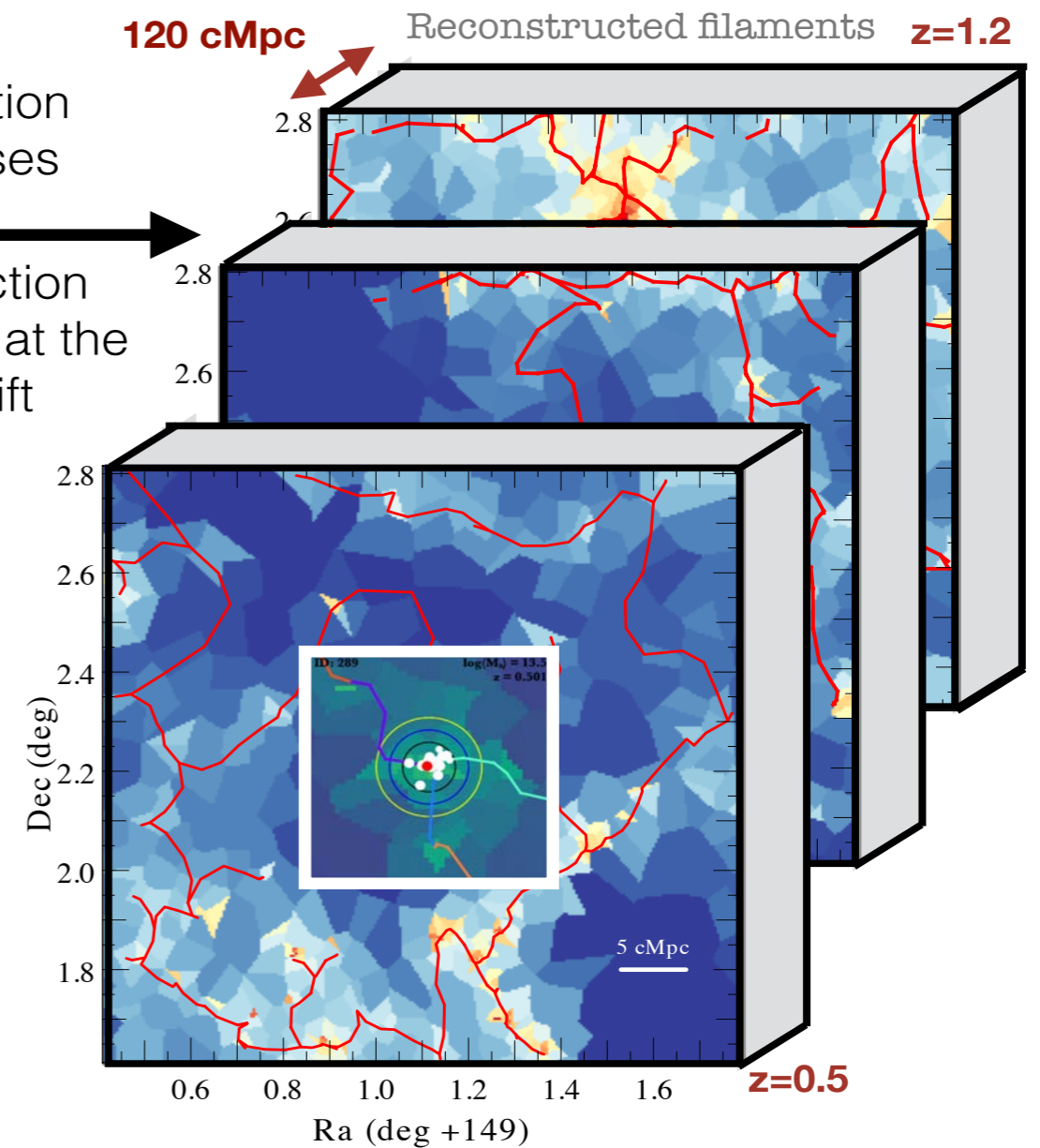
Darragh-Ford, Laigle et al. in prep

COSMOS
reference photometric field
1 million of galaxies



Galaxy extraction
redshift, masses

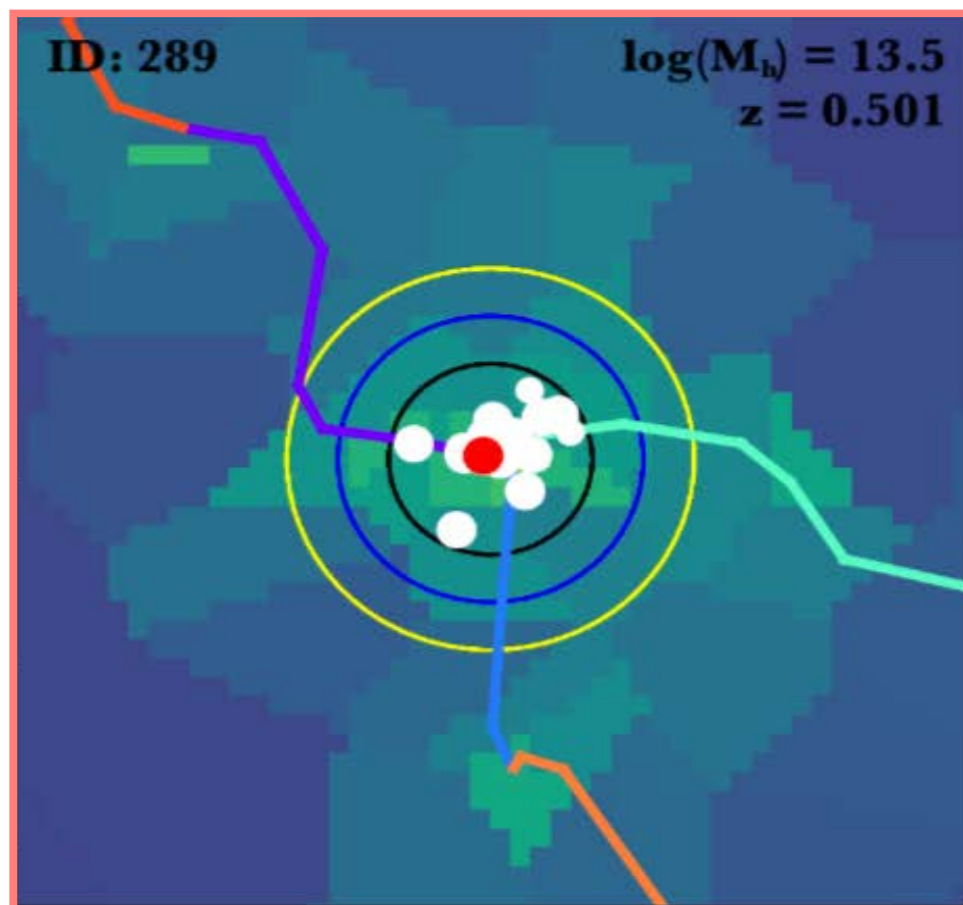
Filament extraction
in slices centred at the
group redshift



Redshift and mass range constrained by galaxy photometric properties:
We work in $0.5 < z < 1.2$ with all galaxies more massive than 10^{10} solar mass

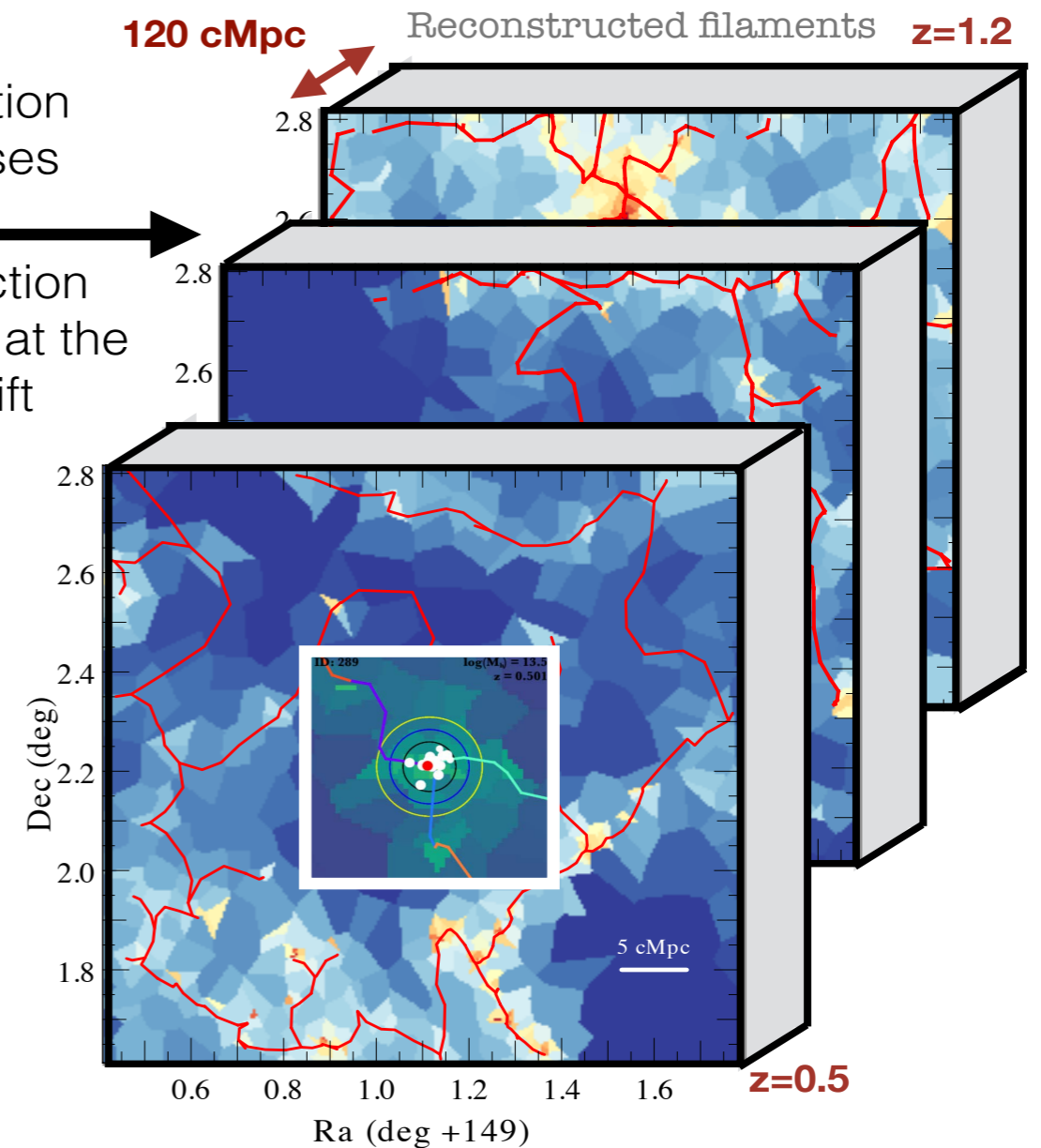
Filament extraction in 2D around groups

Darragh-Ford, Laigle et al. in prep



Galaxy extraction
redshift, masses

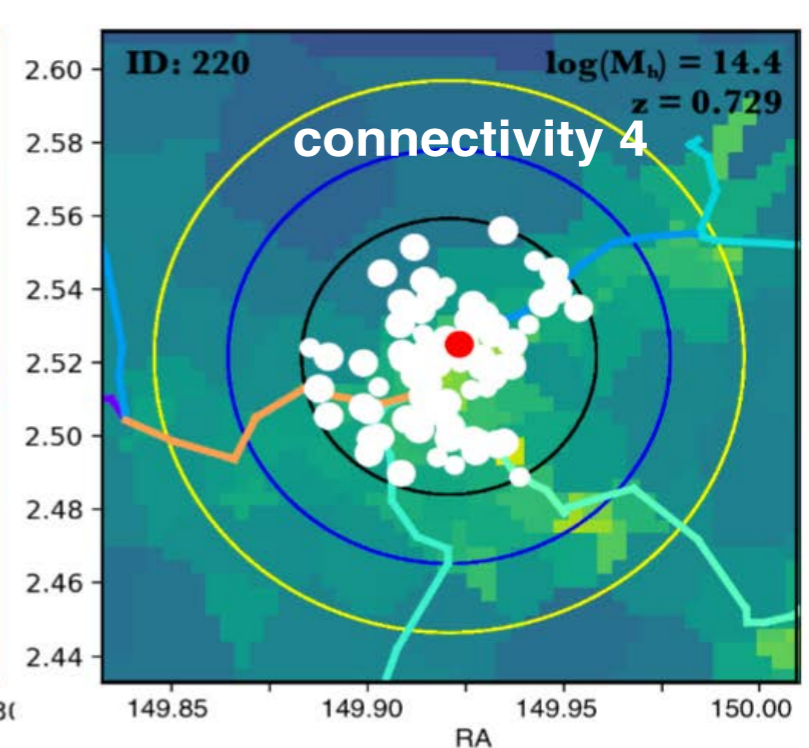
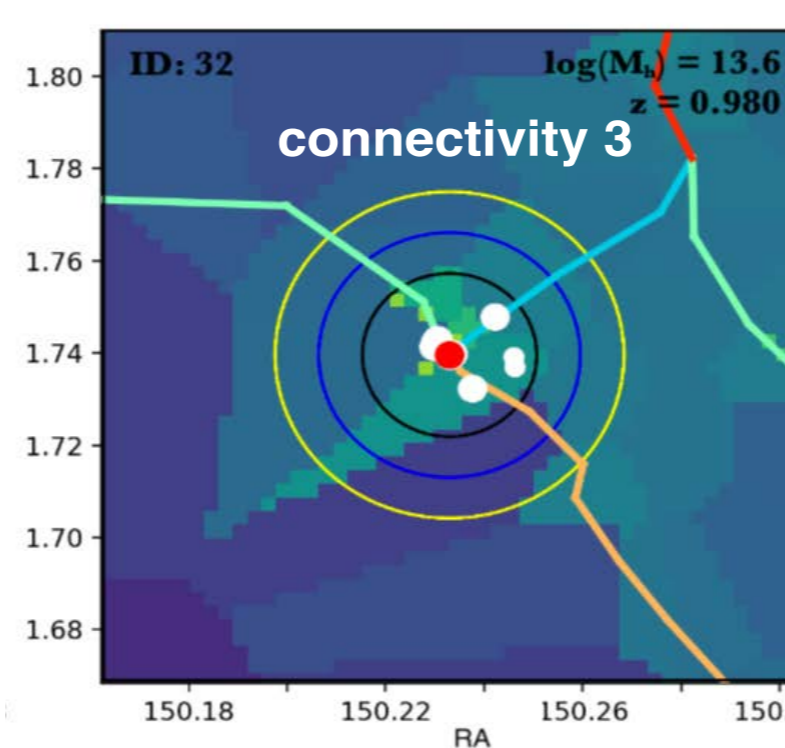
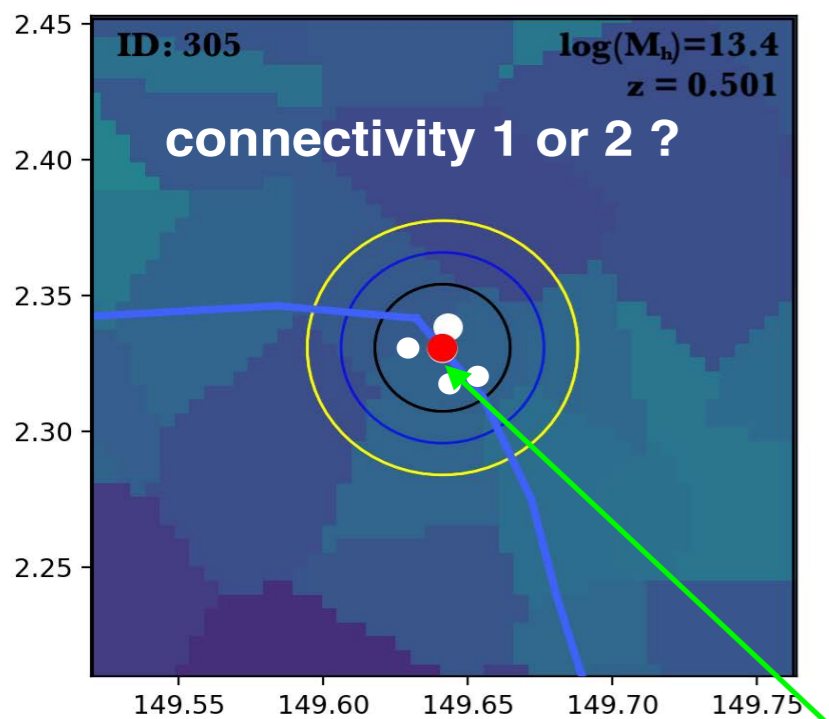
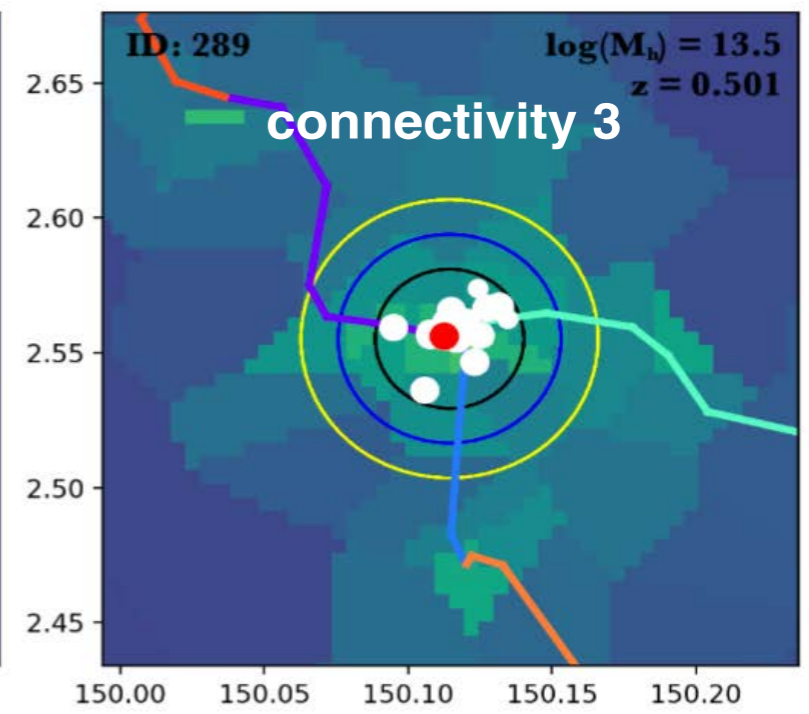
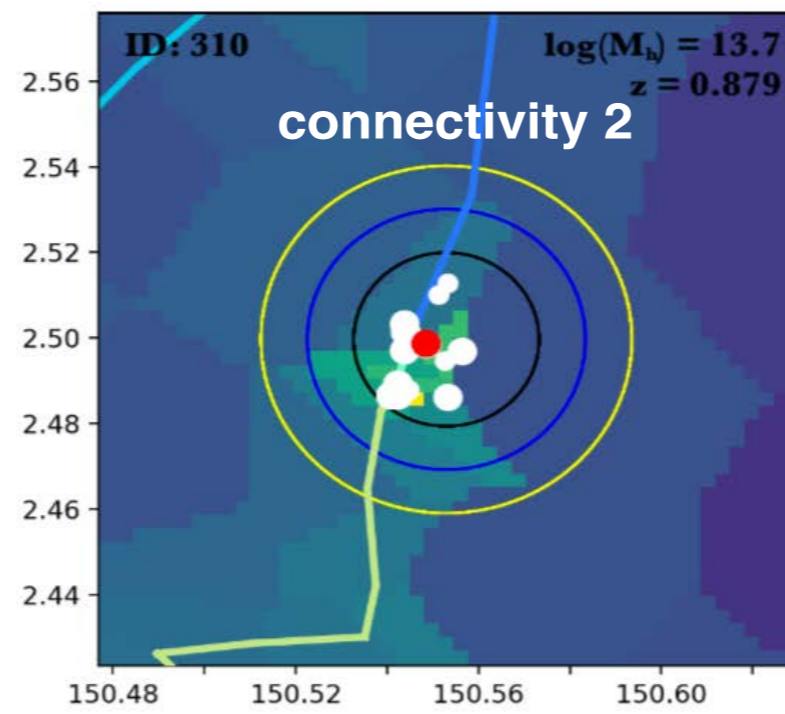
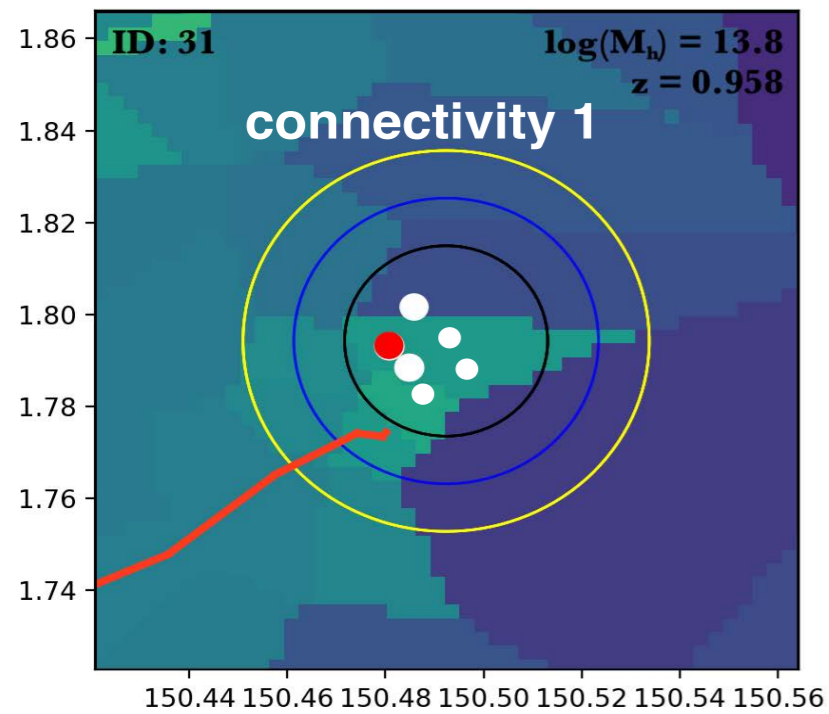
Filament extraction
in slices centred at the
group redshift



Redshift and mass range constrained by galaxy photometric properties:
We work in $0.5 < z < 1.2$ with all galaxies more massive than 10^{10} solar mass

Group Multiplicity

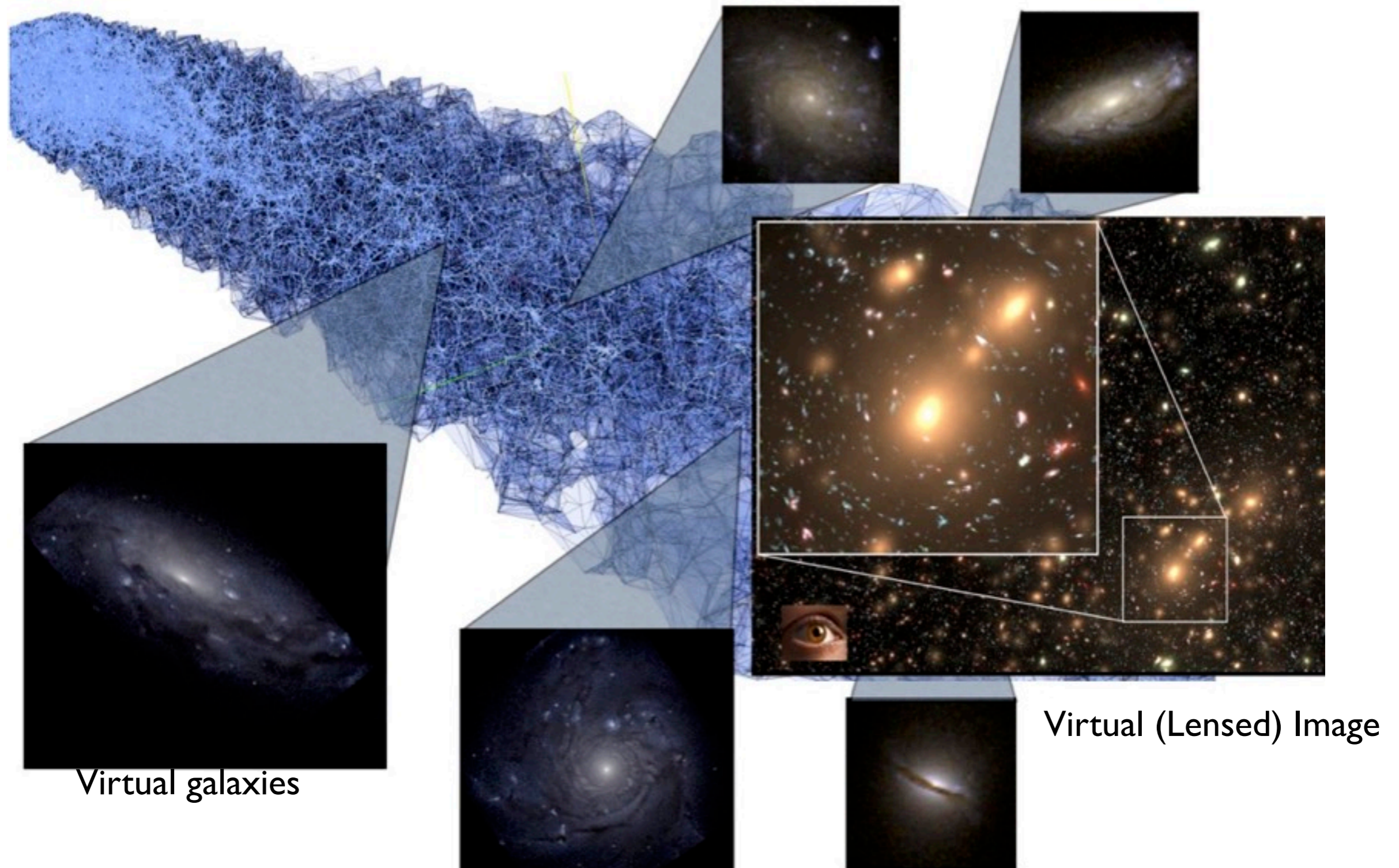
Measuring connectivity with photometric filaments



BGG: brightest group galaxy

Group Multiplicity in Horizon-AGN

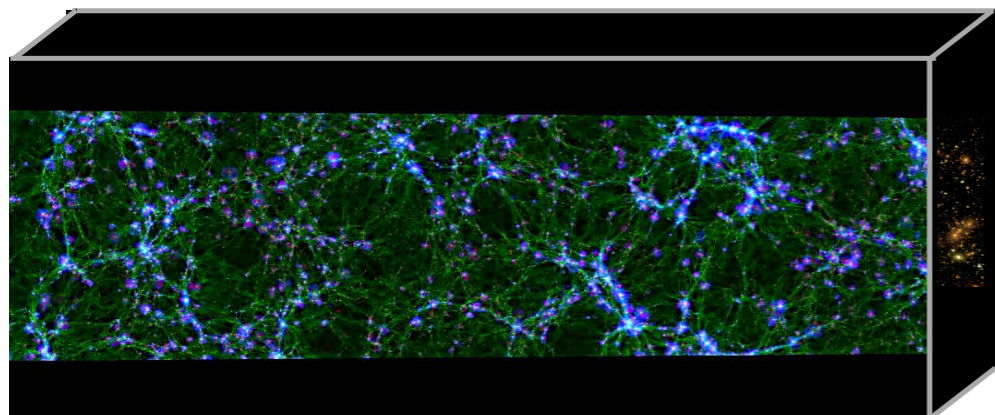
Testing the impact of photometric uncertainties



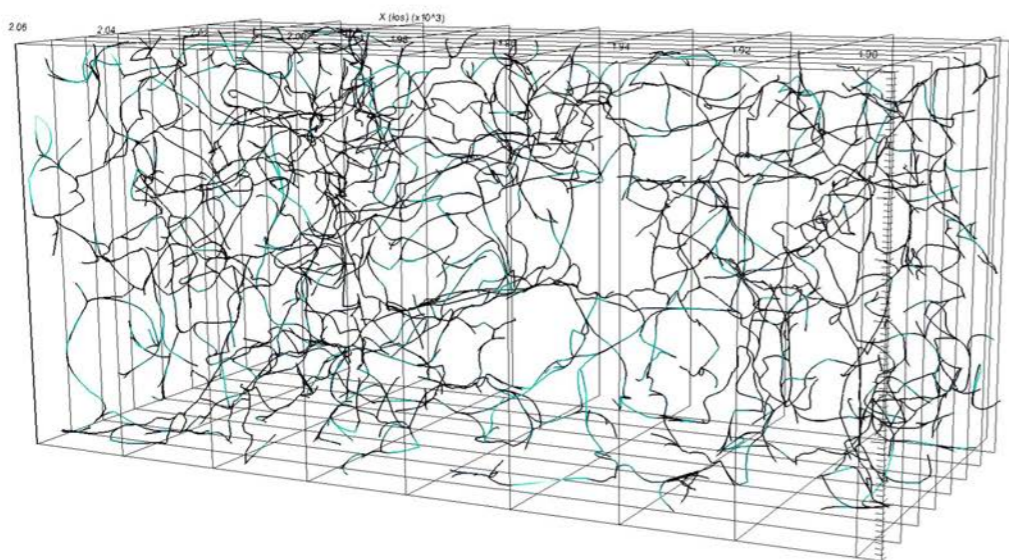
Group Multiplicity in Horizon-AGN

Testing the impact of photometric uncertainties

Hydrodynamical simulation Horizon-AGN
Dubois+14



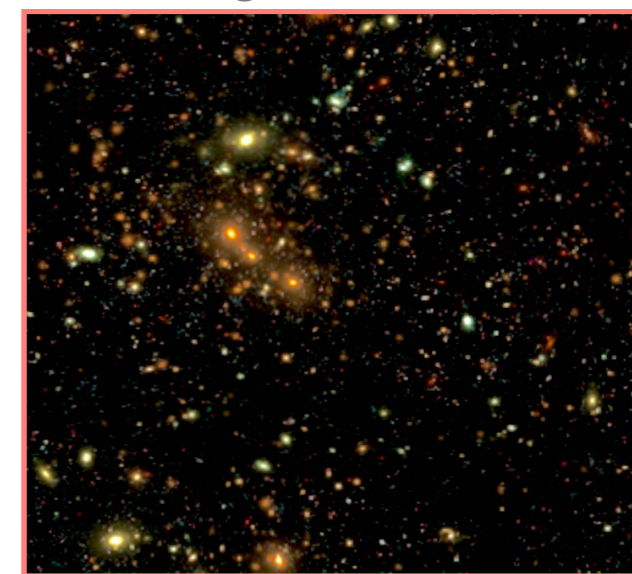
3D reference skeleton



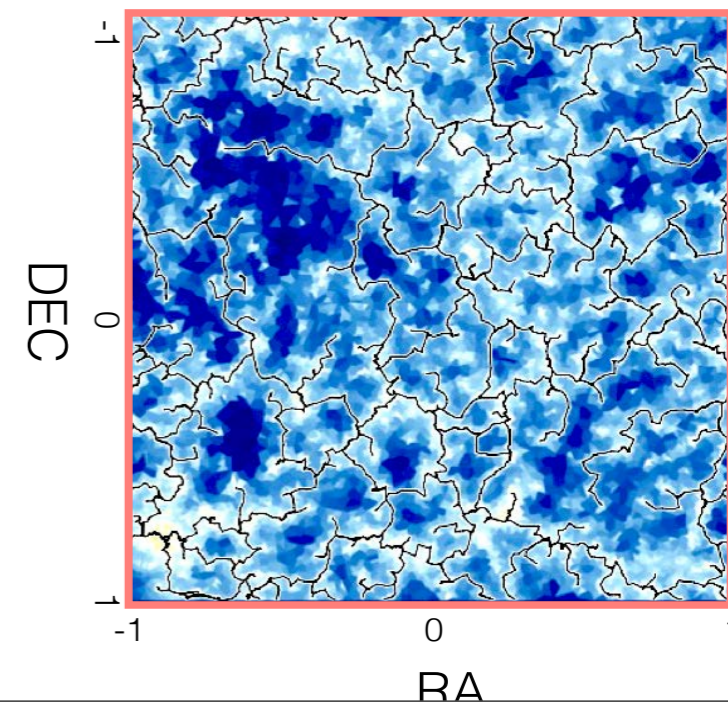
Mock observation generation
(photometry, photo-z, photometric masses)

Adding errors
(including systematics)

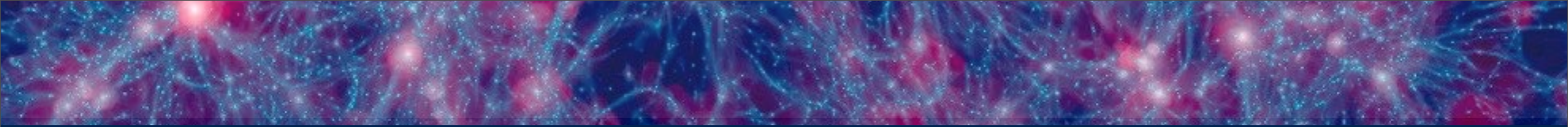
Mock image



Virtually observed skeleton



Confrontation



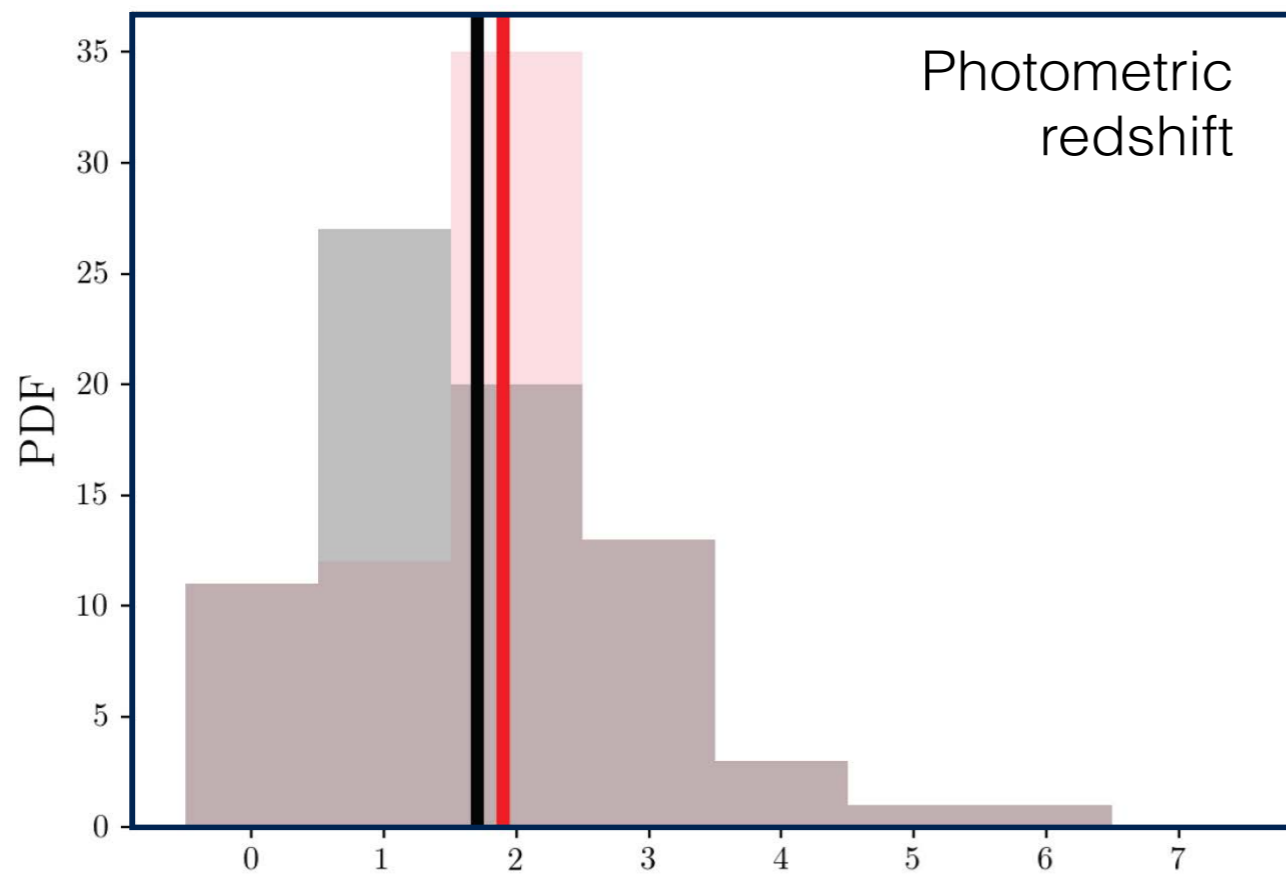
Group Multiplicity

Measuring connectivity with photometric filaments

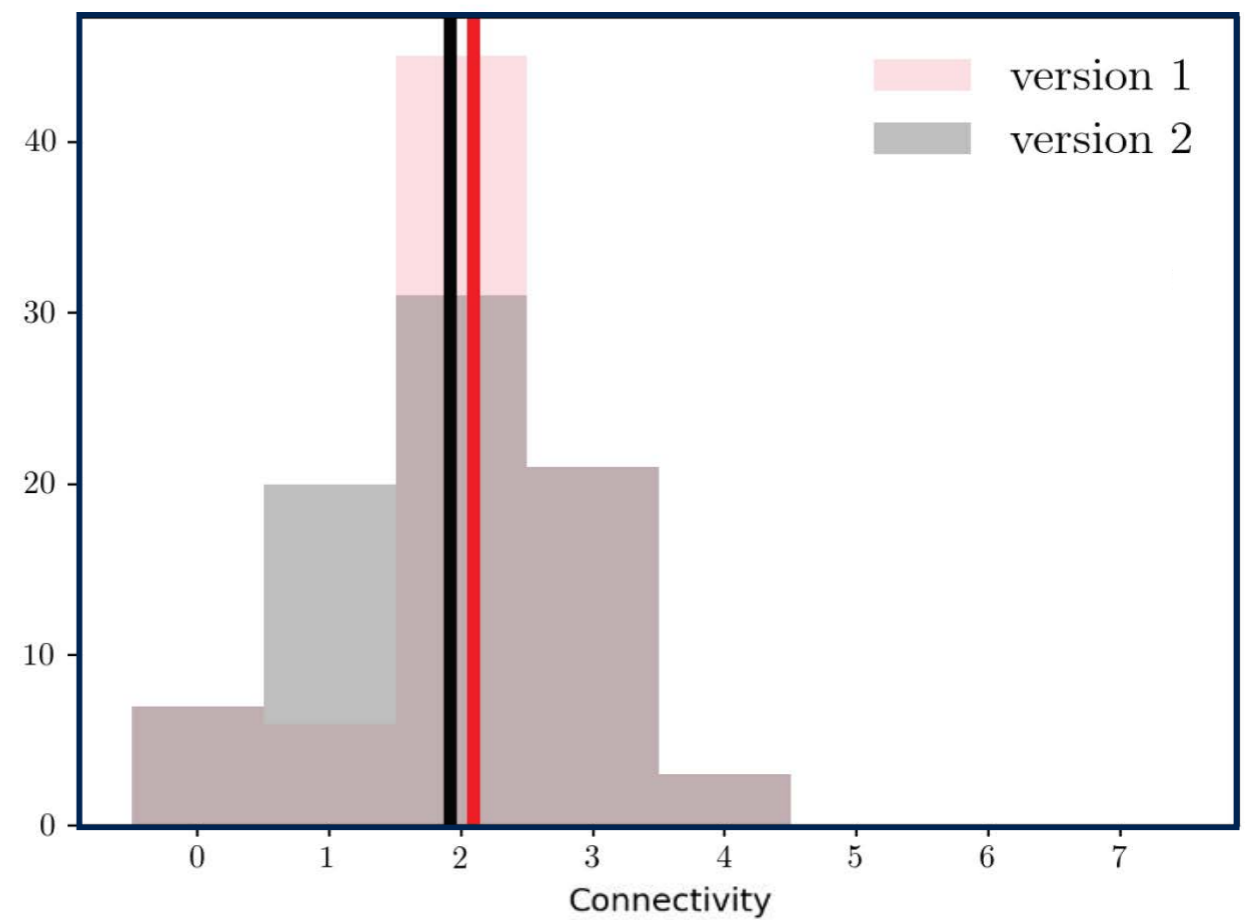
Darragh-Ford, Laigle et al. in prep

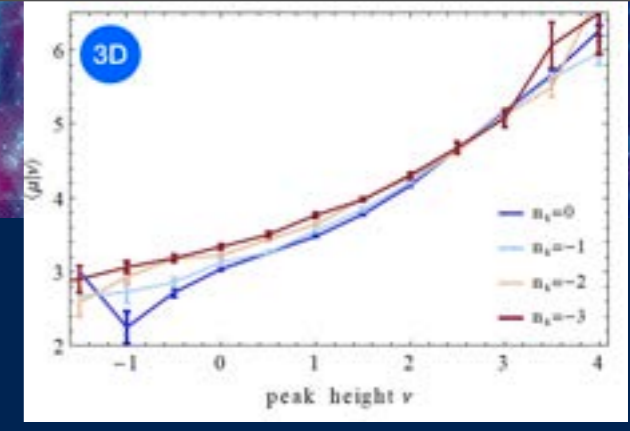
photo-z uncertainties decrease connectivity

Hz-AGN connectivity



COSMOS connectivity





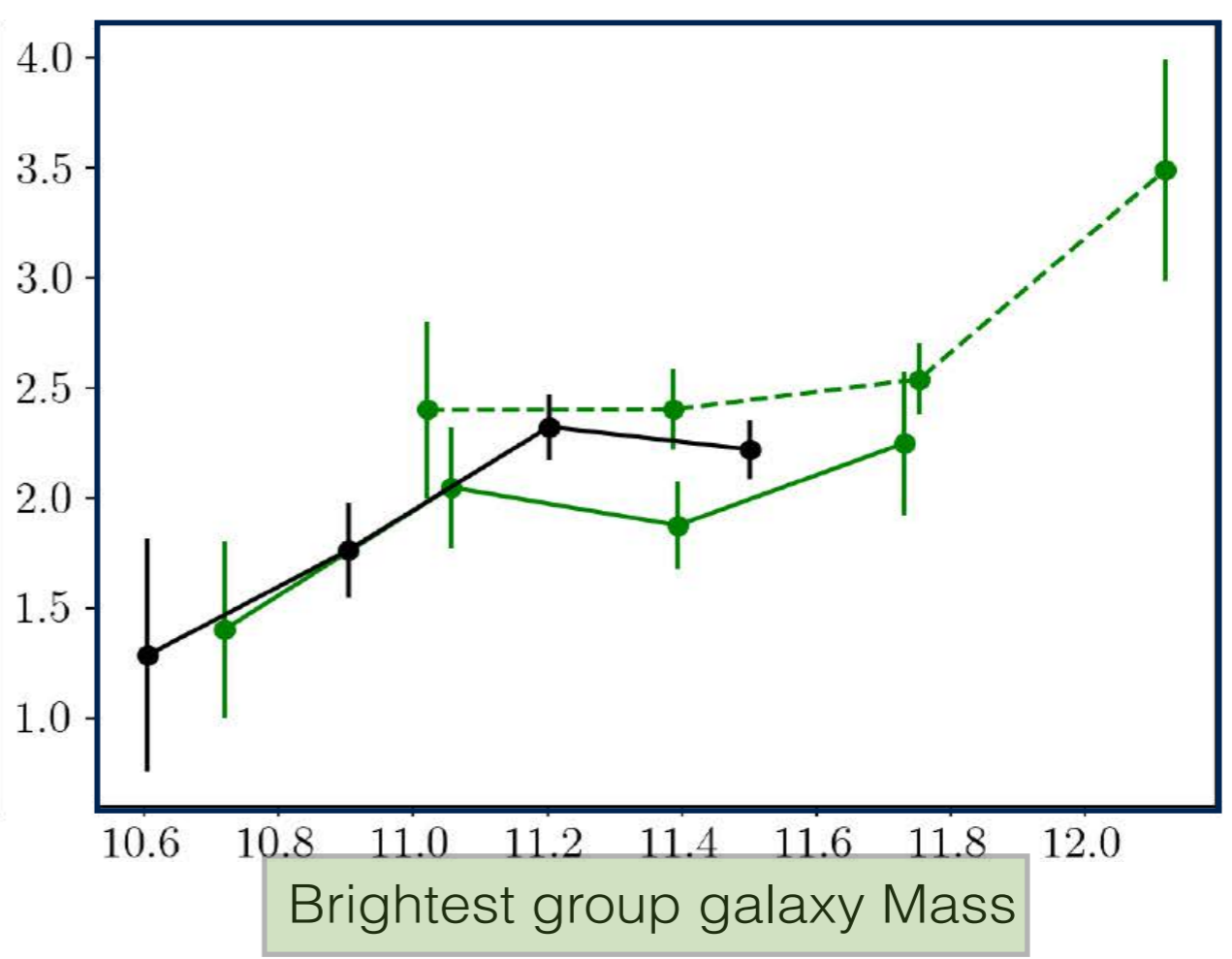
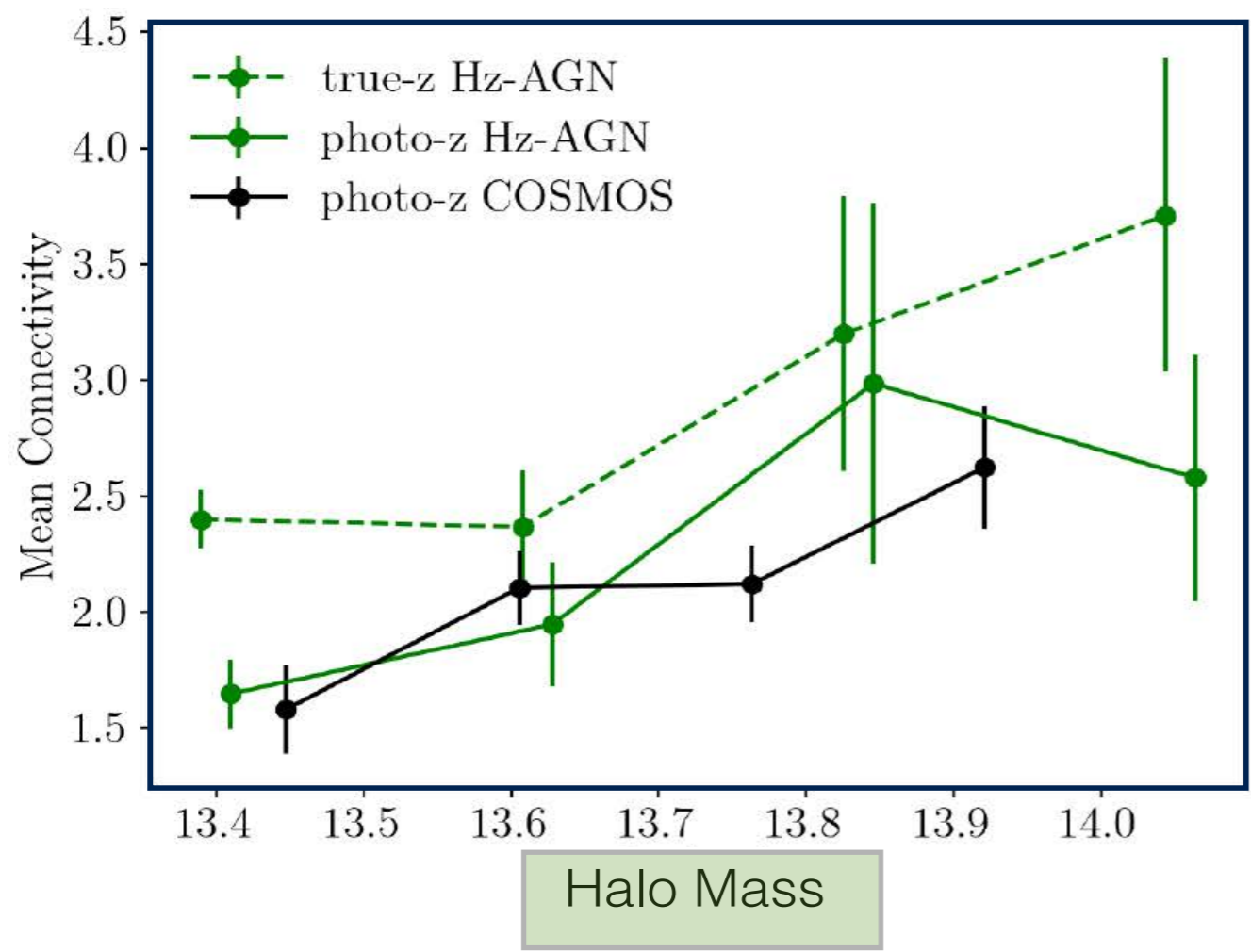
Group Multiplicity

Impact of connectivity on group properties

Darragh-Ford, Laigle et al. in prep

see also
Theoretical predictions from
Codis et al. 2018

Mean connectivity increases with halo/BGG mass

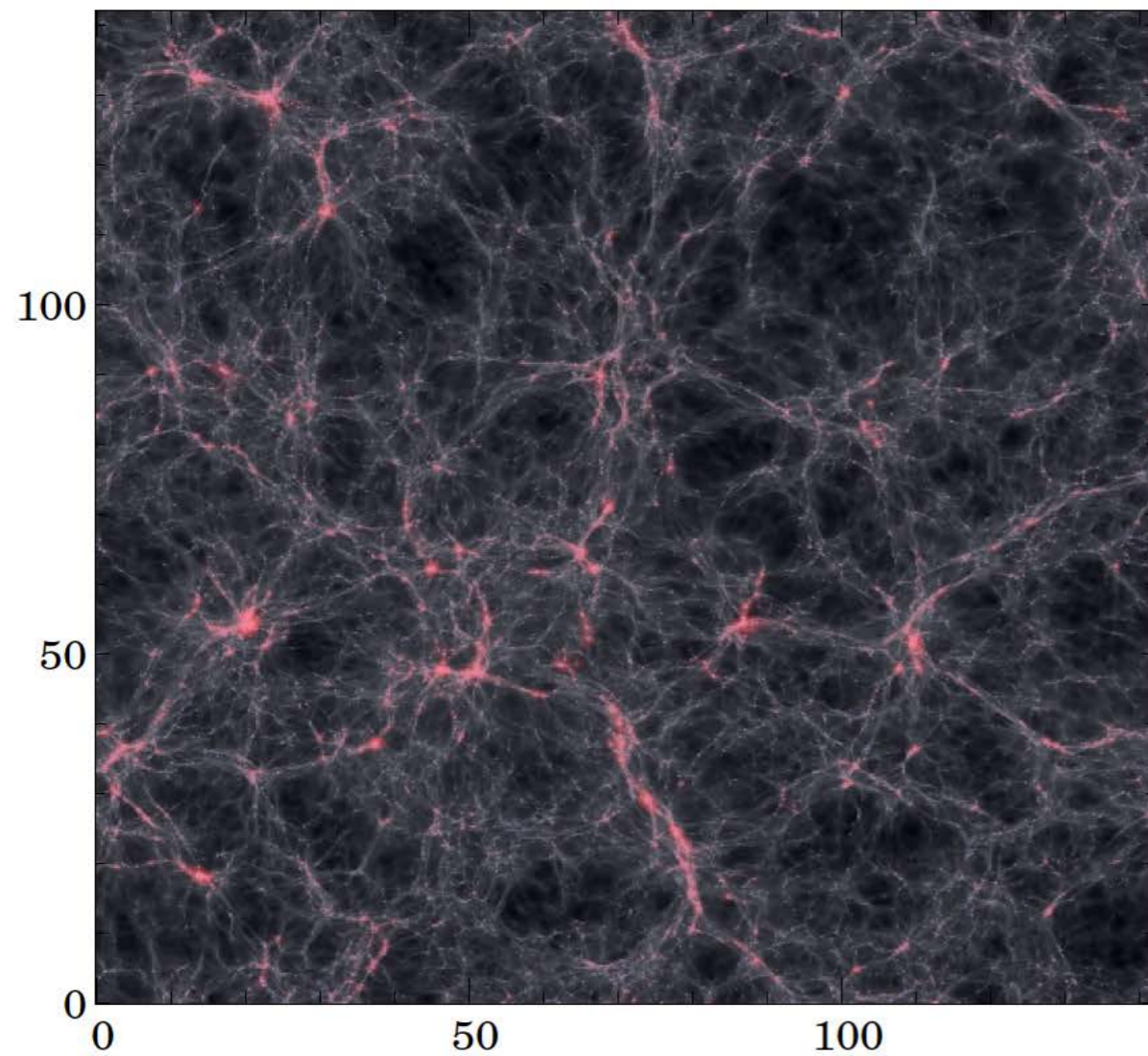


The impact of Multiplicity on BGG properties

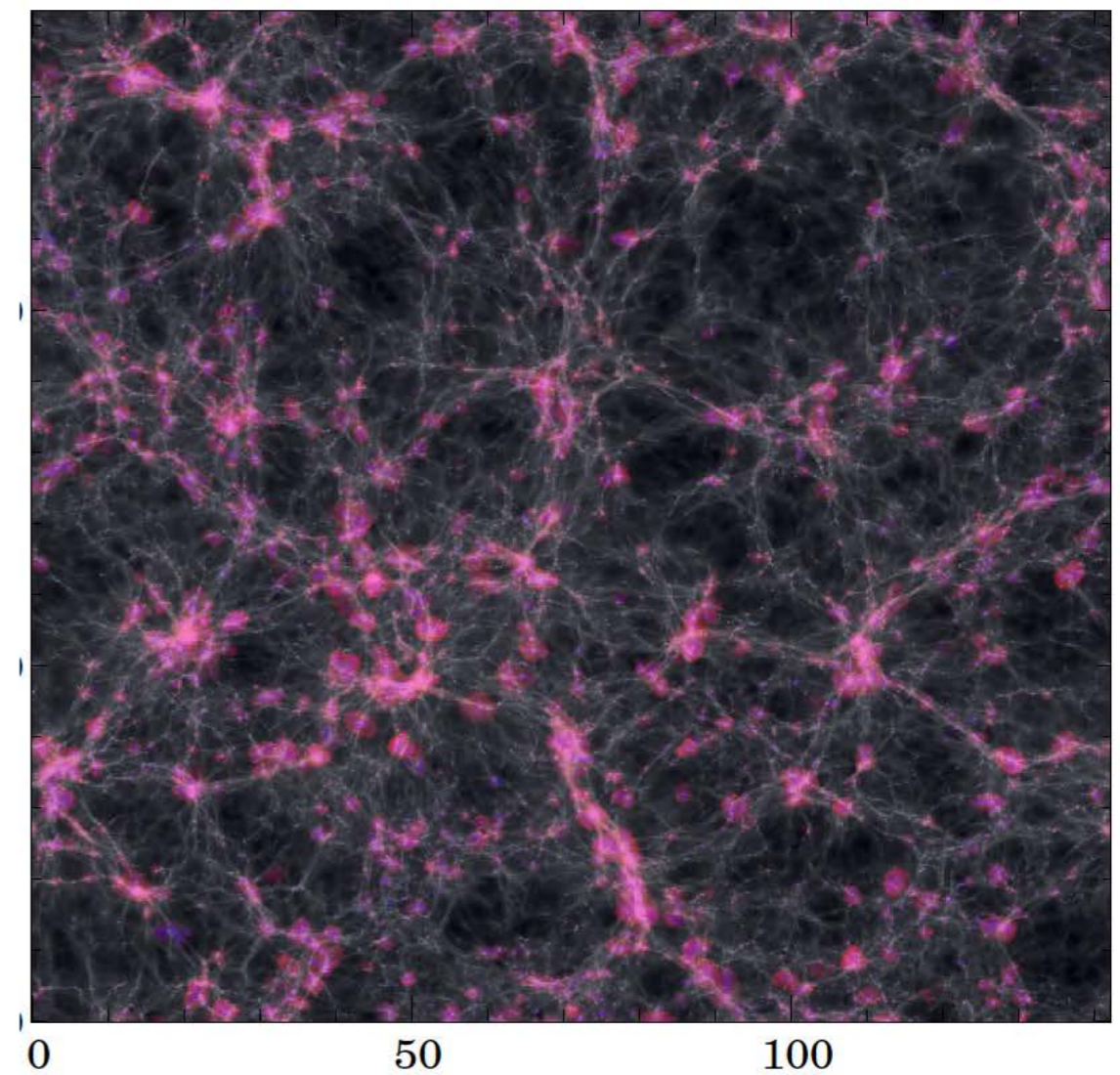
Interpretation from Horizon-AGN simulation

Darragh-Ford, Laigle et al. in prep

Horizon-noAGN



Horizon-AGN



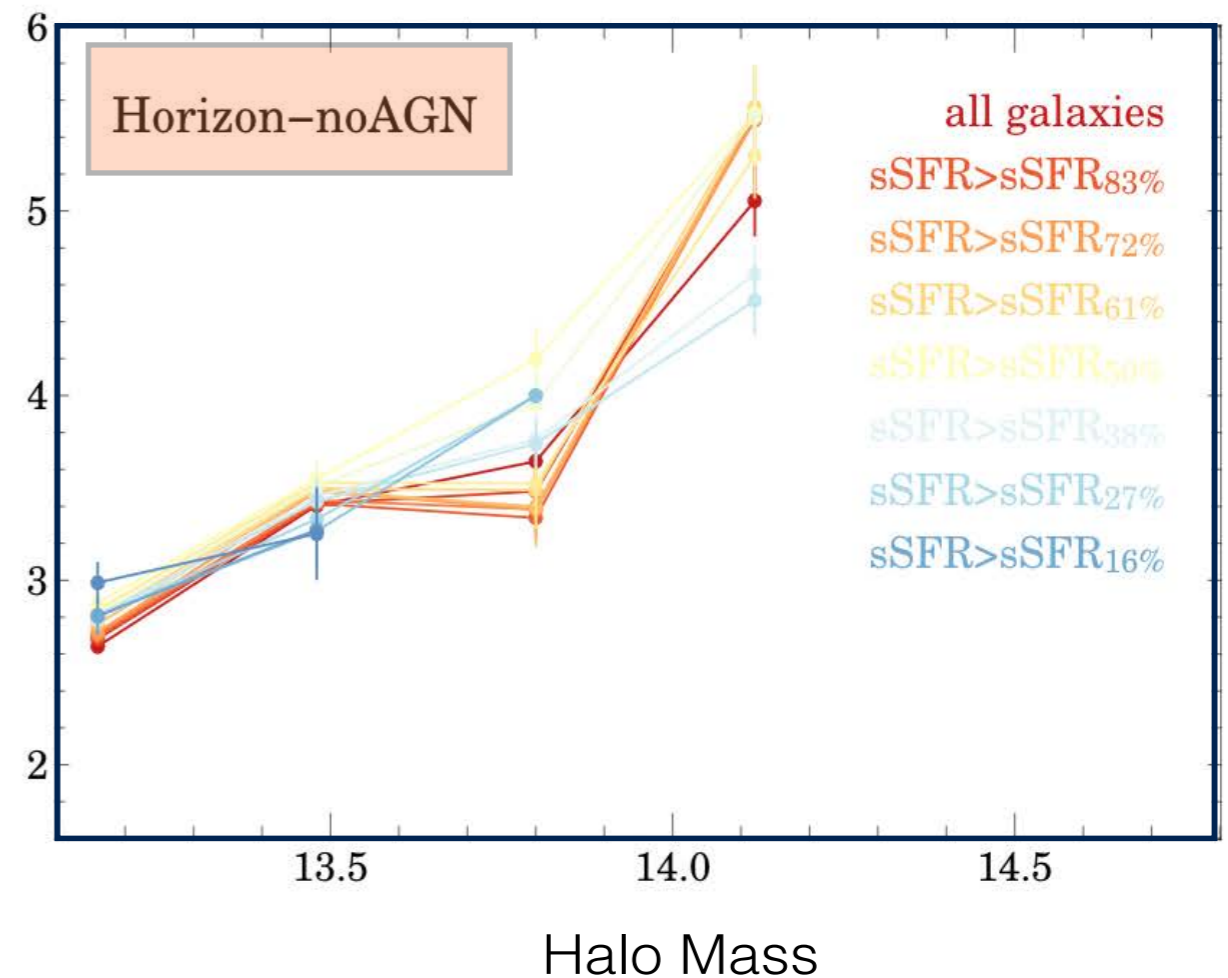
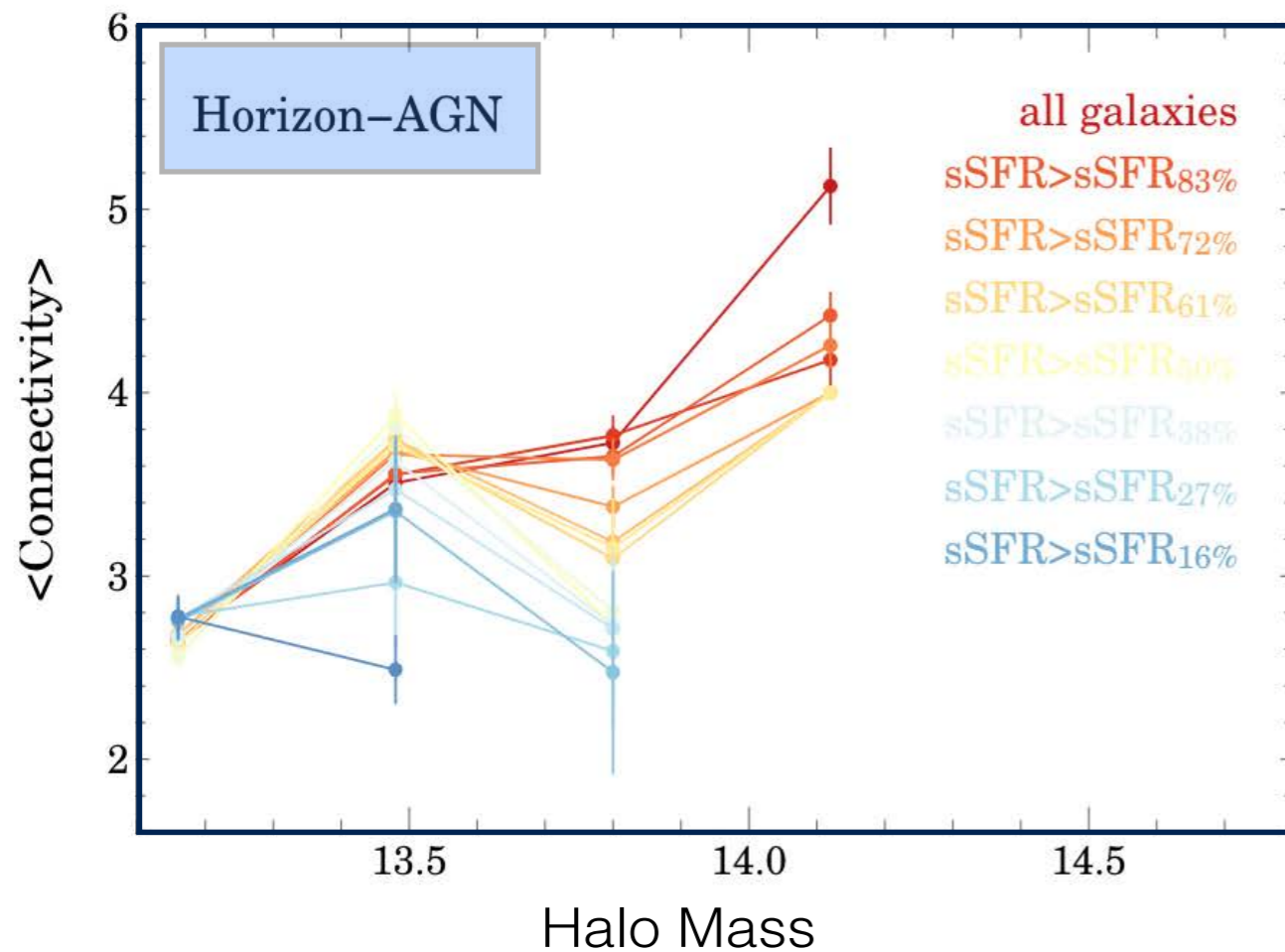
Group Multiplicity

Impact of connectivity on group properties

Darragh-Ford, Laigle, et al in prep

HORIZON-AGN simulation result:

At a given halo mass, “AGN quenching efficiency” is higher at higher connectivity



- Connectivity: proxy for mass of accreted matter; more accretion \Rightarrow higher feedback?
- higher connectivity \Rightarrow accretion more isotropic

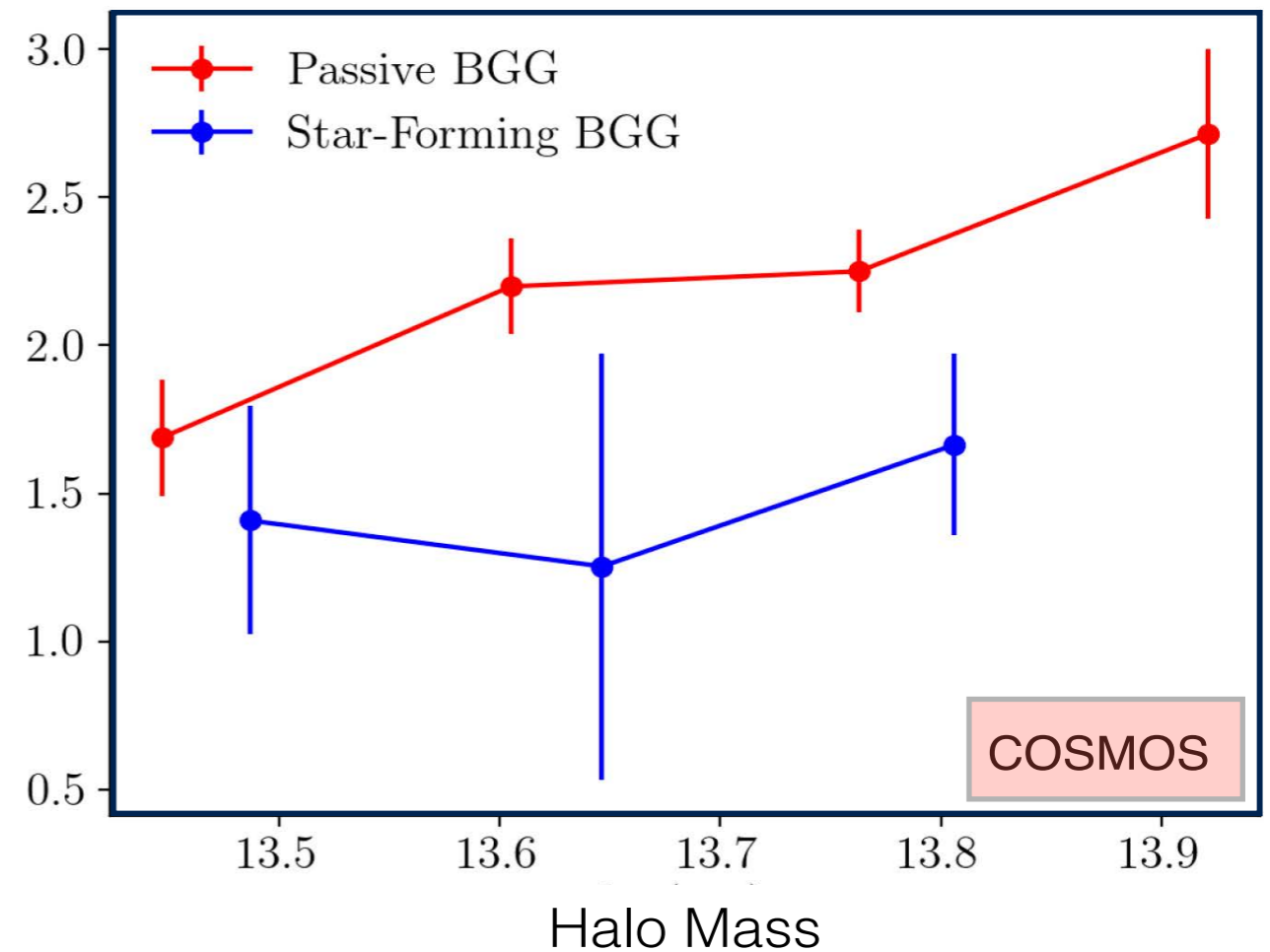
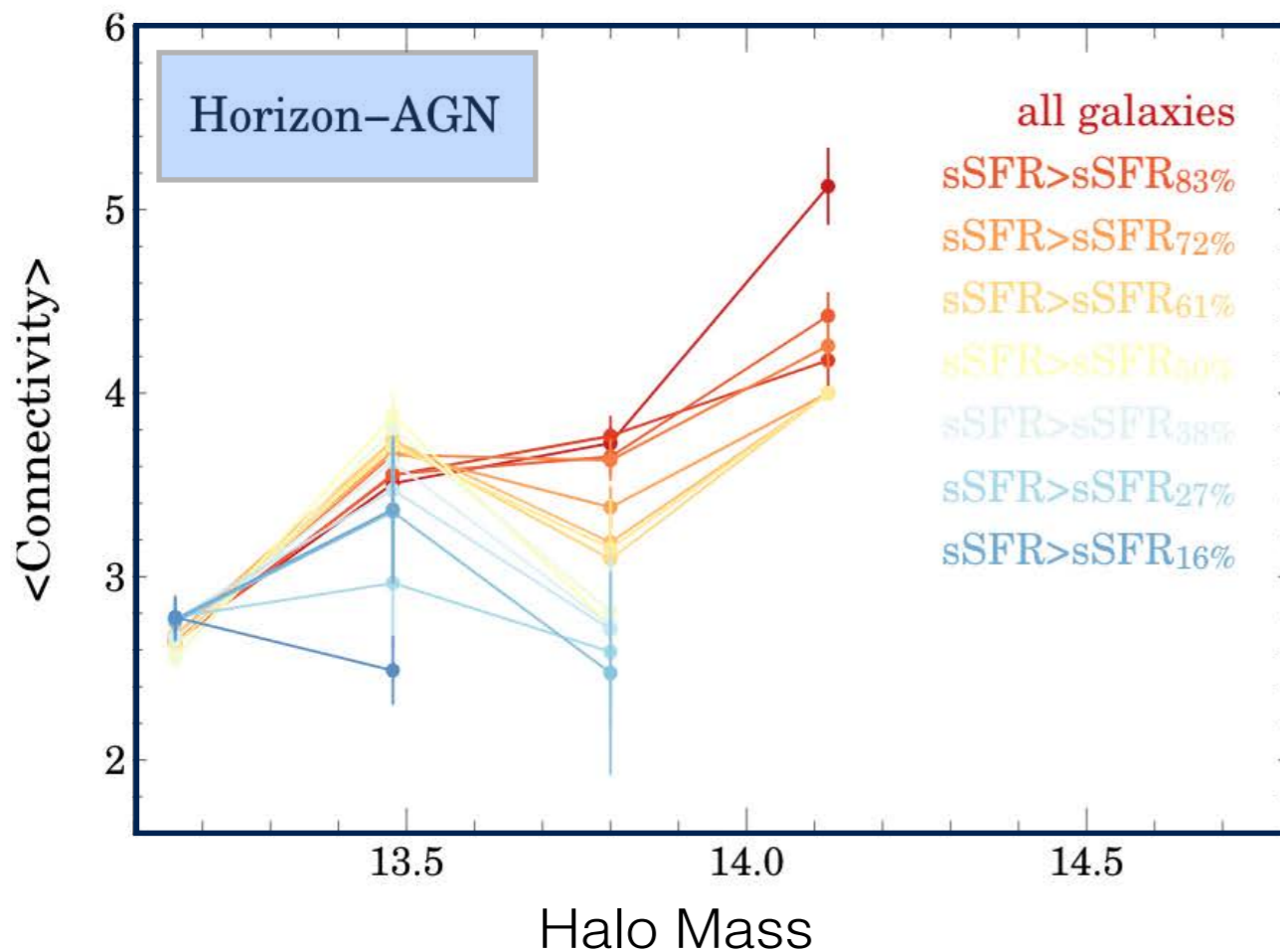
Group Multiplicity

Impact of connectivity on group properties

Darragh-Ford, Laigle, et al in prep

HORIZON-AGN simulation result:

At a given halo mass, “AGN quenching efficiency” is higher at higher connectivity



- Connectivity: proxy for mass of accreted matter; more accretion \Rightarrow higher feedback?
- higher connectivity \Rightarrow accretion more isotropic

Connectivity: measuring DE ?

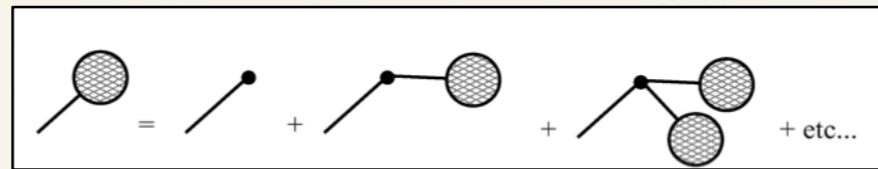
Generalized geometrical S_n

Purpose: Express the invariant **cumulants** in terms of σ (hence $D(z)$) through Perturbation theory *e.g.* $\langle J_1 x \rangle = \text{function}(\sigma)$

$$F_2(\mathbf{k}_1, \mathbf{k}_2) = \frac{5}{7} + \frac{\mathbf{k}_1 \cdot \mathbf{k}_2}{k_1^2} + \frac{2}{7} \frac{(\mathbf{k}_1 \cdot \mathbf{k}_2)^2}{k_1^2 k_2^2} \implies \mathcal{F}_{\alpha, \beta, \gamma}(\mathbf{k}_1, \mathbf{k}_2) = F_2(\mathbf{k}_1, \mathbf{k}_2) \mathcal{G}_{\alpha, \beta, \gamma}(\mathbf{k}_1, \mathbf{k}_2)$$

GRAVITY

Geometric shape factor = powers of k



$$\delta^{(n)}(\vec{k}) = \int d^3 \vec{k}_1 \dots d^3 \vec{k}_n \delta^D(\vec{k} - (\vec{k}_1 + \dots + \vec{k}_n)) F_n(\vec{k}_1, \dots, \vec{k}_n) \delta^{(1)}(\vec{k}_1) \dots \delta^{(1)}(\vec{k}_n),$$

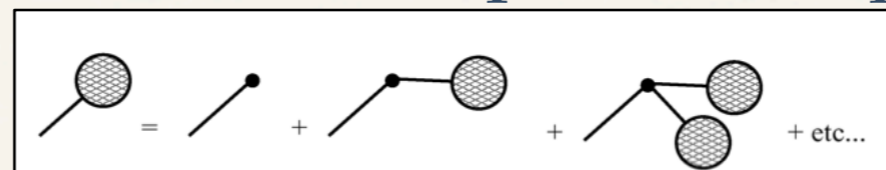
Generalized geometrical S_n

Purpose: Express the invariant **cumulants** in terms of σ (hence $D(z)$) through Perturbation theory *e.g.* $\langle J_1 x \rangle = \text{function}(\sigma)$

$$F_2(\mathbf{k}_1, \mathbf{k}_2) = \frac{5}{7} + \frac{\mathbf{k}_1 \cdot \mathbf{k}_2}{k_1^2} + \frac{2 (\mathbf{k}_1 \cdot \mathbf{k}_2)^2}{7 k_1^2 k_2^2} \implies \mathcal{F}_{\alpha, \beta, \gamma}(\mathbf{k}_1, \mathbf{k}_2) = F_2(\mathbf{k}_1, \mathbf{k}_2) \mathcal{G}_{\alpha, \beta, \gamma}(\mathbf{k}_1, \mathbf{k}_2)$$

GRAVITY

Geometric shape factor = powers of k



power spectrum index

$$\frac{1}{\sigma} \langle x^3 \rangle = 3 {}_2F_1 \left(\frac{3+n}{2}, \frac{3+n}{2}, \frac{3}{2}, \frac{1}{4} \right) - \frac{1}{7} (8 + 7n) {}_2F_1 \left(\frac{3+n}{2}, \frac{3+n}{2}, \frac{5}{2}, \frac{1}{4} \right) .$$

skewness of field

Lokas 94

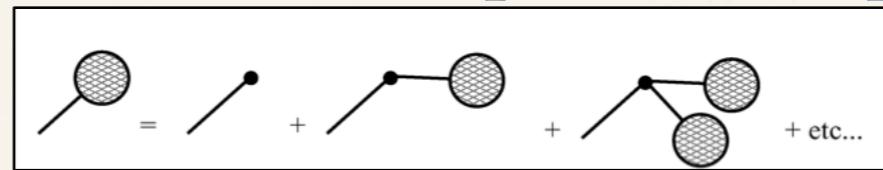
Generalized geometrical S_n

Purpose: Express the invariant **cumulants** in terms of σ (hence $D(z)$) through Perturbation theory *e.g.* $\langle J_1 x \rangle = \text{function}(\sigma)$

$$F_2(\mathbf{k}_1, \mathbf{k}_2) = \frac{5}{7} + \frac{\mathbf{k}_1 \cdot \mathbf{k}_2}{k_1^2} + \frac{2}{7} \frac{(\mathbf{k}_1 \cdot \mathbf{k}_2)^2}{k_1^2 k_2^2} \implies \mathcal{F}_{\alpha, \beta, \gamma}(\mathbf{k}_1, \mathbf{k}_2) = F_2(\mathbf{k}_1, \mathbf{k}_2) \mathcal{G}_{\alpha, \beta, \gamma}(\mathbf{k}_1, \mathbf{k}_2)$$

GRAVITY

Geometric shape factor = powers of k



power spectrum index

$$\frac{1}{\sigma} \langle x^3 \rangle = 3 {}_2F_1 \left(\frac{3+n}{2}, \frac{3+n}{2}, \frac{3}{2}, \frac{1}{4} \right) - \frac{1}{7} (8+7n) {}_2F_1 \left(\frac{3+n}{2}, \frac{3+n}{2}, \frac{5}{2}, \frac{1}{4} \right)$$

skewness of field

Lokas 94

$$\frac{1}{\sigma} \langle x x_1^2 \rangle = \frac{4(48 + 62n + 21n^2)}{21n^2} {}_2F_1 \left(\frac{3+n}{2}, \frac{3+n}{2}, \frac{3}{2}, \frac{1}{4} \right) - \frac{6(3+n)(8+7n)}{21n^2} {}_2F_1 \left(\frac{3+n}{2}, \frac{5+n}{2}, \frac{3}{2}, \frac{1}{4} \right)$$

3pt field- gradient cumulant

$$n = -3 : \quad \frac{1}{\sigma} \langle x^3 \rangle = \frac{34}{7} \implies \frac{1}{\sigma} \langle x x_1^2 \rangle = \frac{34}{7} \frac{2}{3^2}$$

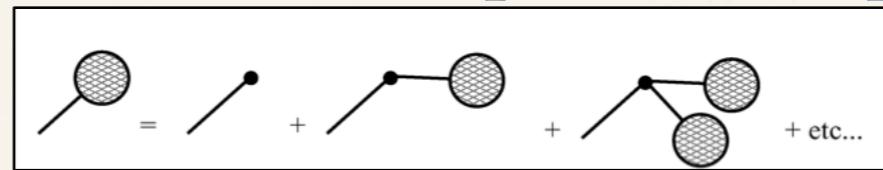
Generalized geometrical S_n

Purpose: Express the invariant **cumulants** in terms of σ (hence $D(z)$) through Perturbation theory *e.g.* $\langle J_1 x \rangle = \text{function}(\sigma)$

$$F_2(\mathbf{k}_1, \mathbf{k}_2) = \frac{5}{7} + \frac{\mathbf{k}_1 \cdot \mathbf{k}_2}{k_1^2} + \frac{2}{7} \frac{(\mathbf{k}_1 \cdot \mathbf{k}_2)^2}{k_1^2 k_2^2} \implies \mathcal{F}_{\alpha, \beta, \gamma}(\mathbf{k}_1, \mathbf{k}_2) = F_2(\mathbf{k}_1, \mathbf{k}_2) \mathcal{G}_{\alpha, \beta, \gamma}(\mathbf{k}_1, \mathbf{k}_2)$$

GRAVITY

Geometric shape factor = powers of k



power spectrum index

$$\frac{1}{\sigma} \langle x^3 \rangle = 3 {}_2F_1 \left(\frac{3+n}{2}, \frac{3+n}{2}, \frac{3}{2}, \frac{1}{4} \right) - \frac{1}{7} (8+7n) {}_2F_1 \left(\frac{3+n}{2}, \frac{3+n}{2}, \frac{5}{2}, \frac{1}{4} \right) .$$

skewness of field

Lokas 94

See also Bouchet for S4

$$\frac{1}{\sigma} \langle x x_1^2 \rangle = \frac{4(48 + 62n + 21n^2)}{21n^2} {}_2F_1 \left(\frac{3+n}{2}, \frac{3+n}{2}, \frac{3}{2}, \frac{1}{4} \right) - \frac{6(3+n)(8+7n)}{21n^2} {}_2F_1 \left(\frac{3+n}{2}, \frac{5+n}{2}, \frac{3}{2}, \frac{1}{4} \right)$$

3pt field- gradient cumulant

$$n = -3 : \quad \frac{1}{\sigma} \langle x^3 \rangle = \frac{34}{7} \implies \frac{1}{\sigma} \langle x x_1^2 \rangle = \frac{34}{7} \frac{2}{3^2}$$

Generalized geometrical S_n

Purpose: Express the invariant **cumulants** in terms of σ (hence $D(z)$) through Perturbation theory *e.g.* $\langle J_1 x \rangle = \text{function}(\sigma)$

$$F_2(\mathbf{k}_1, \mathbf{k}_2) = \frac{5}{7} + \frac{\mathbf{k}_1 \cdot \mathbf{k}_2}{k_1^2} + \dots$$

	$n_s = 0$	
	prediction	measurement
$\langle x^3 \rangle / \sigma$	3.144	3.08 ± 0.08
$\langle x q^2 \rangle / \sigma$	2.096	2.05 ± 0.03
$\langle x^2 J_1 \rangle / \sigma$	-3.248	-3.15 ± 0.06
$\langle x J_1^2 \rangle / \sigma$	3.871	3.75 ± 0.06
$\langle x J_2 \rangle / \sigma$	1.545	1.54 ± 0.02
$\langle q^2 J_1 \rangle / \sigma$	-1.335	-1.28 ± 0.02
$\langle J_1^3 \rangle / \sigma$	-4.644	-4.50 ± 0.08
$\langle J_1 J_2 \rangle / \sigma$	-0.679	-0.65 ± 0.01
$\langle J_3 \rangle / \sigma$	1.304	1.28 ± 0.03

$$F_2(\mathbf{k}_1, \mathbf{k}_2) = F_2(\mathbf{k}_1, \mathbf{k}_2) \mathcal{G}_{\alpha, \beta, \gamma}(\mathbf{k}_1, \mathbf{k}_2)$$

GRAVITY

power spectrum index powers of k

power spectrum index

$$\frac{1}{\sigma} \langle x^3 \rangle = 3 {}_2F_1 \left(\frac{3+n}{2}, \frac{3+n}{2}, \frac{3}{2}, \frac{1}{4} \right) - \frac{1}{7} (8+7n) {}_2F_1 \left(\frac{3+n}{2}, \frac{3+n}{2}, \frac{5}{2}, \frac{1}{4} \right)$$

skewness of field

Lokas 94



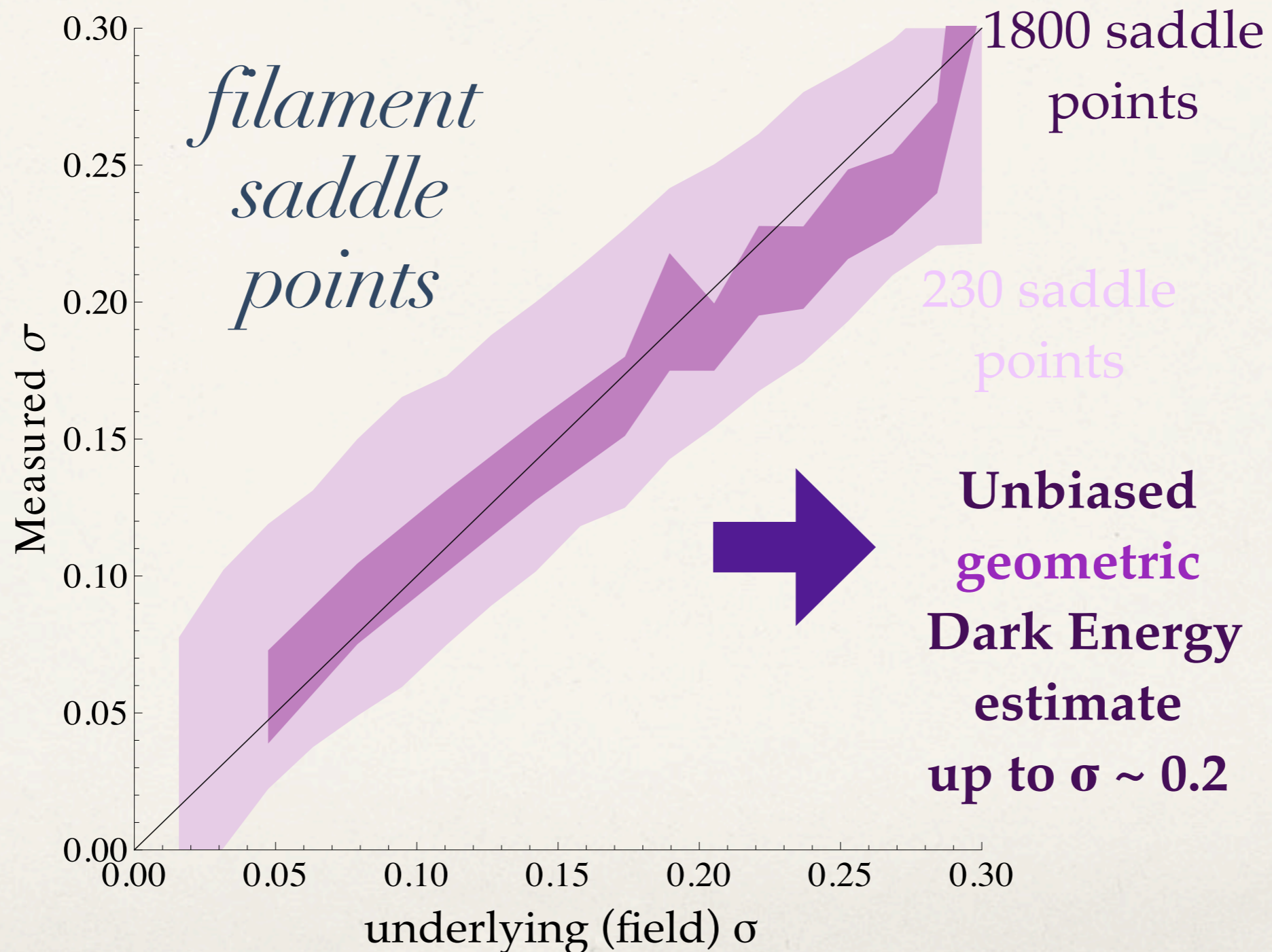
$$\frac{1}{\sigma} \langle x x_1^2 \rangle = \frac{4(48 + 62n + 21n^2)}{21n^2} {}_2F_1 \left(\frac{3+n}{2}, \frac{3+n}{2}, \frac{3}{2}, \frac{1}{4} \right) - \frac{6(3+n)(8+7n)}{21n^2} {}_2F_1 \left(\frac{3+n}{2}, \frac{5+n}{2}, \frac{3}{2}, \frac{1}{4} \right)$$

3pt field- gradient cumulant

$$n = -3 : \quad \frac{1}{\sigma} \langle x^3 \rangle = \frac{34}{7} \implies \frac{1}{\sigma} \langle x x_1^2 \rangle = \frac{34}{7} \frac{2}{3^2}$$

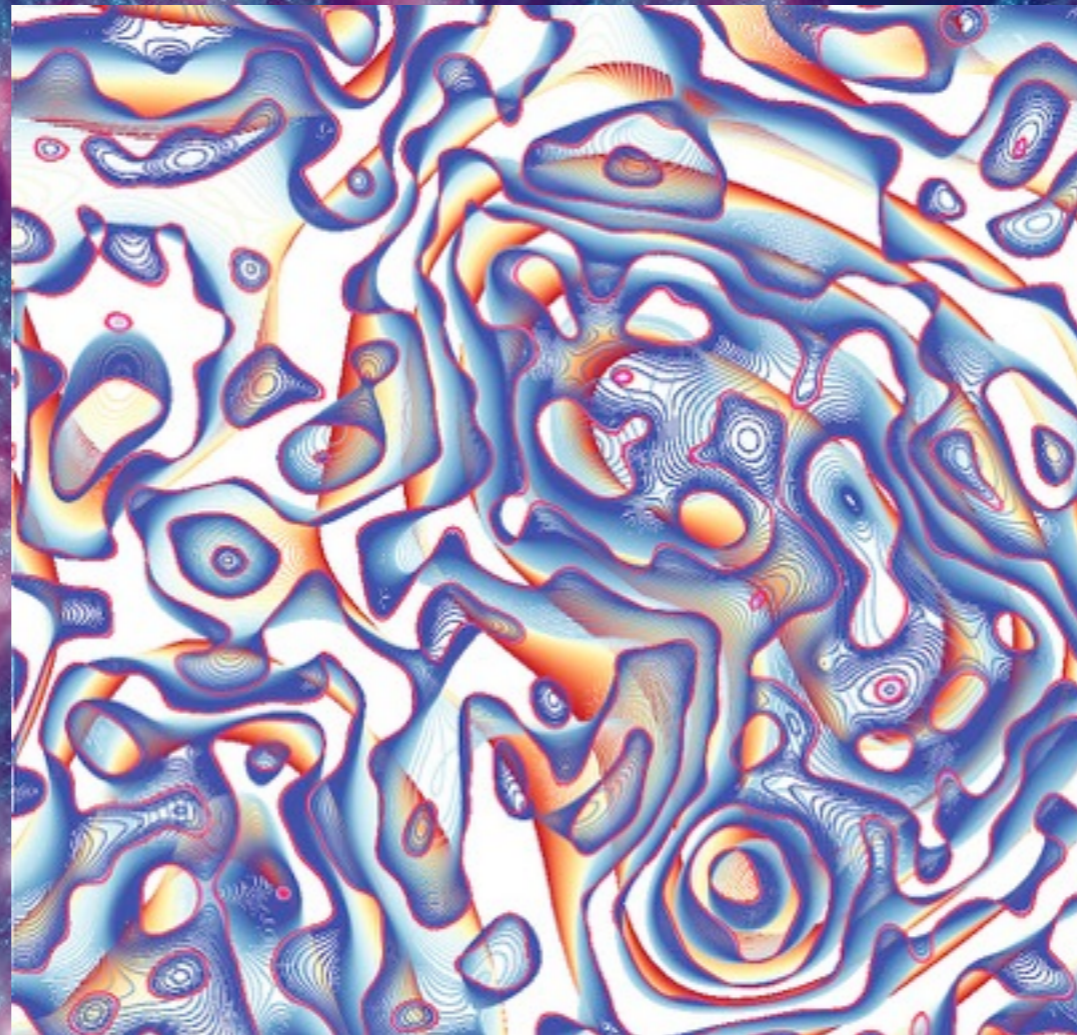
Fiducial DE experiment

- Generate scale invariant ICs
- Evolve them with gravity
- identify critical sets
- compute differential counts
- estimate amplitude of NG **distorsion** via PT
- deduce **geometric** critical set σ



How is the cosmic web woven?

- ▶ Context
- ▶ Random fields, Peak theory, critical events
- ▶ Cosmic connectivity
- ▶ Cosmic multiplicity
- ▶ Application: AGN in groups



$$\left. \frac{\partial^2 n}{\partial R \partial \nu} \right|_{\pm} = \frac{3\sqrt{3}(1-\tilde{\gamma}^2)(25\gamma^4 + 30\gamma^2(2\nu^2 - 1) - 27)R}{20\sqrt{10}\pi^{5/2}(9-5\gamma^2)^{5/2}R_*^3\tilde{R}^2} e^{-\frac{9\nu^2}{2(9-5\gamma^2)}}.$$

